# NSTX Upgrade

# Analysis of the PF1c Mandrel/Case CHI Gap, Thermal/Structural Analysis, Including the Proposed Thermal Shield Design

**NSTXU-CALC-133-15-0**

**Rev 0**

**December, 2014**

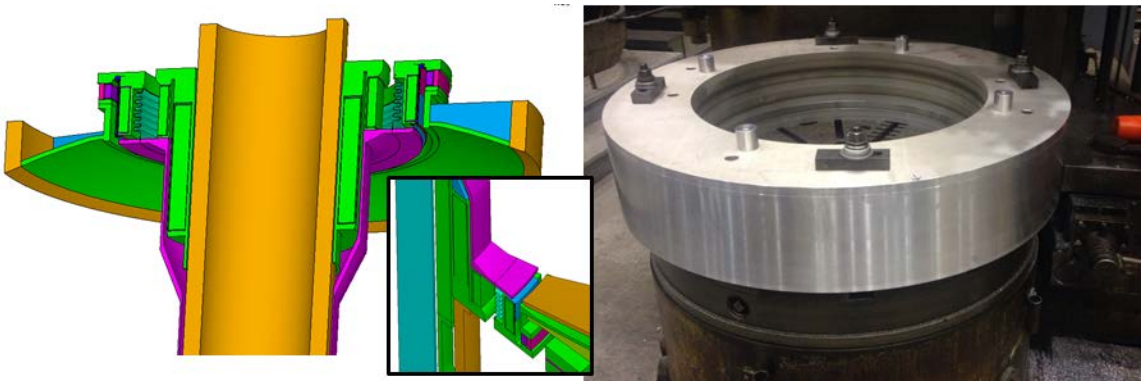


**Prepared By:**

Peter H. Titus

Digitally signed by Peter H. Titus
DN: cn=Peter H. Titus, o, ou=Princeton Plasma Physics Laboratory, email=ptitus@pppl.gov, c=US
Date: 2015.03.10 14:48:27 -04'00'

Peter Titus

**Reviewed By:**

Irving J. Zatz

Digitally signed by Irving J. Zatz
DN: cn=Irving J. Zatz, o, ou=PPPL, email=zatz@pppl.gov, c=US
Date: 2015.03.09 17:26:26 -04'00'

**Irving Zatz**

## PPPL Calculation Form

Calculation # **NSTXU-CALC-12-01-01** Revision # **00** ____ WP #, **1672**
(ENG-032)

Purpose of Calculation: (Define why the calculation is being performed.)

The purpose of this calculation is to provide guidance on the initial design and qualification of the PF1c outer mandrel shell. A thermal shield was recommended for the CHI Gap to protect the mandrel shell, but time and budget constraints dictated omission of the shield. What is presented is a best effort assessment of the heat loads and mandrel shell stresses that will result from operations due to heat loads that enter the CHI gap. Additionally, the inner PF mandrel outer shell closure welds are evaluated, consistent with the requirements of Len Myatt's inner PF analysis.

References (List any source of design information including computer program titles and revision levels.)

These are included in the body of the calculation, in section 6.2

Assumptions (Identify all assumptions made as part of this calculation.)

The significant assumption made in this analysis is that there will be sufficient monitoring of the case temperature, and sufficient constraint on the flux lines near the CHI gap, such that acceptable case temperatures can be maintained.

Full heat flux for a full 5 second pulse would have damaged the as-designed 1/16th inch thick 316 SST thermal shield. Thickening the shield to improve the thermal inertia would encroach on the CHI gap, posing operational problems for the CHI and greater difficulty in assembling the centerstack. Thermocouples in the CHI gap divertor tiles and a pyrometer viewing the shield were intended to provide an adequate indication of the peak shield temperature. Elimination of the thermal shield due to assembly difficulties and time constraints led to the addition of a thermocouple positioned at the mandrel corner that sees the highest heat flux (see figure 4.0-9). It is assumed that during the operation of NSTX, these sensors will be monitored well enough to avoid shots that impose unacceptable heat fluxes on the mandrel shell for unacceptable times. The number of planned equilibria that use the full PF1c current is limited. This is shown in figure 8.1-2. For design and analysis, it will be assumed that each normal operating pulse heats the coil to 100C.

Calculation (Calculation is either documented here or attached)

These are included in the body of the following document

Conclusion (Specify whether or not the purpose of the calculation was accomplished.)

The PF1c mandrel/case shell has been instrumented to monitor the effects of heat entering the CHI gap. Shell temperatures resulting from only plasma radiation for a 5 second shot fails the 20,000 pulse S-N fatigue requirements. Fracture mechanics assessments show an acceptable result with no direct plasma impingement and 200C temperature from radiative heating. Shell temperatures greater than 200C degrees may eventually fatigue the closure weld and potentially can spoil the vacuum. Coil centering functions are now provided by a silicon band wound around the outside of the coil. The original concept for the closure welds of the outer mandrel shell was converted from a O-ring seal groove to a small full penetration weld. This was replaced with a mandrel shell casing in which the corner weld was done in the shop and the closure weld was at a more favorable location.

Addition of the thermal shield may still be required, once there is operating experience with the actual heat loads measured in the CHI gap.

Cognizant Engineer's printed name, signature, and date

Digitally signed by Lawrence E. Dudek
Date: 2015.03.11 13:52:07 -04'00'

**I have reviewed this calculation and, to my professional satisfaction, it is properly performed and correct.**

Checker's printed name, signature, and date

Irving J. Zatz
Digitally signed by Irving J. Zatz
DN: cn=Irving J. Zatz, o, ou=PPPL, email=zatz@pppl.gov, c=US
Date: 2015.03.09 17:26:54 -04'00'

## 2.0 Table of Contents


| | |
|---|---|
| Title Page | 1.0 |
| ENG-33 Forms | |
| Table Of Contents | 2.0 |
| Revision Status Table | 3.0 |
| Executive Summary | 4.0 |
| Input to Digital Coil Protection System | 5.0 |
| Design Input | 6.0 |
| Criteria | 6.1 |
| References | 6.2 |
| Photos and Drawing Excerpts | 6.3 |
| Materials and Allowables | 6.4 |
| Heat Fluxes | 6.5 |
| Normal Operation Plasma Radiation | 6.5.1 |
| Particle Flux from X Point | 6.5.2 |
| Heat Flux from CHI Currents | 6.5.3 |
| Lorentz Loads, Max Currents | 6.6 |
| Disruption and Halo Current Input | 6.7 |
| Thermal Expansion Cycles | 6.8 |
| Models | 7.0 |
| Magnetic Stability, and Required Alignment Shell Stiffness | 8.0 |
| Inner PF Outer Mandrel Shell Closure Welds | 9.0 |
| Final August 2014 Weld Design with Mid Silicon Band and Thermocouple | 9.1 |
| Fracture Mechanics Assessment of Closure Weld | 9.2 |
| Closure Weld Configuration Studies | 9.3 |
| PF1c Mandrel Shell and Heat Shield Thermal Transients | 10.0 |
| No Thermal Shield | 10.1 |
| With Thermal Shield | 10.2 |
| Moly Shield | 10.2.1 |
| PF1c Mandrel Shell and Heat Shield Normal CHI Current Heating | 11.0 |
| Transient Electromagnetic Disruption Results | 12.0 |

Appendix A - email from Roger Ramen on PF1c Heat-Up During CHI Operations
Appendix B - Flex Shell Centering System and Closeout Weld
Appendix C - “Rubber Bumpers “ Centering System
Appendix D - More on the Unused Moly Thermal Shield
Appendix E - True Basic Shield Thermal Analysis Program


## 3.0 Revision Status Table

| | |
|---|---|
| Rev 0 | Initial Issue |

## 4.0 Executive Summary

The objective of this calculation is to provide guidance on the initial design and qualify the final design of the PF1c hardware in the vicinity of the CHI gap. The qualification needs to consider larger upgrade loads and thermal conditions. This area has proved to be an extremely difficult area to properly design to satisfy Lorentz load stresses, coil centering requirements, and protect from thermal loads from the CHI gap. The PF1c case is a part of the vacuum boundary of the vessel, and would temporarily end operation if a vacuum leak developed. The divertor tiles near PF1c have been extended to cover the vessel flange, but the PF1c outer mandrel is still exposed to significant heat flux if the X point is positioned over the CHI gap. The surface normal heat flux on the case for a 8.2 MW/m^2 heat load with a 15 degree grazing angle is 2.1 MW/m^2 – See section 6.5.2 and ref [5]. The CHI tile evaluation is included in Art Brooks' tile calculation [5]. The design as of October 2014 does not include a shield, but it may be needed in the future. The corner of the PF1c case is instrumented with a thermocouple on the inside of the case mounted on the winding. This will be monitored during operation.

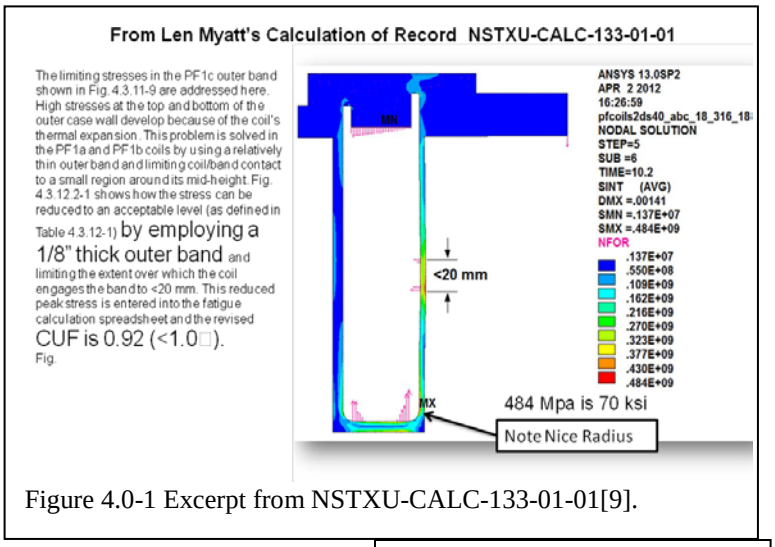

Figure 4.0-1 Excerpt from NSTXU-CALC-133-01-01[9].

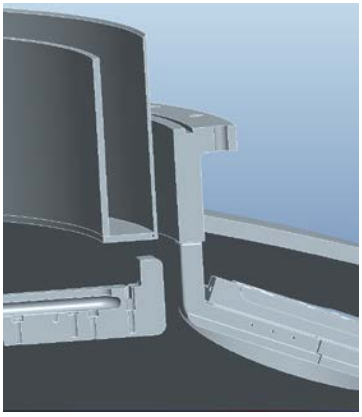
Figure 4.0-2 CAD model of the PF1c mandrel shell before revisions to the weld detail.

Work on this detail of the inner PF coils, began by Leonard Myatt, and is documented in NSTXU-CALC-133-01-01[9]. The original concept was based on winding the coil on a temporary mandrel then transferring it to a case in which it would be potted. The case was intended to have appropriate flexibility, strength, and adequate corner radii to avoid unacceptable stress concentrations. The thermal excursion of the coil from 12C to 100C produced unacceptable bending strains in the case wall. Introduction of a gap to allow the radial growth then necessitated addition of a centering mechanism to ensure the coil would not shift and add error fields or adversely load the terminal break-outs that were fixed to solid bus bar. The bus bar and terminal bending stress are addressed in rev 2 of [9] prepared by A. Zolfaghari [10].

The outer shell of the case was used as a spring/flex and bore on the winding through an epoxy band. This system of epoxy bands and an outer flex shell is used in PF1a and b with split outer shells. A similar system is retained in the final design of PF1c, but the epoxy band was replaced with a silicon band. Flex of the outer case shell is also used in PF1a, and b, but these coils are not a part of the vacuum boundary and the outer shells are segmented and have less carefully prepared welds. For all the inner PF coils, the manufacturing process was changed from winding on a temporary mandrel to making the case into the mandrel and adding a temporary outer shell as a VPI pressure boundary. O-ring seals were used for the VPI. The intent was then to add an outer shell to the mandrel using the O-ring seal groove geometry to weld to. The lips of the O-ring seal provided a thickness of only .054 inches to make a vacuum sealed weld that had to take end moments from the outer shell cyclic flexure as the coil went from 12C to 100C.

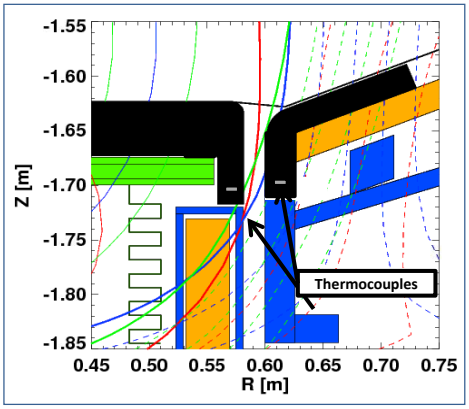

Figure 4.0-3 Figure from Stefan Gerhardts presentation on the potential for flux lines intercepting the corner of the pF1c case outer shell.

The integrity of this seal weld is an important component in the reliability of the operation of NSTX-U. The outer shell of the mandrel is loaded by coil thermal motions and Lorentz forces and, in addition, it will see heating from the plasma if a thermal shield is not provided. There have been a few evolutions of the seal weld design. Weld designs that attempted to use the O-ring seal groove were unacceptable.

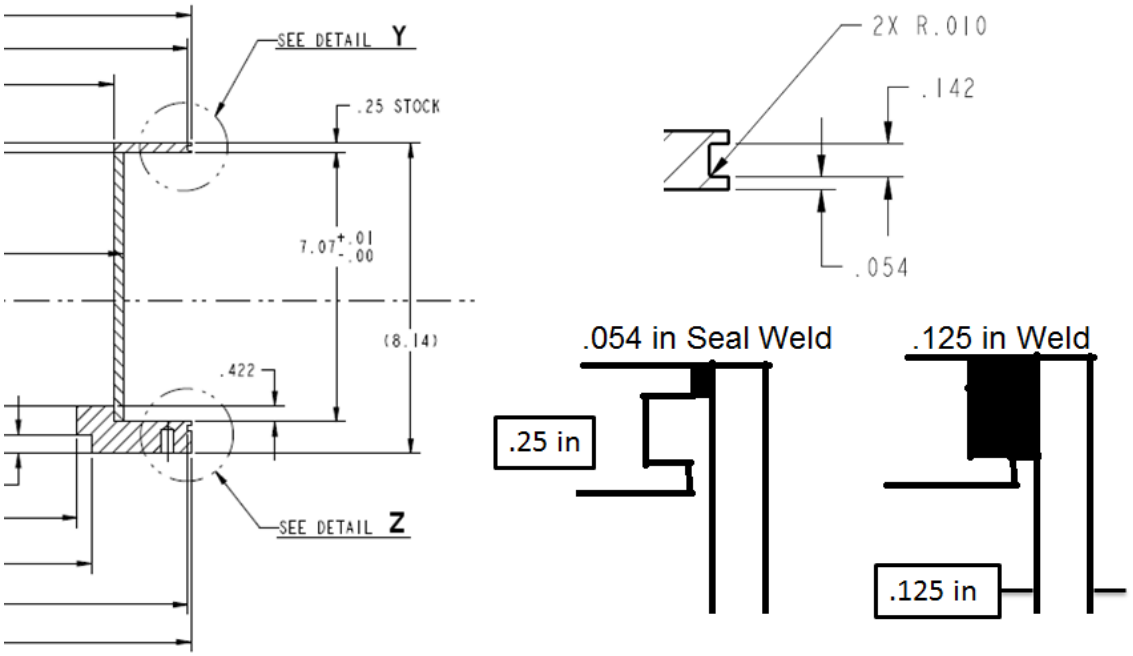


Figure 4.0-4 Lip Seal Weld and Better, but not Adequate filled Weld

There were a number of reviews of the design throughout 2013 and 2014. The status of the analysis was presented in a Peer review on Jan 10, 2014.

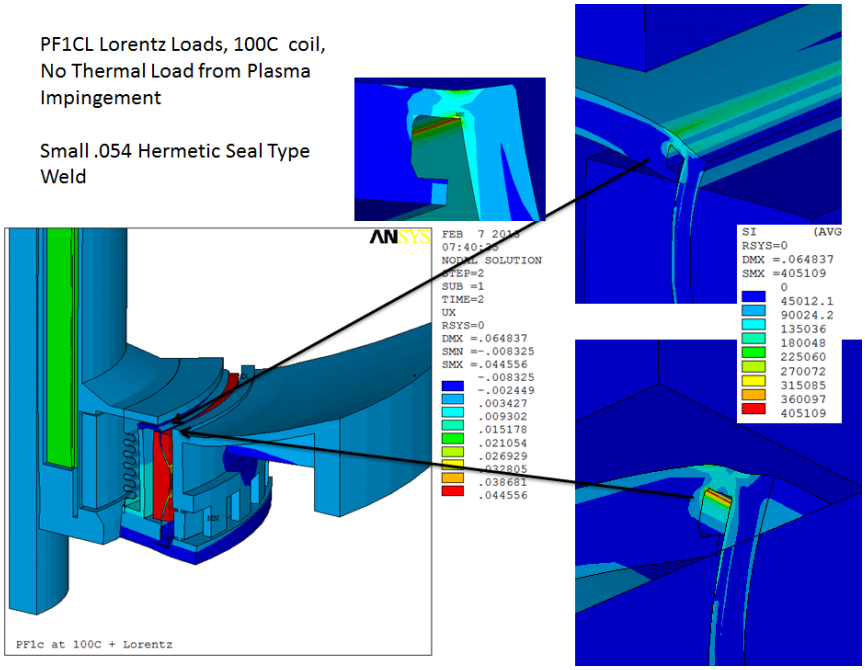


Figure 4.0-5 405 ksi Stress in the Lip Seal Weld . Peak Stress =405ksi

The tiny lip seal weld was highly overstressed. This is shown in figure 4.0-5. There was a lot of work done by Larry Dudek, Steve Raftopolis and Steve Jurzynski to develop a better weld detail than that originally intended based on the tiny lip left by the O-ring seal groove. A few cross sections were investigated based on the lip seal geometry as a starting point for the weld prep.

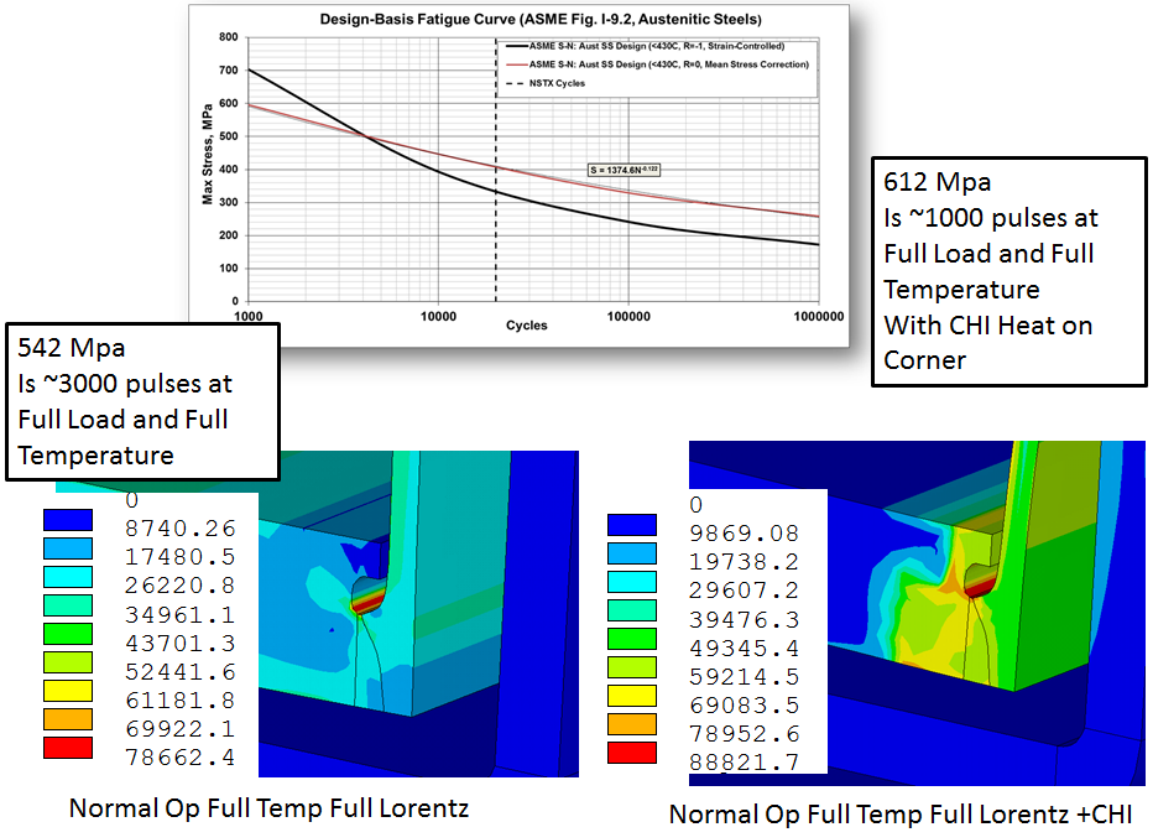


Figure 4.0-6 Outer Shell with Thicker Section Added for a Weld Prep

Figure 4.0-6 shows the stress analysis (Appendix D, June 27th Status) of a weld prep that required a thicker section be added to the outer shell, with the lip seal geometry machined down to obtain a larger radius relief at the back side of the closure weld. The thicker section could be added with a full penetration weld and then ground smooth. The relief and remaining lip provided thermal protection for the insulation from the weld heat. This geometry was mocked up and tested with a machined plate stacked on G-10. The G-10 was not overheated during welding, but great care had to be taken to avoid overheating the insulation.

At this point in the project it was clear that design and installation of the shield would be a schedule problem. Operation with the X point over the CHI gap could be avoided during operation by appropriate shaping of the plasma, and with the addition of instrumentation. Use of the tile thermocouples, possibly in concert with a pyrometer viewing the tiles from available ports for CHI penning gauges, should allow acceptable operating temperatures. The pyrometers were dropped and an additional thermocouple was installed on the OD of the coil near the corner of the PF1c case corner. The CHI gap tile thermocouples were retained.

Elimination of the shield provided space at the horizontal flange of the mandrel to add another annular ring/flange. This allowed the most delicate corner weld to be replaced by a heavier full size fillet that could be inspected from both sides. The closure weld is also a full size fillet. The extra annular plate was supposed to take only the space allocated for the shield, but at assembly, the coil can interfered with the divertor tiles that had been extended for thermal protection of the CHI gap. The welds are still a sensitive area and after insertion of the centerstack in the machine in October 2014, a vacuum leak was detected

[14]. At first, both inner and outer welds were suspect, but later it was determined that the corner fillet was OK and the leak was in the closure fillet which sees much lower stress.

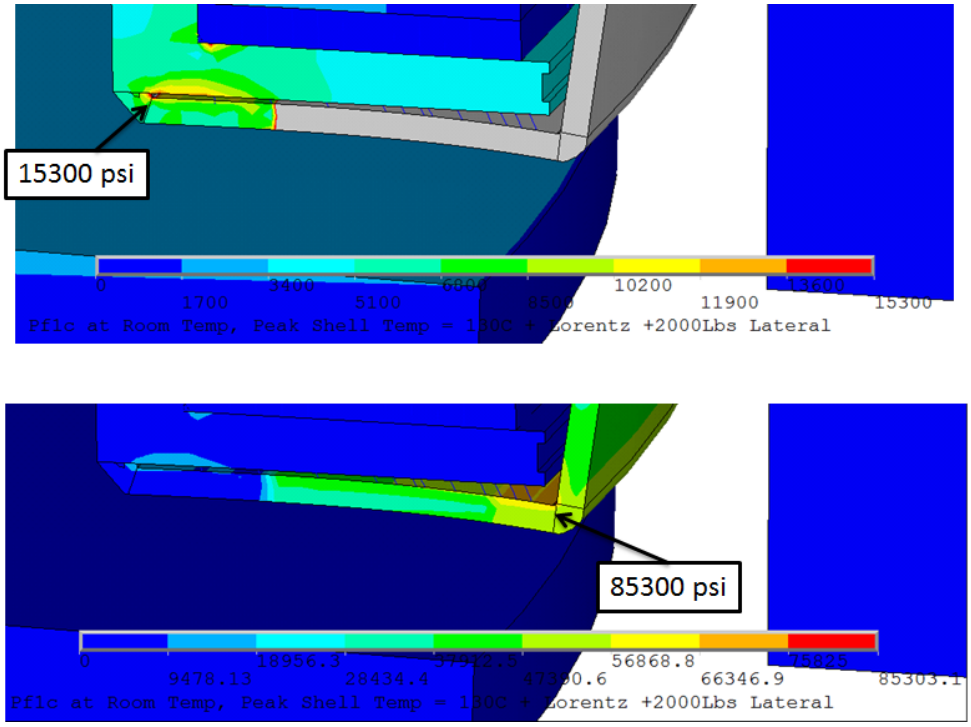


Figure 4.0-7 Added annular plate with full penetration corner weld and larger section fillet closure weld

The latest closure weld at the ID of the coil is much better. The outer weld is highly stressed even with only plasma radiation heating. For 5 second operation, radiant heating will heat the outer shell to 158C, and produce stresses of 85 ksi. This is above the fatigue allowable of 51ksi to 70 ksi tabulated in section 6.4.1. Multiple pulses can ratchet up to 248C(see Figure 6.5.1-1). If operations that heat the corner aren't avoided, it will be a problem. If there is direct plasma impingement, the temperature can be significantly higher. The thermocouples don't solve the problem; they only tell when operation must be restricted. Stresses in the welds are above S-N type allowables for modest heating.

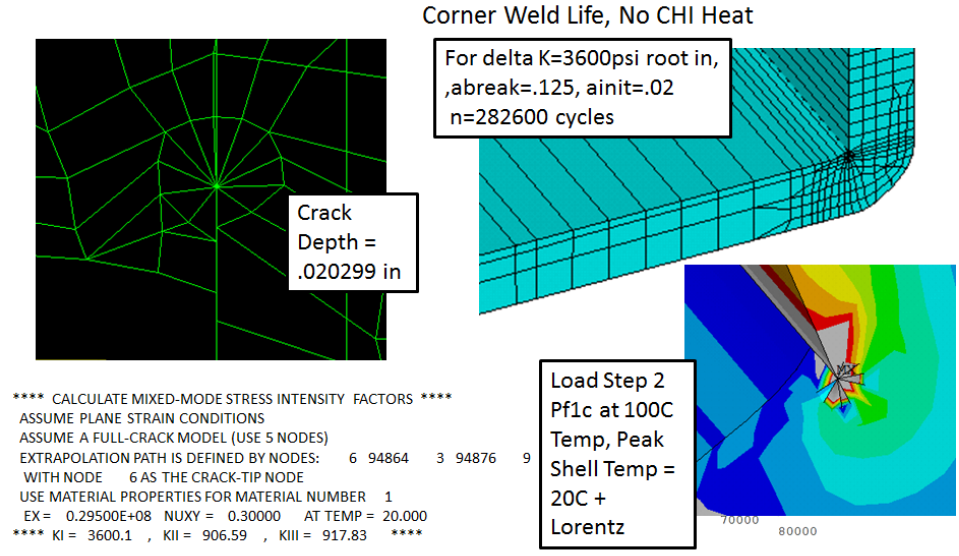


Figure 4.0-8 Fracture Mechanics Assessment of the Corner Weld

PF1c case welds were investigated with fracture mechanics calculations. The closure weld was not the limiting weld. The deformations imposed on the annular flange from CHI gap thermal loads and Lorentz loads produced lower stresses in the final closure fillet than in the corner weld. The corner weld was made with the outer shell and annular flange off the coil form. It could be inspected and polished from both sides. A large crack is extremely unlikely because of the care with which the weld was made, and the inspectability of the weld. The closure weld could only be seen from the outside when made, and the fillet forms a natural crack-like configuration at the root. The assessment of the corner weld shown in figure 4.0-8 concludes a predicted life of 282,600 cycles for a peak temperature of 200C in the case. The NSTX criteria requires a factor of safety of 2 on cycles for a fracture mechanics calculation, so this calculation would qualify the case for 140,000 cycles – well above the required 20,000 full power design shots. The position of the postulated cracks was chosen based on peak Tresca stresses, but it turned out that the tensile stresses normal to the postulated cracks were not as severe as the Tresca. Large hoop compressions from restrained thermal growth contributed to the Tresca, but not the crack growth. Because of the complexity of the thermal and mechanical loading, there is some uncertainty that the worst conditions were captured in the calculation. Monitoring the thermocouples during operation is still recommended.

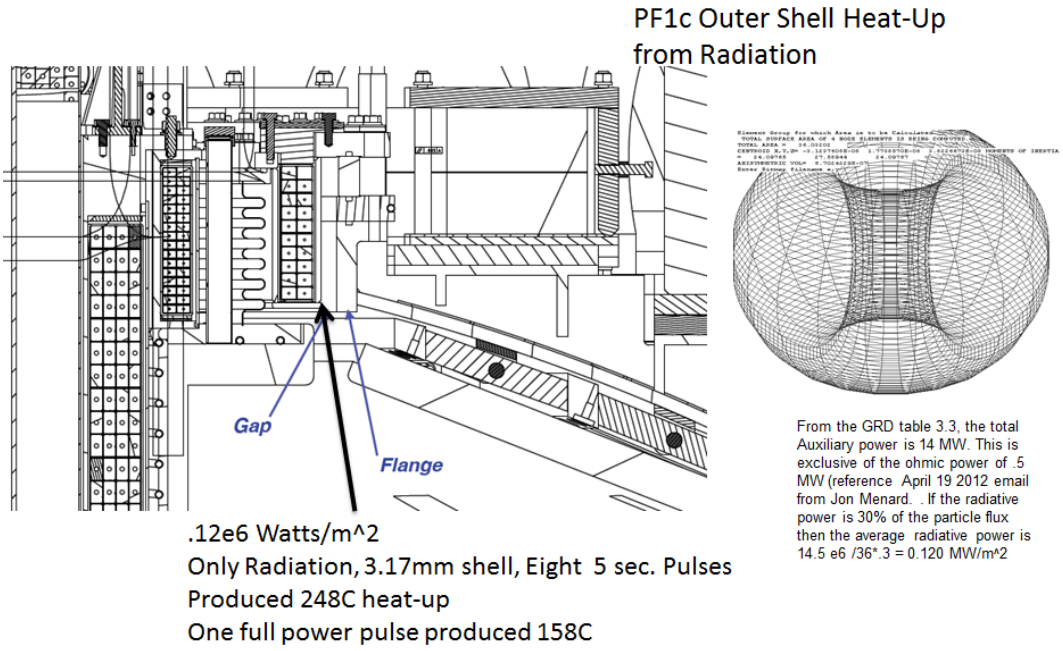


Figure 4.0-9 PF1c Outer Shell Heat-up with Only the Radiation Heat load

The IR radiation heat load from the CHI gap "viewing" the plasma is still sufficient to heat the case shell. Multiple, full 5 second pulses produce 248C case temperature. The fracture mechanics qualification was run at 130C and 200C. Even with monitoring the X point position with respect to the CHI gap, temperatures could ratchet to unacceptable levels during a run day.

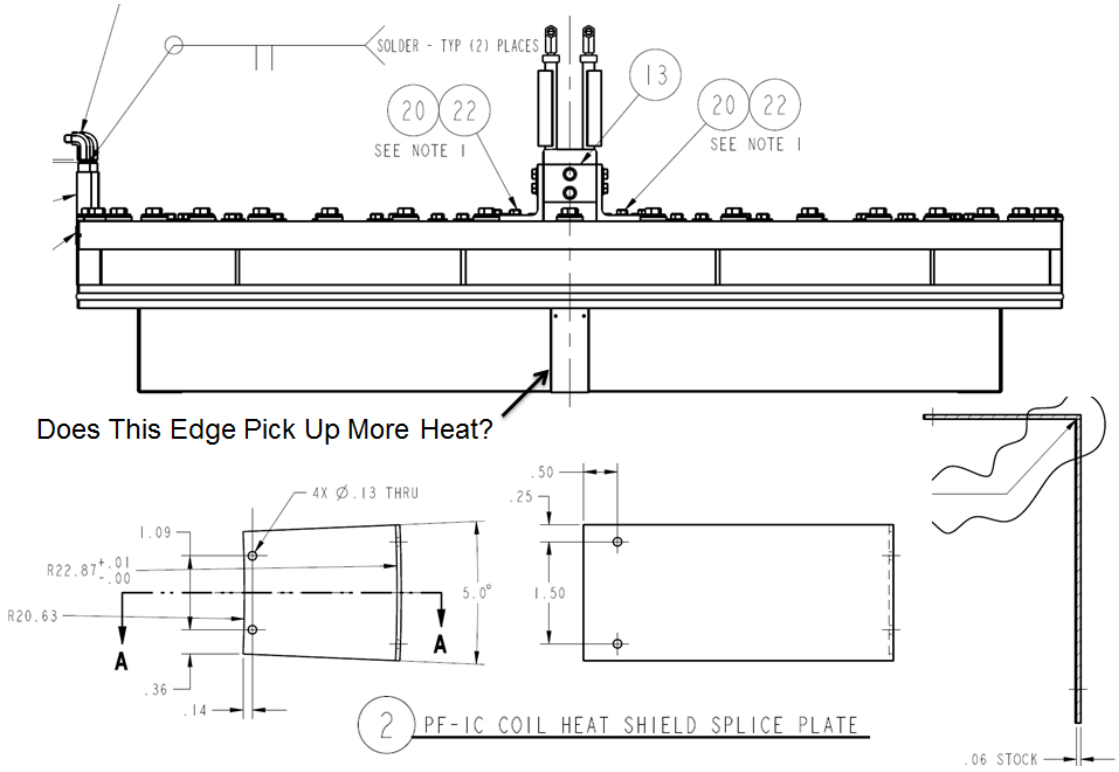


Figure 4.0-10 Thermal Shield Design that was not Implemented

Figure 4.0-10 shows a thermal shield concept that progressed to a design drawing. The edge of the splice plate over the shield joint potentially would have picked up most of the heat impinging on the shield. This was discussed at the Jan 10, 2014 meeting, and it was agreed that it should be removed. Later in the year, the shield itself was dropped.

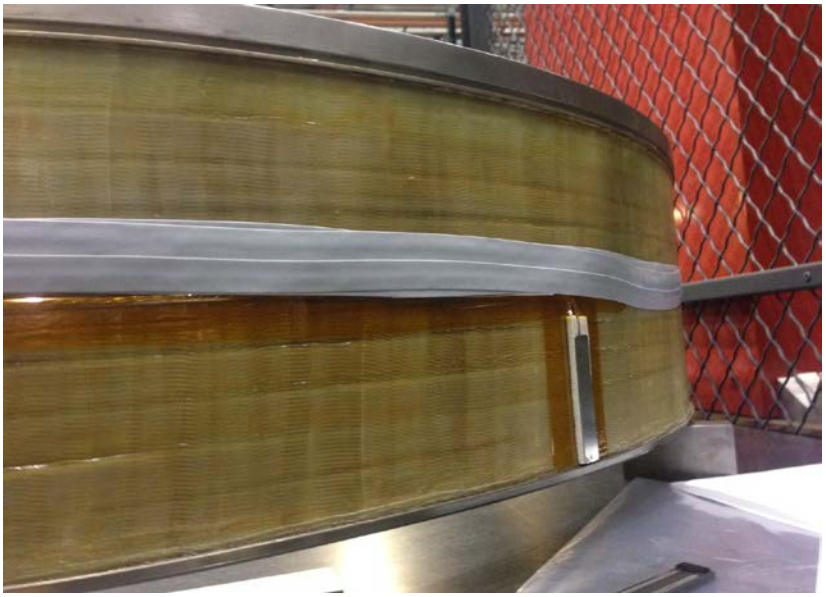

Figure 4.0-11 Thermocouple intended to read the casing temperature

Figure 4.0-11 shows the silicon band that bears agains the outer mandrel shell. The thermocouple is also shown. This is intended to measure the case temperature during operation.

Eventually, we should take another look at adding the thermal shields. Temperatures above 200C will flex the can and "exercise" and potentially propagate a crack or imperfection in the weld. One known imperfection was sealed by an epoxy [14]. We have upped the surveillance and instrumentation intending to minimize thermal loads on the can and intend to limit operation that might put heat loads in the CHI gap. With appropriate monitoring of the case temperature, and avoidance of experiments that cause significant plasma flux into the CHI gap, the PF1c case should remain leak tight and the coil should avoid overheating. With more operating experience, the addition of a shield may still be needed.

## 5.0 Digital Coil Protection System (DCPS)

There is no input to the DCPS planned for disruption loading of components or for thermal response of components caused by plasma heat loads. There are plans for instrumenting the area around the CHI gap to monitor the temperature of the tiles and PF1c thermal shield, but these will be examined after the shots. Subsequent shots will be adjusted to improve thermal loading on the CHI gap components, if needed. The loading calculated for the PF1c thermal shield and other components in this calculation is based on the maximum toroidal field for the upgrade, and the maximum poloidal fields for the 96 scenarios specified in the design point spreadsheet.

## 6.0 Design Input

### 6.1 Criteria

Stress Criteria are found in the NSTX Structural Criteria Document. Disruption and thermal specifications are outlined in the GRD - [7] and are discussed in more detail in section 6.5. Cyclic requirements for the PF1c mandrel shell shall be 20,000 full power operating pulses. These are assumed to develop the full 100C temperature, which imposes a full radial deflection on the coil centering components. Actually, looking at figure 6.6-1, the number of planned equilibria that use the full PF1c current is limited. For design and analysis, it will be assumed that each normal operating pulse heats the coil to 100C.

### 6.2 References


[1] NSTX-U Design Point Spreadsheet, **NSTXU-CALC-10-03-00** C. Neumeyer, http://w3.pppl.gov/~neumeyer/NSTX_CSU/Design_Point.html

[2] Disruption specification J. Menard spreadsheet: disruption_scenario_currents_v2.xls, July 2010. NSTX Project correspondence, input to Reference [1]

[3] "DISRUPTION ANALYSIS OF PASSIVE PLATES, VACUUM VESSEL AND COMPONENTS", NSTXU-CALC-12-01-01,February, 2012, P. Titus, and Yuhu Zhai

[4] ITER material properties handbook, ITER document No. G 74 MA 15, file code: ITER-AK02-22401.

[5] "Stress Analysis of ATJ Center Stack Tiles and Fasteners" NSTXU-CALC-11-03-01 Revision 1 by Art Brooks

[7] NSTX Upgrade General Requirements Document, NSTX_CSU-RQMTS-GRD Revision 0, C. Neumeyer, March 30, 2009

[8] Inductive and Resistive Halo Current s in the NSTX Centerstack, A.Brooks, Calc # NSTX-103-05-00

[9] Inner PF Coils (1a, 1b & 1c), Center Stack Upgrade NSTXU-CALC-133-01-01 March 30, 2012 Rev 0/1 by Len Myatt.

[10] Inner PF Coils (1a, 1b & 1c), Center Stack Upgrade NSTXU-CALC-133-01-02 May, 2014 Rev 2 by Len Myatt. Rev 2 by A Zolfaghari and A Brooks

[12] Modeling of the Toroidal Asymmetry of Poloidal Halo Currents in Conducting Structures N. Pomphrey, J.M. Bialek_, W. Park Princeton Plasma Physics Laboratory,

[13] An Experimental Investigation of Fatigue Crack Growth of Stainless Steel 304L S. Kalnaus, F.Fan, Y Jiang, A.K. Vasudevan University of Nevada and Office of Naval Research , International Journal of Fatigue, Volume 31, Issue 5, May 2009

[14] On Wed, Oct 22, 2014 at 10:31 AM, William Blanchard <wblancha@pppl.gov> wrote: All,
The majority of leaks are on the inside of the can in the 10-7 t-l/sec range. We recommend these be sealed with leak sealer (good to 450 C). There appears to be one leak on the outside corner that will have line of

sight to the plasma. S. Vinson is localizing and measuring the leak rate. If it is in the 10-7 range, we recommend using leak sealer for that leak also. Bill Blanchard Joseph Winston
[17] Fatigue Crack Propagation in Stainless Steel Weldments at High Temperature
BY P. SHAHINIAN, H. H. SMITH AND J. R. HAWTHORNE The performance of submerged arc welds and base metals of Types 304 and 316 stainless steels are compared on the basis of fracture mechanics analysis
[18] Damping in ANSYS/LS-Dyna Prepared by: Steven Hale, M.S.M.E Senior Engineering Manager CAE Associates (Web Search Results)
[19] Disruption Load Calculations Using ANSYS Transient Electromagnetic Simulations for the ALCATOR C-MOD Antennas, P Titus Plasma Sci. & Fusion Center, MIT, Cambridge, MA; Fusion Engineering, 2002. 19th Symposium on Fusion Engineering 02/2002; DOI: 10.1109/FUSION.2002.1027634 ISBN: 0-7803-7073-2
[20] Email from Stefan Gerhart
>> > 2) I suspect that the toroidal symmetry should be fairly good...better
>> > than
>> > the symmetry (or lack thereof) for the halo current entrance points. I
>> > think
>> > that a peaking factor of 1.5 could be assumed for a first analysis
>> > (max/average = 1.5). If this poses a problem, please let me know and we can revisit. Note that there are no measurements of this peaking, so it will be a guess no matter what.
>> >
[22] OH-PF1a/b Magnetic Stability NSTXU-CALC-133-11-00 Rev 0 P. Titus, Checked by A. Zolfaghari, March 2 2010
[23] "Molybdenum" Metallwerk Plansee GhmbH A-6600 Reuttee, http://www.plansee.com/english/
[24] email from Roger Ramen 11/13/12 included in Appendix A
[25] email from Roger Ramen
Roger Raman
Dec 1 (1 day ago)
to me, Raki

Hi Pete,
Yes, the Hi - pot should be for 9kV, eventually. But, for 2015, we will operate CHI at 2kV. Raki takes care of the Hi - pots for CHI.
Roger

On Dec 1, 2014 9:56 AM, "Peter Titus" <ptitus@pppl.gov> wrote:

Could you clarify the GRD CHI specs:?
Section 3.2.2 says 2kV upgradable to 4kV and a highpot of 5kV
If the highpot is usually 2E+1 shouldn't it

## 6.3 Photos and Drawing Excerpts

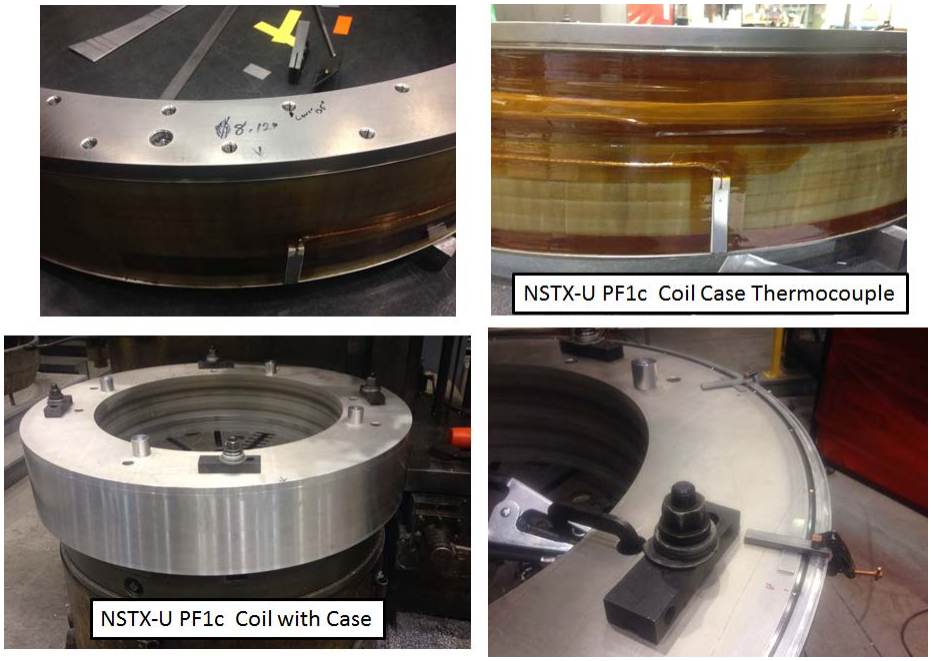


Figure 6.3-1 Photos of the Outer Shell Welding

Figure 6.3-2 Photo of the Outer Shell Welding

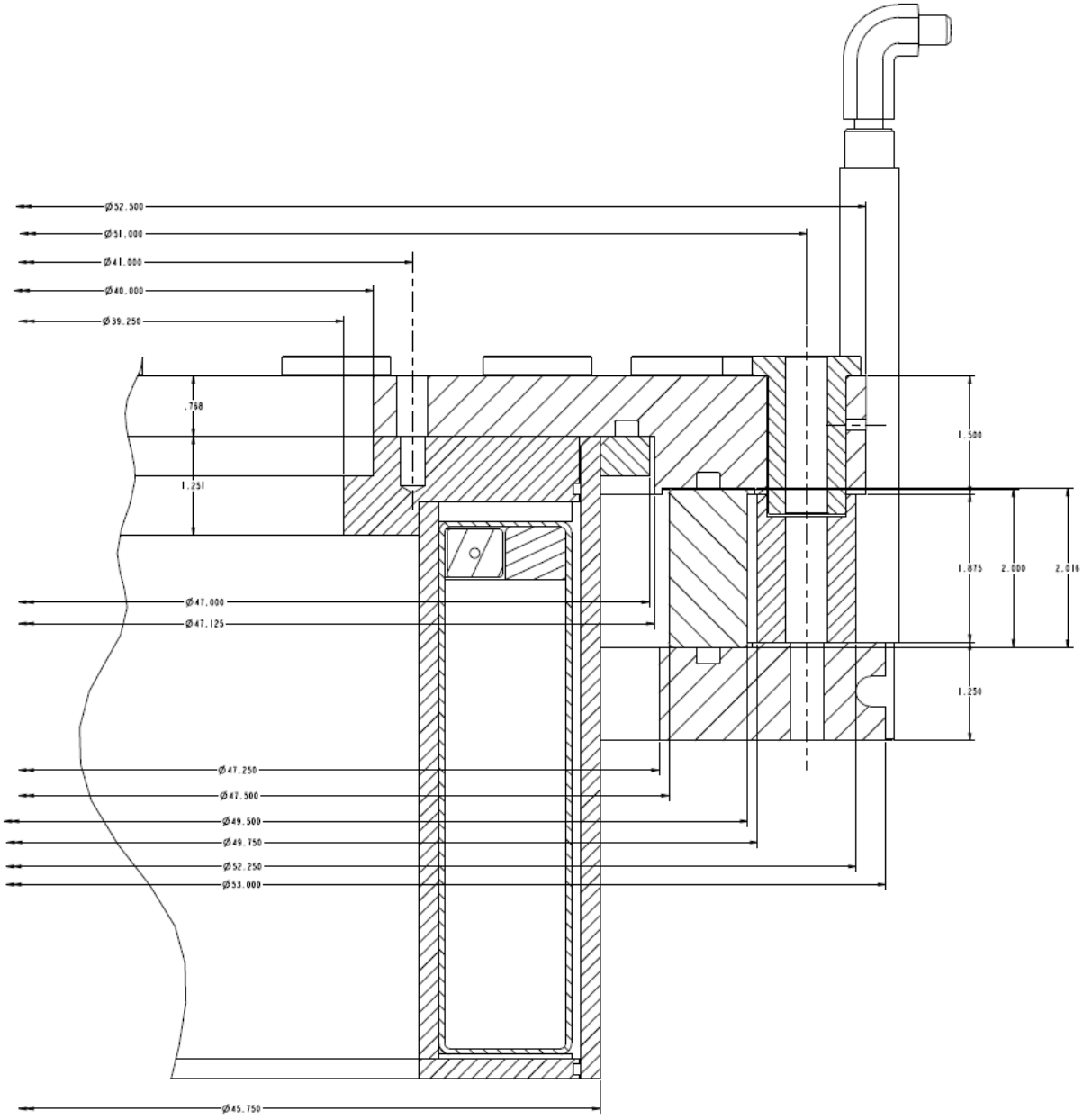


Figure 6.3-3 Dimensional Study from Lew Morris with dimensions used in making the FEA Model

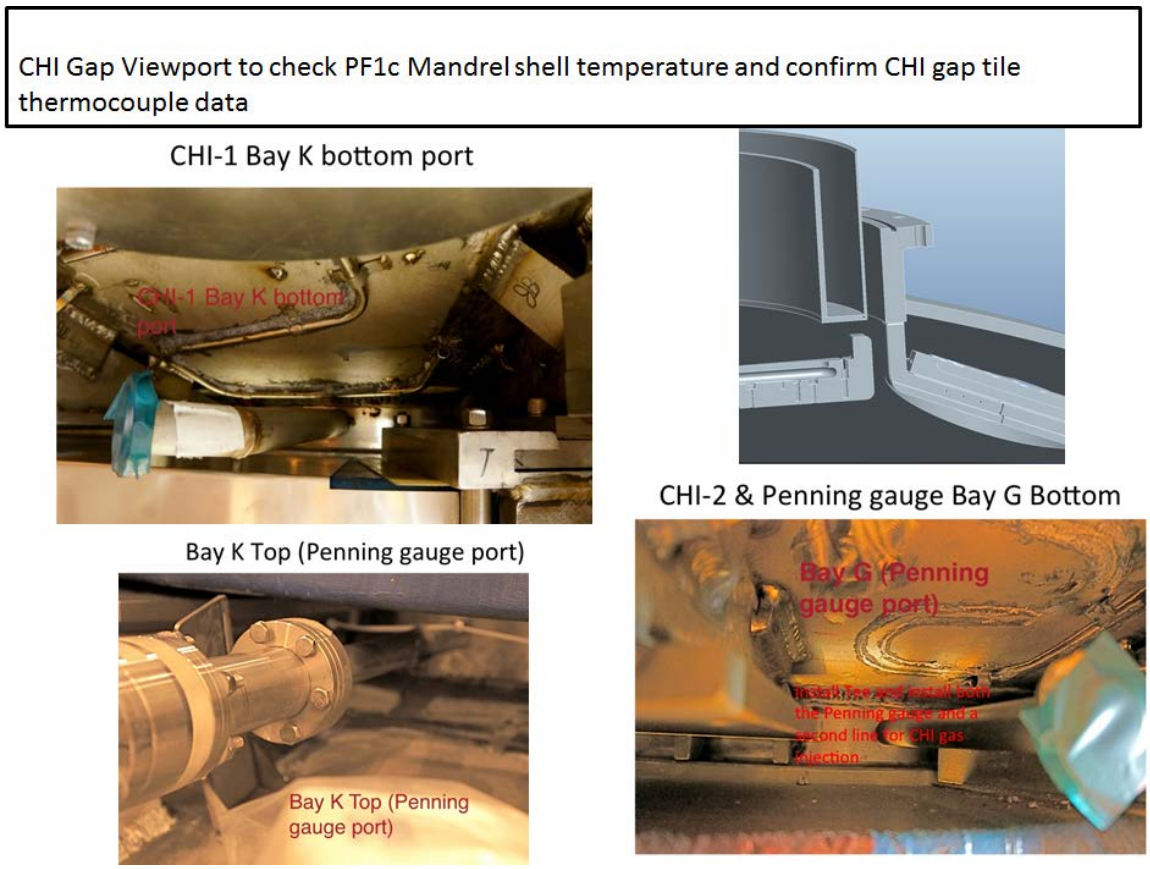


Figure 6.3-4 Photos of Potential Locations of a Pyrometer

Roger Raman Oct 2

to Kelsey, Lawrence, William, James, me, Stefan, Dennis, Jonathan

All,

It would be best if we could add one or two more ports like these in the photos. This could be done when we install the new 2-3/4 inch ports on the outer vessel.
If that is not possible, these CHI gas injection ports could be modified to add an optical detector at the end.
The Bay G port is for both the Penning gauge and the CHI gas injection.
The orientation of the Penning gauge is shown in the file Bay-G-Top-with-penning-gauge

## 6.4 Materials and Allowables

### 6.4.1 Stainless Steel Fatigue Allowable

The fatigue allowables have been collected from a few sources below:

| | | | |
|---|---|---|---|
| RCC-MR | 30,000 cycles | 483 MPa | 70 ksi |
| NSTX Criteria | 30,000 cycles | 275 MPa | 40 ksi |
| ASME (corrected for R=.1) | 30,000 cycles | 400 MPa | 58 ksi |
| ITER in-vessel Components [18] | 1e6 cycles | 351 MPa | 51ksi |

The choice of a S-N allowable is made somewhat moot and superseded by the inclusion of fracture mechanics assessments of the expected life of the case welds.

316 Allowables for 30,000 cycles

| | R=-1<br>Strain Controlled Max Stress | R=0 Strain Controlled<br>Max Stress | Strain Controlled Stress Range |
|---|---|---|---|
| ASME/Myatt | 340 MPa | 410 MPa | 410 to 680 |
| NIST/Titus<br>2 and 20 | 205 MPa | 275 MPa | 275 to 410 |
| RCC-MR | | | 483 MPa |
| ITER In Vessel Criteria | | | >308 Mpa ( 308 Mpa is for 1e6 Cycles, Load Controlled) |

Table 6.4.1-1 316 Allowable Fatigue Stress – 483 MPa is 70 ksi

Design Life = 30,000 Full Power Pulses, With a factor of 20, The requirement is 600,000 cycles which yields a 420 MPa =60.9ksi, At 30,000 cycles the criteria based on 2*stress yields 550 MPa/2 = 275MPa = 40 ksi

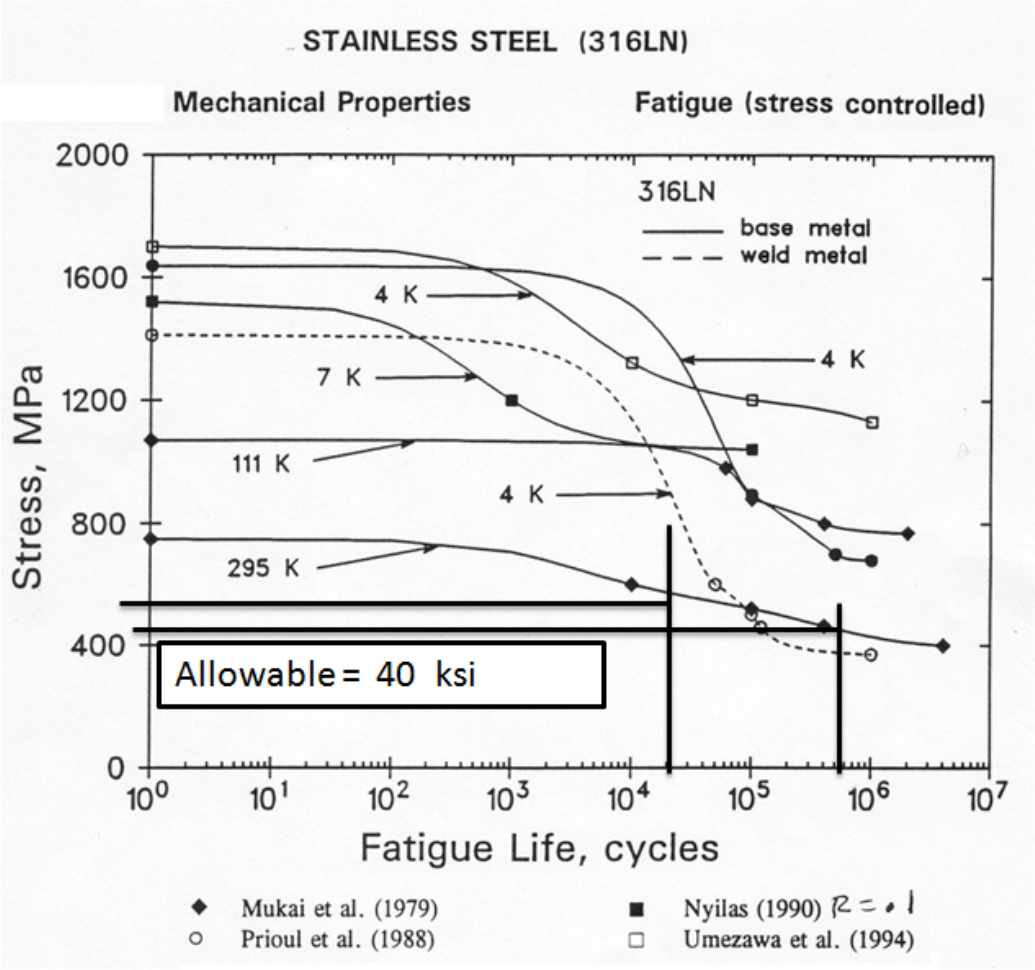


Figure 6.4.1-1 NIST Fatigue Data for 316 LN

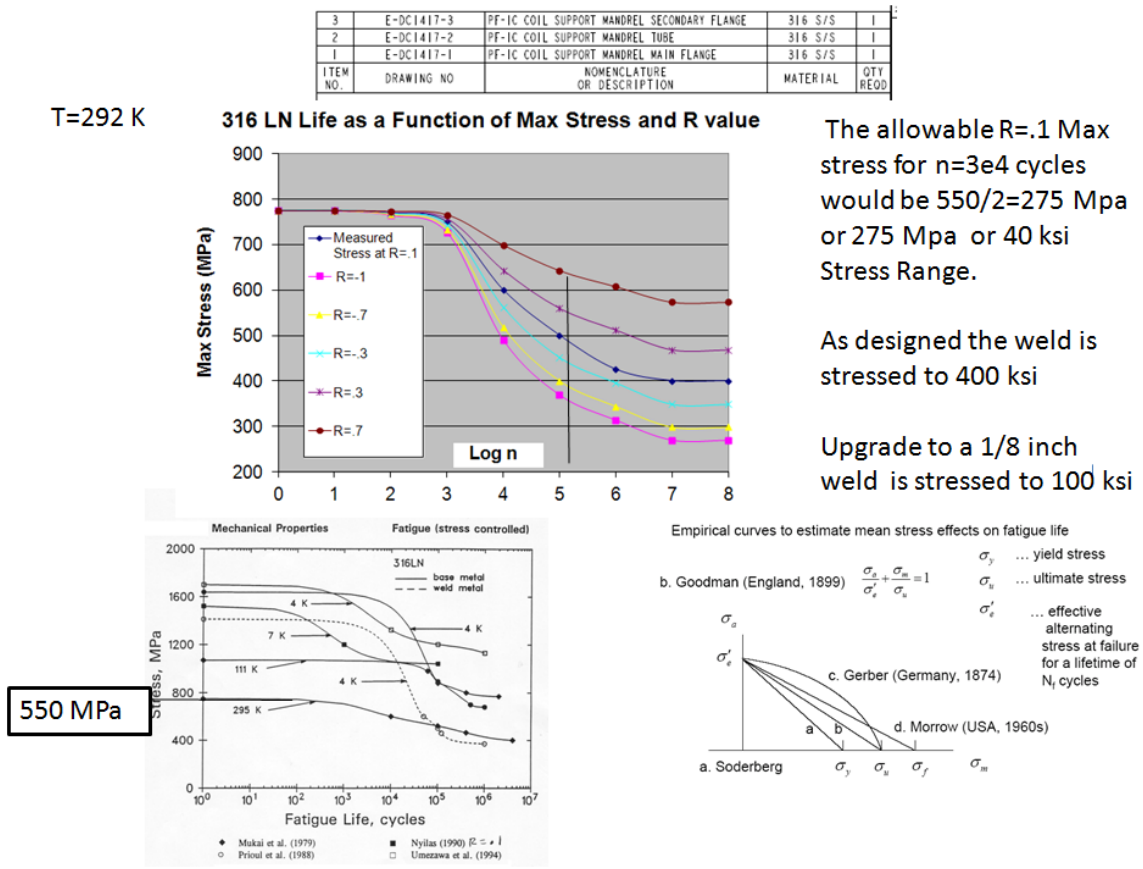


Figure 6.4.1-2 Recommended Strain Range (%) Values from the 316 SST section of [18] (structural Design Criteria for In-Vessel Components, Material Section)

| T⇓/N⇒ | $10^6$ | $10^7$ | $2.10^8$ | $4.10^{11}$ |
|---|---|---|---|---|
| 20°C | 0.190 | 0.147 | 0.111 | 0.107 |
| 425°C | 0.183 | 0.140 | 0.106 | 0.102 |
| 550°C | 0.167 | 0.128 | 0.097 | 0.094 |

**Table A.S1.5.5-2: Recommended fatigue design values Stress controlled for N > $10^6$.**

Figure 6.4.1-3 The allowable fatigue stress for 1e6 cycles from [18] is .00190*185e9=351 MPa, or 51 ksi.

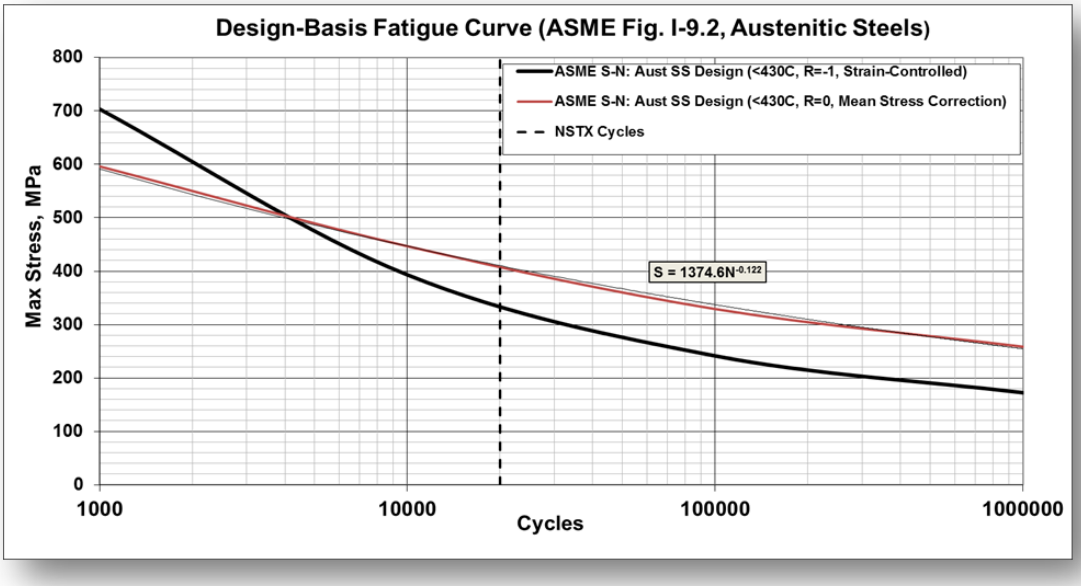


Figure 6.4.1-4 ASME Design SN curve with R=0 Correction by L. Myatt [81]

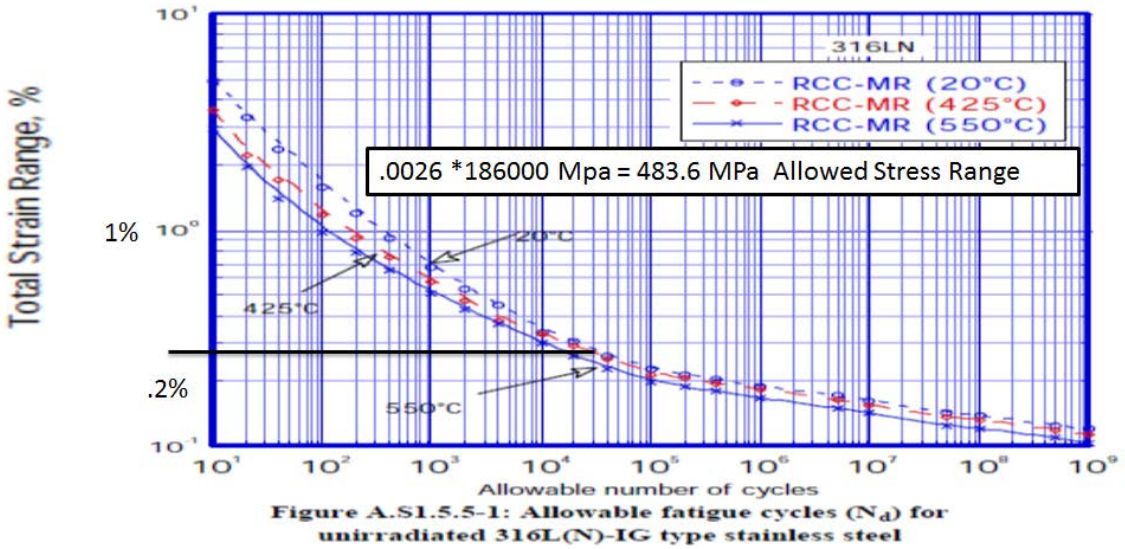


**Figure A.S1.5.5-1: Allowable fatigue cycles ($N_d$) for unirradiated 316L(N)-IG type stainless steel**

Figure 6.4.1-5 RCC-MR Design Design Fatigue curve Total Strain Range

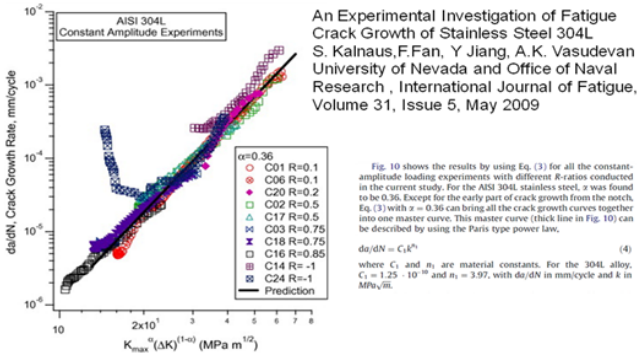


An Experimental Investigation of Fatigue Crack Growth of Stainless Steel 304L
S. Kalnaus, F.Fan, Y Jiang, A.K. Vasudevan
University of Nevada and Office of Naval Research , International Journal of Fatigue, Volume 31, Issue 5, May 2009

Fig. 10 shows the results by using Eq. (3) for all the constant-amplitude loading experiments with different $R$-ratios conducted in the current study. For the AISI 304L stainless steel, $\alpha$ was found to be 0.36. Except for the early part of crack growth from the notch, Eq. (3) with $\alpha = 0.36$ can bring all the crack growth curves together into one master curve. This master curve (thick line in Fig. 10) can be described by using the Paris type power law,

$$da/dN = C_1 k^{n_1} \quad (4)$$

where $C_1$ and $n_1$ are material constants. For the 304L alloy, $C_1 = 1.25 \cdot 10^{-10}$ and $n_1 = 3.97$, with $da/dN$ in mm/cycle and $k$ in $MPa\sqrt{m}$.

**Table 2. $\Delta K_{th}$ values and Paris equation parameters ($da/dN = C(\Delta K)^n$) at different temperatures for $R = 0.1$ (units are MPa$\sqrt{m}$ and m/cycle)**

| Temperature (°C) | $\Delta K_{th}$ | $C$ | $n$ |
|---|---|---|---|
| 25 | 8.2 | $3.1\times10^{-13}$ | 3.3 |
| 475 | — | $6.8\times10^{-12}$ | 2.8 |
| 500 | 11.8 | $6.8\times10^{-12}$ | 2.4 |
| 600 | 6.5 | $5.5\times10^{-12}$ | 2.9 |
| 700 | 5.1 | $2.6\times10^{-11}$ | 2.6 |
| 800 | – | $2.4\times10^{-12}$ | 5.1 |

Figure 6.4.1-6 Fracture Mechanics Properties of Stainless Steel

## 6.4.2 Molybdenum Properties

At this point of the design process (June 2014), Molybdenum is not being used, but in anticipation of the possibility of the stainless steel shield being switched out for Molybdenum, the Molybdenum properties are retained here.

Molybdenum Properties

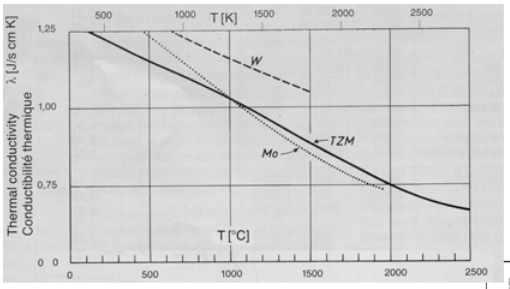


| MATERIAL | TEMP °F (°C) | e-EMISSIVITY |
|---|---|---|
| Molybdenum | 100 (38) | .06 |
| Molybdenum | 500 (260) | .08 |
| Molybdenum | 1000 (538) | .11 |
| Molybdenum | 2000 (1093 | .18 |
| Oxidized at 1000¡F | 600 (316) | .80 |
| Oxidized at 1000¡F | 700 (371) | .84 |
| Oxidized at 1000¡F | 800 (427) | .84 |
| Oxidized at 1000¡F | 900 (482) | .83 |
| Oxidized at 1000¡F | 1000 (538) | .82 |

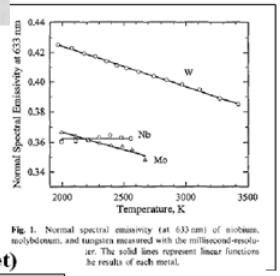


Fig. 1. Normal spectral emissivity (at 633 nm) of niobium, molybdenum, and tungsten measured with the millisecond-resolution. The solid lines represent linear functions the results of each metal.

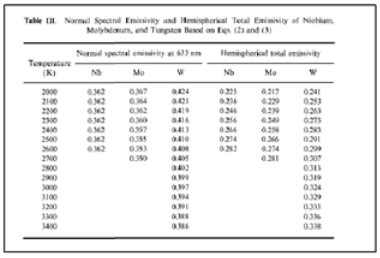

Table III. Normal Spectral Emissivity and Hemispherical Total Emissivity of Niobium, Molybdenum, and Tungsten Based on Eqs. (2) and (3)

| Temperature (K) | Normal spectral emissivity at 633 nm | | | Hemispherical total emissivity | | |
|---|---|---|---|---|---|---|
| | Nb | Mo | W | Nb | Mo | W |
| 2000 | 0.362 | 0.367 | 0.424 | 0.225 | 0.217 | 0.241 |
| 2100 | 0.362 | 0.364 | 0.421 | 0.216 | 0.229 | 0.253 |
| 2200 | 0.362 | 0.362 | 0.419 | 0.246 | 0.239 | 0.263 |
| 2300 | 0.362 | 0.360 | 0.416 | 0.256 | 0.249 | 0.273 |
| 2400 | 0.362 | 0.357 | 0.413 | 0.266 | 0.258 | 0.283 |
| 2500 | 0.362 | 0.355 | 0.410 | 0.274 | 0.266 | 0.291 |
| 2600 | 0.362 | 0.353 | 0.408 | 0.282 | 0.274 | 0.299 |
| 2700 | | 0.350 | 0.405 | | 0.281 | 0.307 |
| 2800 | | | 0.402 | | | 0.315 |
| 2900 | | | 0.399 | | | 0.319 |
| 3000 | | | 0.397 | | | 0.324 |
| 3100 | | | 0.394 | | | 0.329 |
| 3200 | | | 0.391 | | | 0.333 |
| 3300 | | | 0.388 | | | 0.336 |
| 3400 | | | 0.386 | | | 0.338 |

**Molybdenum Properties (from the Internet)**

| | |
|---|---|
| Electrical Conductivity % IACS | 30% |
| Resistivity microhm-cm at 20°C | 5.7 |
| Thermal Conductivity at 20°C | 0.35 cal/cm^2/cm°C/sec |
| Linear Coefficient of Expansion per °C | 4.9 x 10^-6 |

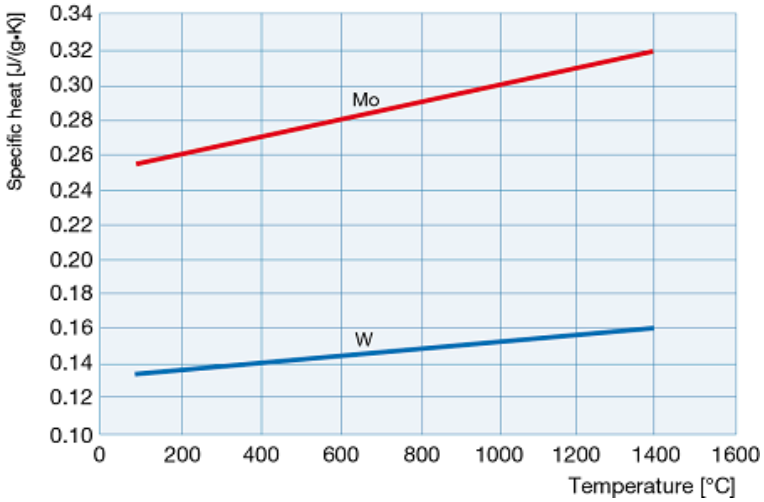


138 W/(m K) at room temp, about 100 at 1000C

Properties of TZM:

Elongation : < 20 %
Modulus of Elasticity : 320 GPa
Tensile Strength : 560 - 1150 MPa (81 ksi to 167 ksi)

### 6.4.3 Rubber

The modulus of rubber was input to ANSYS as 300 psi of RuANSYS Input: ex,14,300 !psi Silicon Rubber Approx Durometer 60 ( ~ twice the 30 shore A durometer in Wikipedia)

From the Internet:

The Young's Modulus, the slope of the stress-strain curve, is the other important setting. For very stiff rubbers, such as you find on the solid tires of a fork-lift, the Durometer might be 80 or 85, and the Young's modulus should be around 1400-1500 psi. A car tire would be more like 70 duro, with a Young's Modulus around 1000 psi. For very soft silicone seals, the Durometer might be as low as 30 (Shore-A), and the Young's Modulus should be about 130 psi. This **Wikipedia Article** shows you that there are several semi-empirical correlations offered by researchers to compute the Young's Modulus from a particular Durometer value, (but be warned, use any such correlation with a grain of salt).

Shore-A to Young's Modulus (in MPa):
=EXP((***Shore-A Durometer)****0.0235-0.6403)

Shore-D to Young's Modulus (in MPa):
=EXP((***Shore-D Durometer*** + *50*)*0.0235-0.6403)

## 6.5 Heat Fluxes

### 6.5.1 Normal Operation Plasma Radiation, No Particle Flux

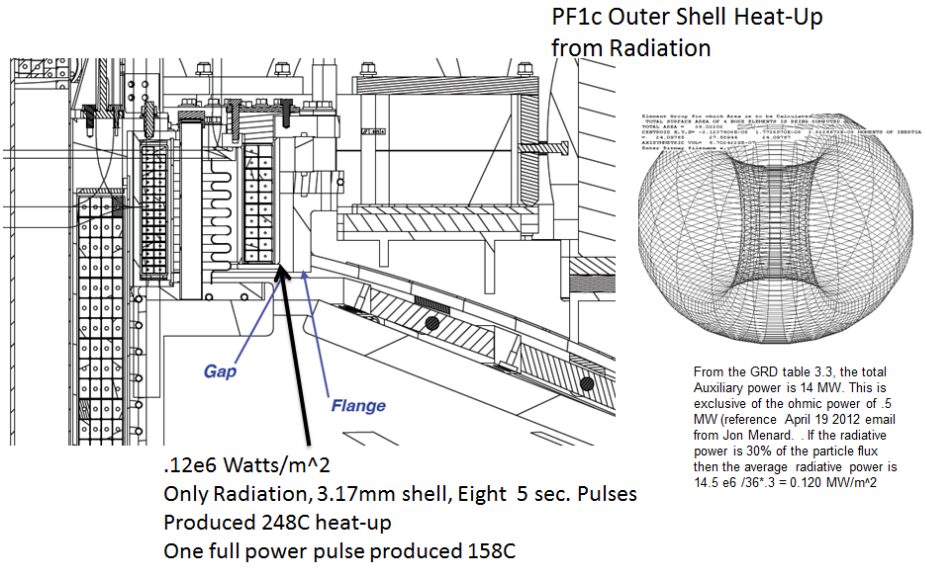


Figure 6.5.1-1 Plasma Radiation Heat Flux

### 6.5.2 Particle Flux from X Point

Figure 6.5.2-1 comes from a power point prepared by Art Brooks that was input to the CHI gap tile Peer review. This led to the upgrading of the tiles and extension of those below the CHI gap opening. The tiles could not be extended to cover the PF1c case because the case is an electrode for the CHI system.

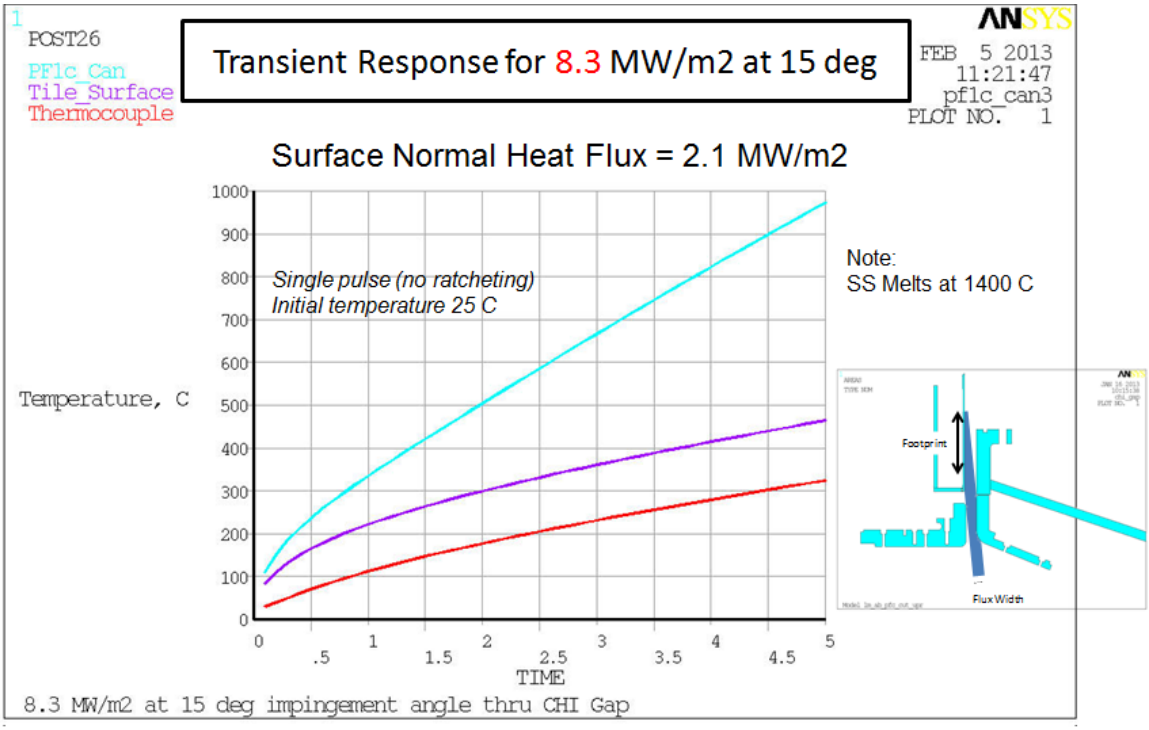


Figure 6.5.2-1 Particle Flux from X Point, (A. Brooks, Feb 2013)

The revision of the tile calculation that includes the redesign of the tiles is [5] "Stress Analysis of ATJ Center Stack Tiles and Fasteners" NSTXU-CALC-11-03-01 Revision 1, by Art Brooks.

### 6.5.3 Heat Flux from CHI Operations

The following is based on an email from Roger Ramen dated 11/13/12 and included in Appendix A [24]. During the CHI operation, current flows through the outer case of PF1c, across the plasma gap and enters the vessel flange. The metallic conduction path across this gap is broken by the ceramic ring. Currents in the mandrel/case outer shell will heat the shell. Normal operation produces a temperature increase of only .04 degrees C. In faulted conditions, the temperature increase is from 20 to 80C depending on the current path.

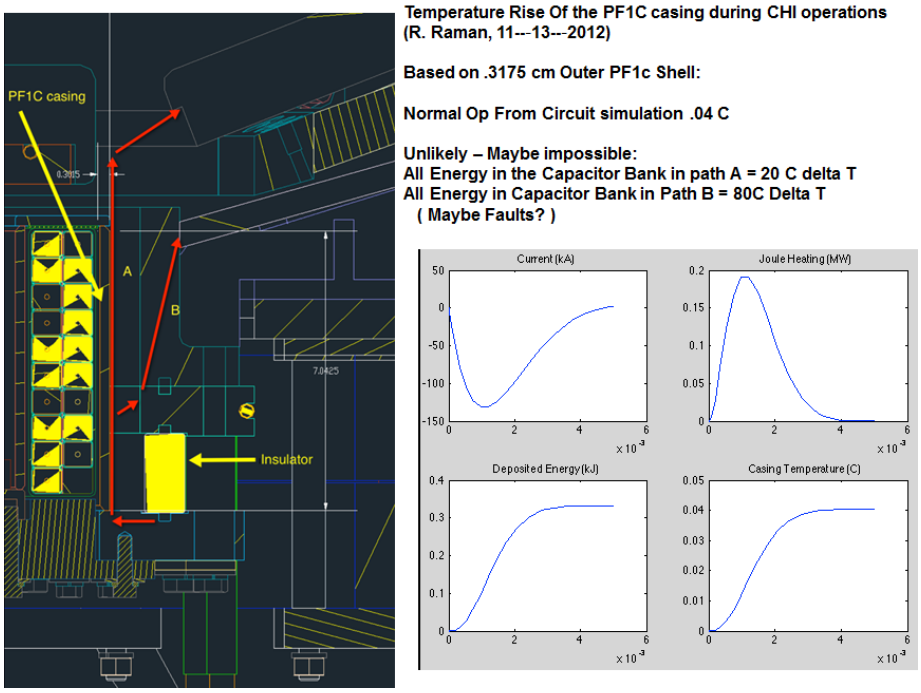


Figure 6.5.3-1 Heating Potential from CHI operations

## 6.6 Design Currents and Lorentz Forces

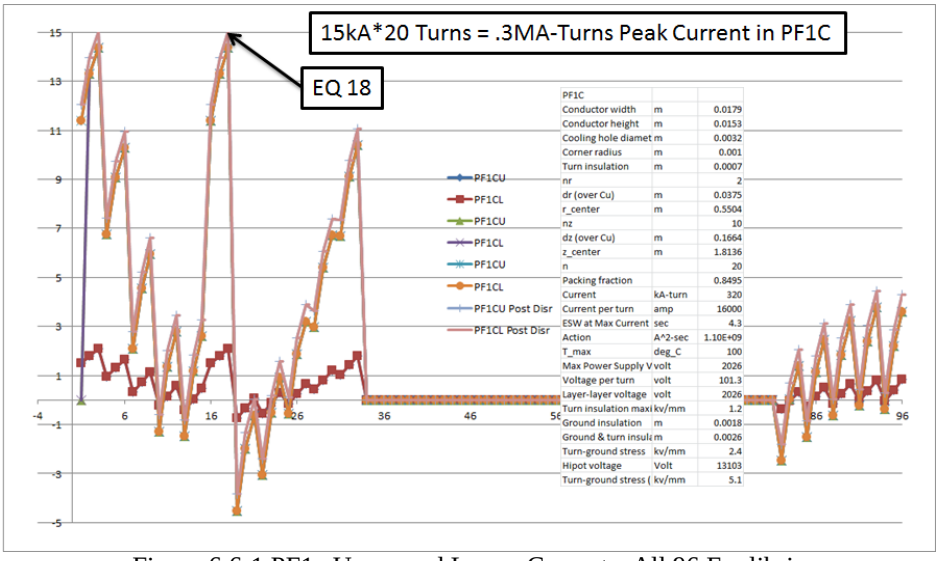


Figure 6.6-1 PF1c Upper and Lower Currents  All 96 Equlibria

The PF1c Upper and Lower Currents are plotted in Figure 6.6-1 for all design equilibria including the post disruption “equilibria”.

| Fr(lbf) | PF1aU | PF1bU | PF1cU | PF1cL | PF1bL | PF1aL |
|---|---|---|---|---|---|---|
| Min w/o Plasma | -35364 | -39917 | -71314 | -71290 | -5460 | -35367 |
| Min w/Plasma | -86091 | -3452 | -51380 | -51356 | -3452 | -86092 |
| Min Post-Disrup | -56775 | -1387 | -49577 | -49552 | -1387 | -56777 |
| Min | -86091 | -39917 | -71314 | -71290 | -5460 | -86092 |
| Worst Case Mi | -308932 | -259553 | -280590 | -280542 | -259506 | -308941 |
| Max w/o Plasma | 244828 | 141199 | 98727 | 46515 | 141221 | 124108 |
| Max w/Plasma | 390442 | 176824 | 17578 | 17561 | 176800 | 221474 |
| Max Post-Disrup | 271221 | 159652 | 18316 | 18297 | 159632 | 139721 |
| Max | 390442 | 176824 | 98727 | 46515 | 176800 | 221474 |
| Worst Case Ma | 1202680 | 427957 | 291802 | 291843 | 427989 | 1202670 |

| Fz(lbf) | PF1aU | PF1bU | PF1cU | PF1cL | PF1bL | PF1aL |
|---|---|---|---|---|---|---|
| Min w/o Plasma | -80237 | -34659 | -18534 | -58912 | -84182 | -42574 |
| Min w/Plasma | -71687 | -49080 | -32610 | -50407 | -78646 | -31269 |
| Min Post-Disrup | -95770 | -33155 | -22126 | -59782 | -83221 | -35298 |
| Min | -95770 | -49080 | -32610 | -59782 | -84182 | -42574 |
| Worst Case Mi | -169764 | -204276 | -126322 | -114523 | -139881 | -300586 |
| Max w/o Plasma | 53473 | 84182 | 58912 | 20585 | 34659 | 80236 |
| Max w/Plasma | 37012 | 78647 | 50408 | 32609 | 49080 | 71686 |
| Max Post-Disrup | 46450 | 83220 | 59782 | 22125 | 33155 | 95770 |
| Max | 53473 | 84182 | 59782 | 32609 | 49080 | 95770 |
| Worst Case Ma | 300589 | 139882 | 114523 | 126322 | 204275 | 118263 |

```
! For the Full 360 degree Model:
esel,mat,17 $nelem
f,all,fy,59782/49725   ! 352 nodes per 2.5 degree slice
```

```
! For the 40 degree Model
esel,mat,17 $nelem
f,all,fy,59782/(325*16)   ! 325 nodes per 2.5 degree slice
```

Figure 6.6-2 Loads from the Design Point Spreadsheet [1]

## 6.7 Disruption Loads and Halo Currents

Halo currents have not been postulated for the PF1c case or the proposed shield. The behavior of the upgrade configuration may behave differently and future operations might experience halo currents in the case. NSTX operation did experience halo currents crossing the CHI gap, so it is conceivable that halo loading might be a concern for the PF1c case, in the future. Inductive disruption eddy currents have been calculated in section 12.0 of this calculation. Disruption loads on the PF1c case are very small. If a Molybdenum shield is added in the future, the disruption eddy currents may be more significant. The requirements for disruption analysis are outlined in the NSTX Upgrade General Requirements Document [7]. The latest (August 2010) disruption specification were provided by Jon Menard as a spreadsheet: disruption_scenario_currents_v2.xls.[2] This reference includes a suggested time phasing of the inductively driven currents and the halo currents.

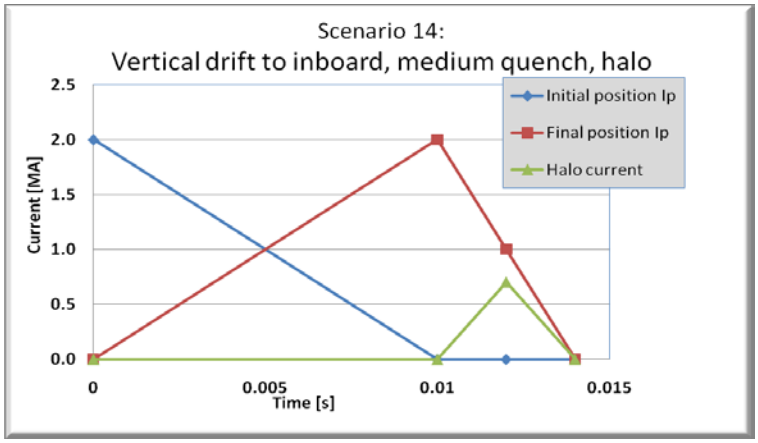


Figure 6.7-1 Time phasing of the plasma current changes that induce currents in the vessel and vessel components, and the halo currents. From J. Menard.

Criteria from the GRD:

Current and field directions (referring to Figure 2.2-2) shall be as follows: Plasma current Ip into the page (counter-clockwise in the toroidal direction, viewed from above); Halo current exits plasma and enters the structure at the entry point, exits the structure and re-enters the plasma at the exit point (counter-clockwise poloidal current, in the view of the figure); Toroidal field into the page (clockwise in the toroidal direction, viewed from above).

## 6.8 Thermal Expansion Cycles

Thermal stresses in the outer shell of the case result from the PF coil heating and radially expanding. In addition, the case can be heated by the plasma through the CHI gap. Thermal loading of the case due to radiation from the plasma occurs each shot. Thermal loading on the PF1c coils and the outer shell of the case due to direct plasma impingement and from the largest of the coil Joule heating is relatively in-frequent. In figure 6.6-1, the PF1c currents are plotted and the number of equilibria that use PF1c significantly are a small percentage of the total. CHI operations are a small percentage of the total and operations which place the X point near the CHI gap are supposed to be avoided. So, the number of thermal cycles applied to the case wall should be a fraction of the 20,000 planned full power shots.

# 7.0 Models

## 7.1 Structural Model

The structural models are swept from a 2D mesh. The last one (p1cz.dat) analyzed, shown in figure 7.1-1, includes a new annular plate that places the close-out weld away from the O-ring detail and allows a much larger weld cross section.

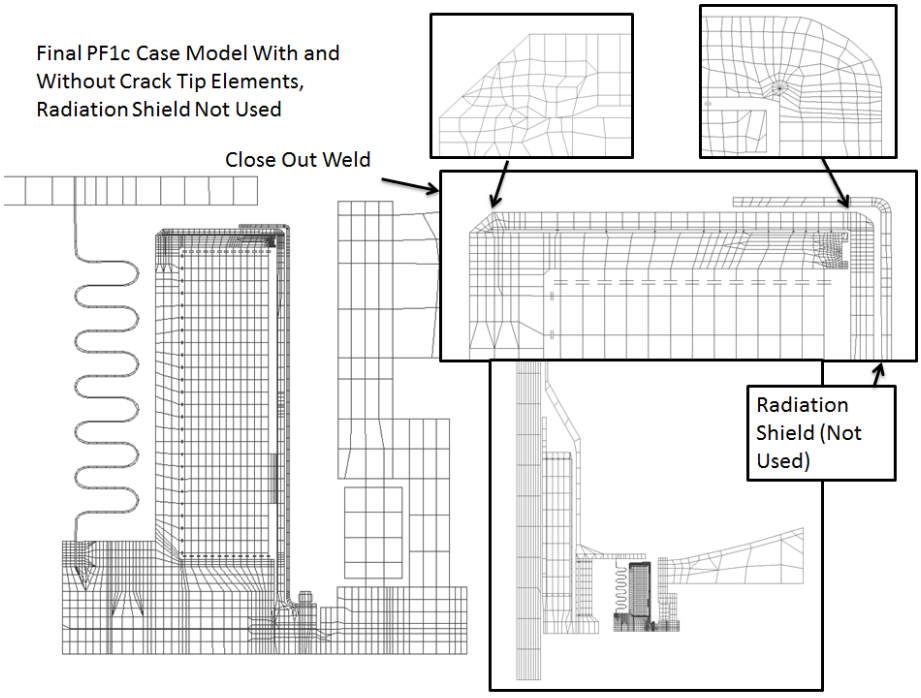


Figure 7.1-1 July 2014 Model with Added Annular Plate. Crack Tip Elements Added in December 2014.

The primary model used in this calculation is a 3D, 360-degree model shown in figure 7.1-3. This was swept from 2D meshes shown in Figures 7.1-1 and-2.

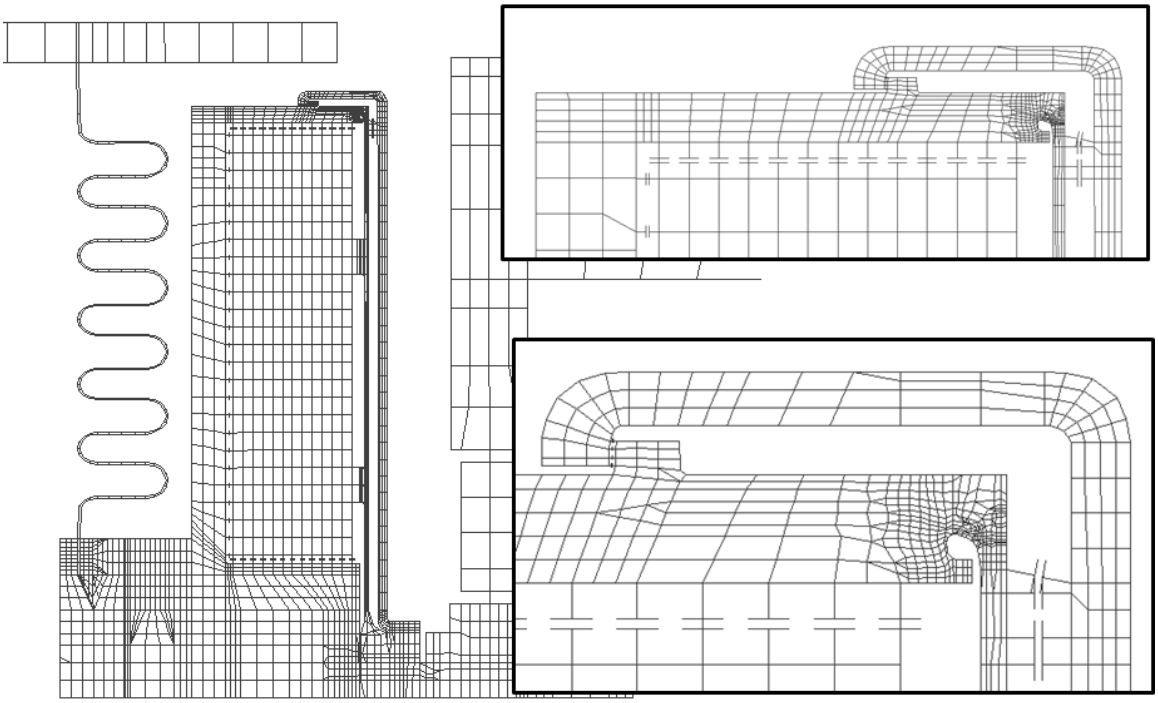

Figure 7.1-2 Earlier Model with Thermal Shield and Close-Out Weld Formed from the O-ring Seal Groove

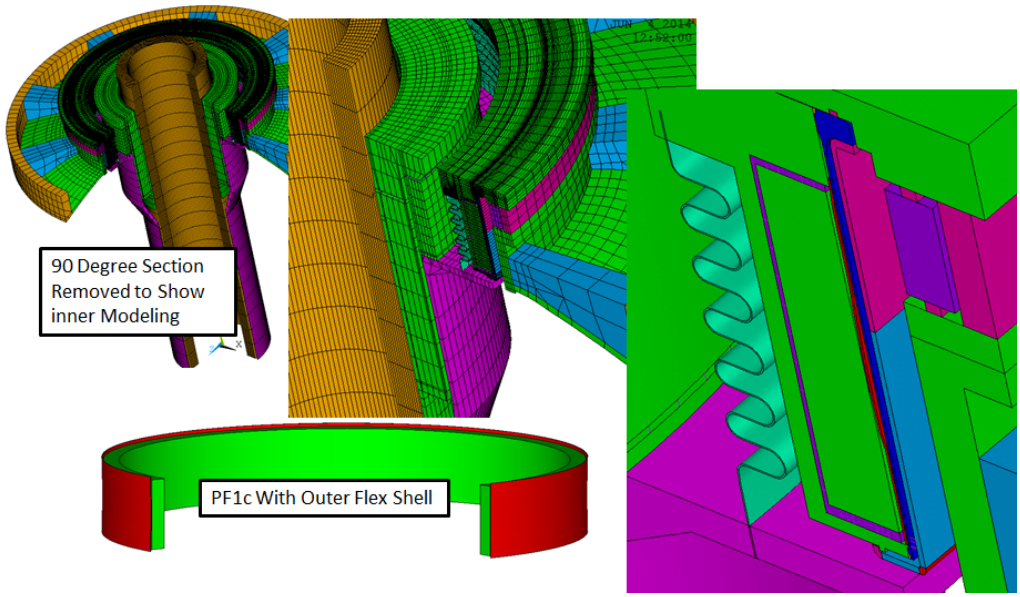


Figure 7.1-3 June 27, 2014 Model With Flex Shell Centering Mechanism

This model went through many evolutions of corner/close-out weld details and inclusions and deletions of thermal shields. The thermal shield is still included in the model in figure 7.1-2.

## 7.2 Disruption Model

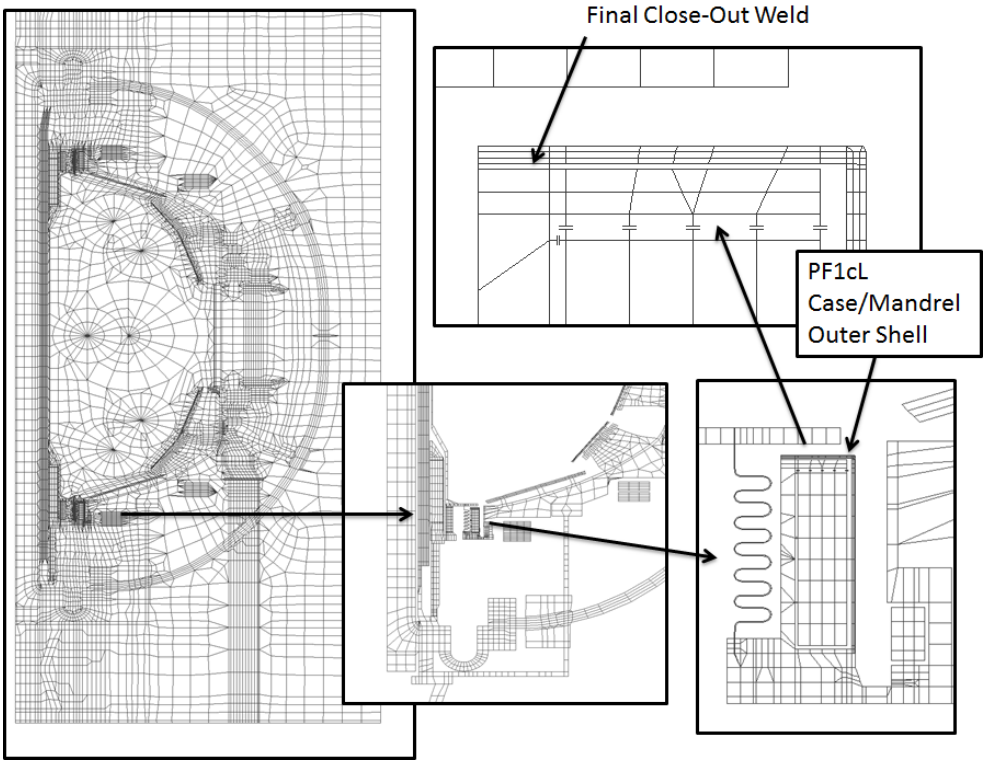


Figure 7.2-1 2D model used for the Swept Mesh

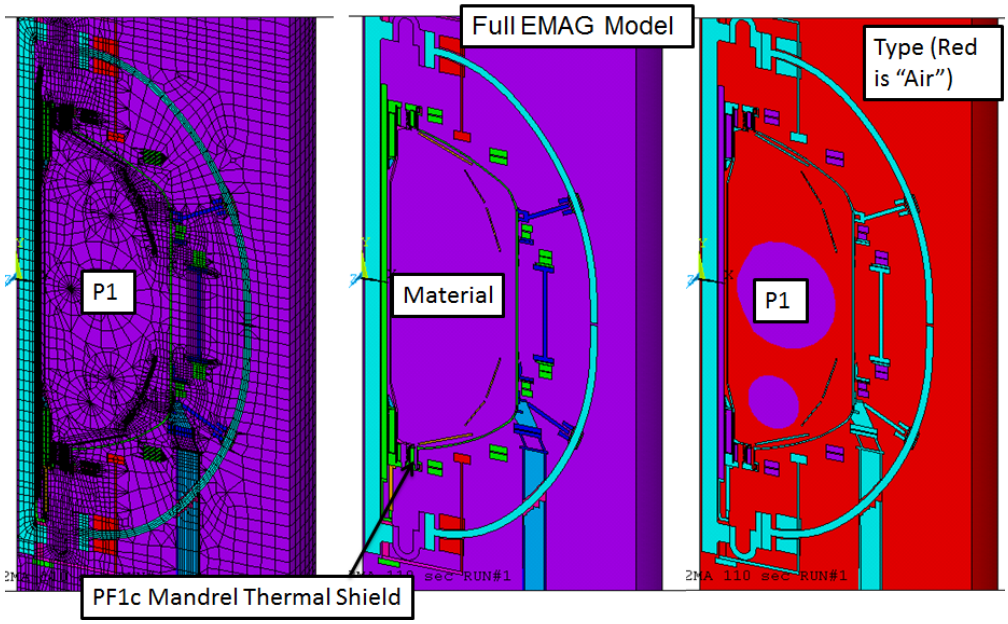


Figure 7.2-2 ANSYS Electromagnet (Disruption) Model

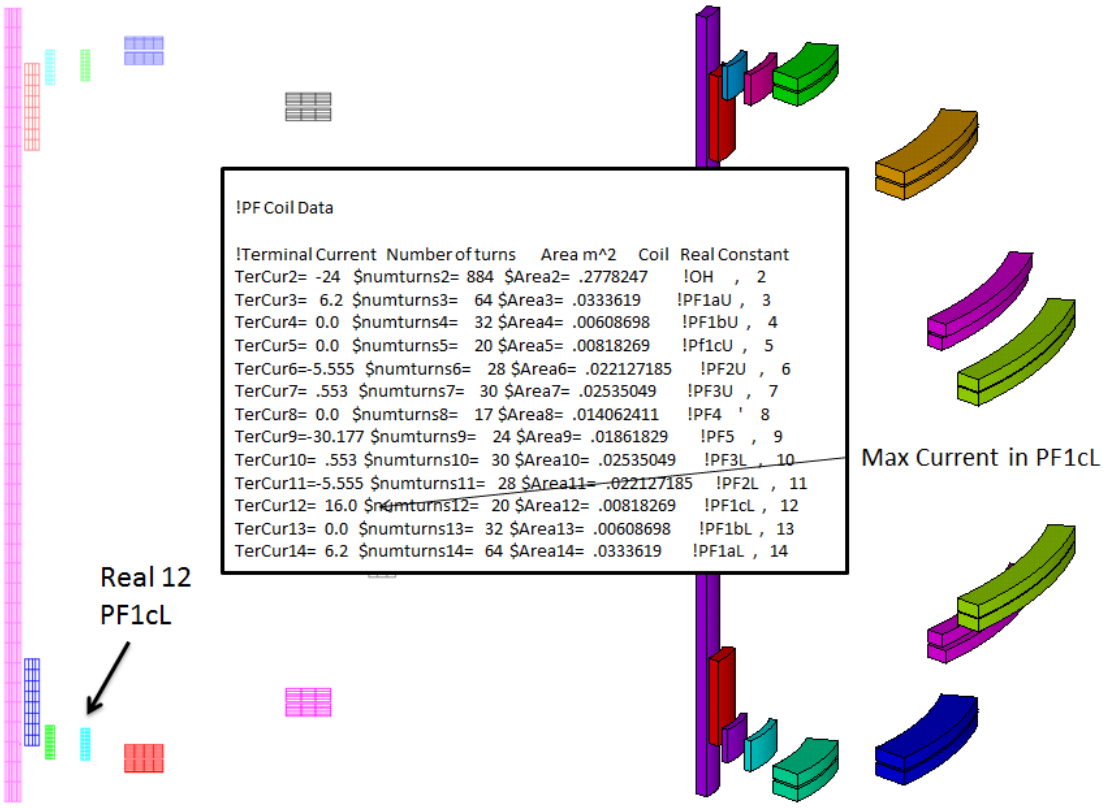


Figure 7.2-3 ANSYS Electromagnet (Disruption) Model PF Coil Input

## 8.0 Magnetic Stability, and Required Alignment Mechanism Stiffness

### 8.1 Silicon Band Centering System and Magnetic Load

The "final" concept used for the centering systems is a silicon band around the middle of the coil – See Figure 8.1-1. The load calculated in this section 8.0 is ~2000 lbs for a 5mm offset, or 10,160 lbs per inch. The band is about 1 inch high, about ¼ inch thick and effectively around 20 inches wide. The A*E/L stiffness is 1*20*300*/.137 = 43,800 lbs/in.

The stiffness of the spring needs to be above the magnetic stiffness of the off center PF1c coil. The analysis of the required stiffness was performed using similar methodology as for the PF1a and b stiffness requirements in calculation OH-PF1a/b Magnetic Stability NSTXU-CALC-133-11-0 March 2, 2010, [22]

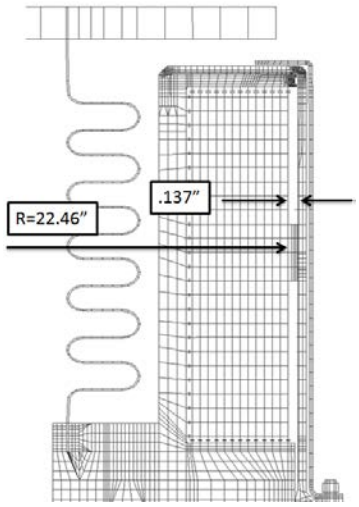

Figure 8.1-1 PF1c Centering Silicon Band

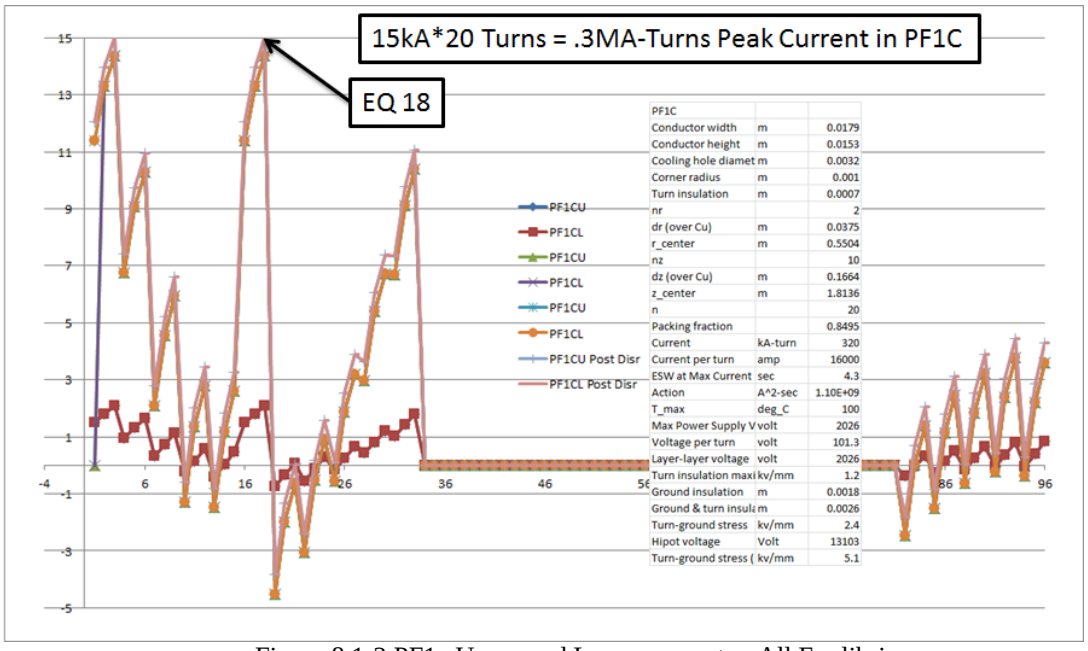

Figure 8.1-2 PF1c Upper and Lower currents - All Equlibria.

The PF1c Upper and Lower Currents are plotted in figure 8.1-2 for all design equilibria including the post disruption "equilibria". EQ 18 was chosen to represent the worst case. For this EQ, PF1c Upper and Lower were shifted laterally 5 mm and the net lateral load was computed.

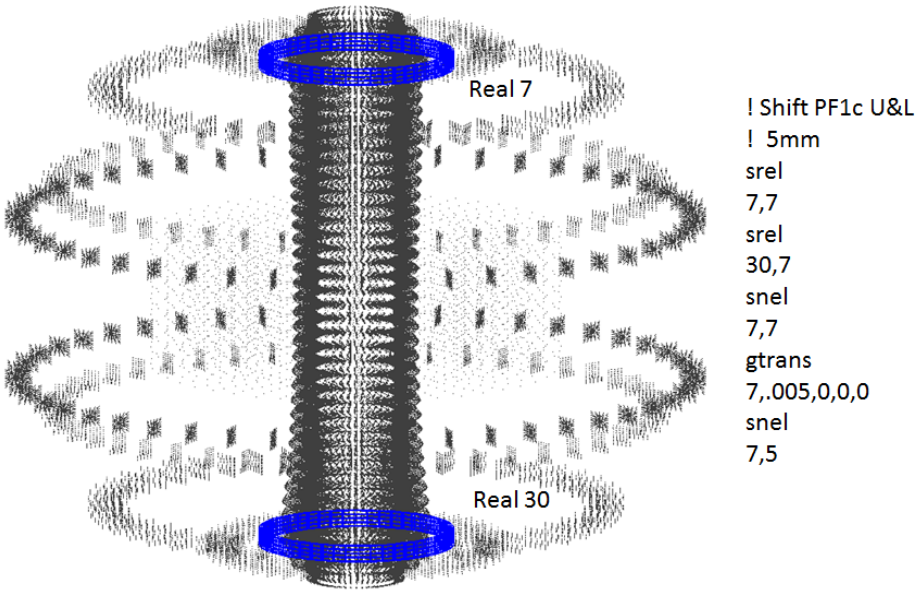


Figure 8.1-3 Biot Savart Model Showing Nodes and the PF1c Elements,

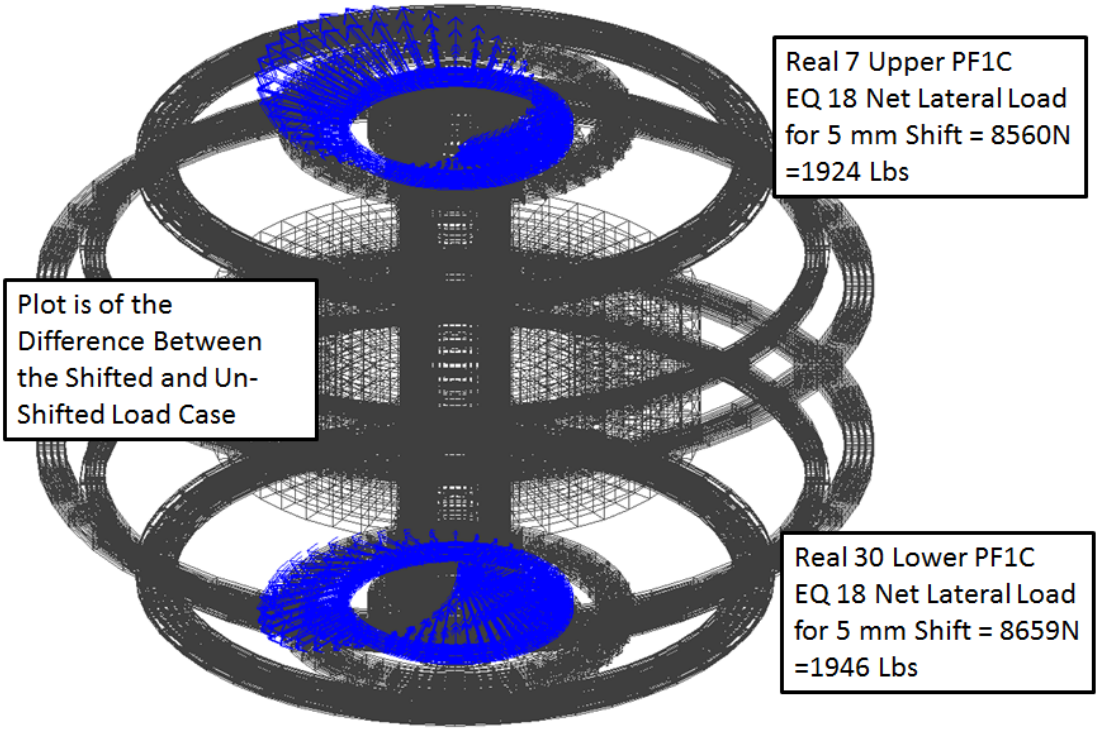


Figure 8.1-4 Biot Savart Model with Force Differences Plotted

As a result of this analysis, 2000 pound net lateral load is used to assess the lateral stiffness of any proposed centering systems.

## 8.2 Flex Shell Centering System

This describes a concept that ultimately was not used but illustrates a mechanism that would have provided the needed centering. It would not have loaded the PF1c Case outer shell. This proposed design

improvement was suggested in June 2014 by S. Raftopoulos to separate the vacuum structure from the centering structure. Radial motion of the coil when it experiences Joule heating to 100C would flex the outer shell of the case and this was a principal contributor to the closure weld stress. In the flex shell design, a thin shell is used as a spring on the outside of the coil.

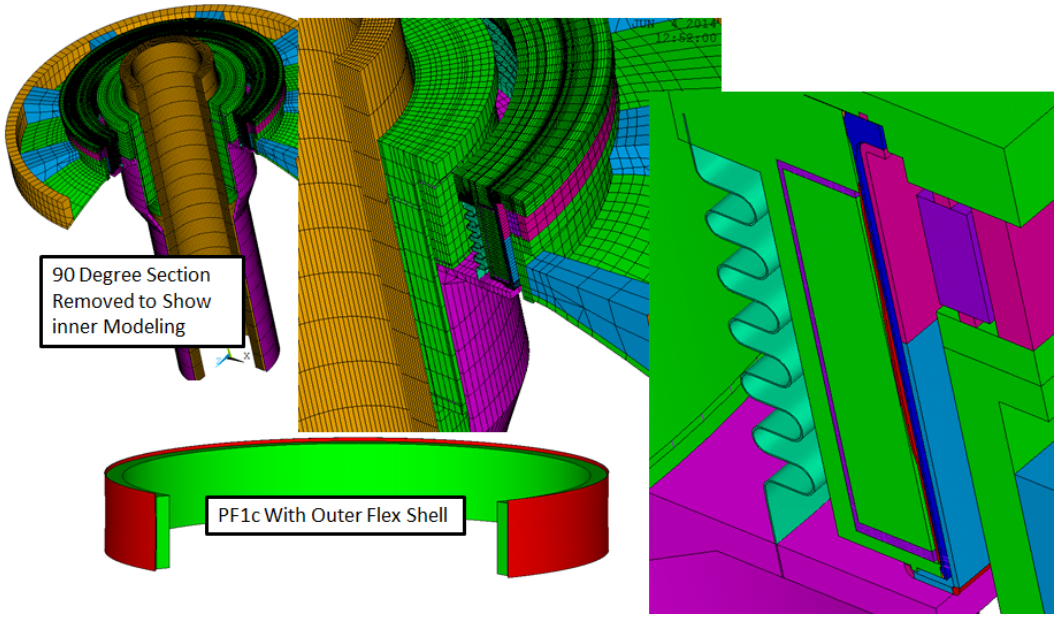


Figure 8.2-1 360 Degree Model Used to Quantify Lateral Stiffness

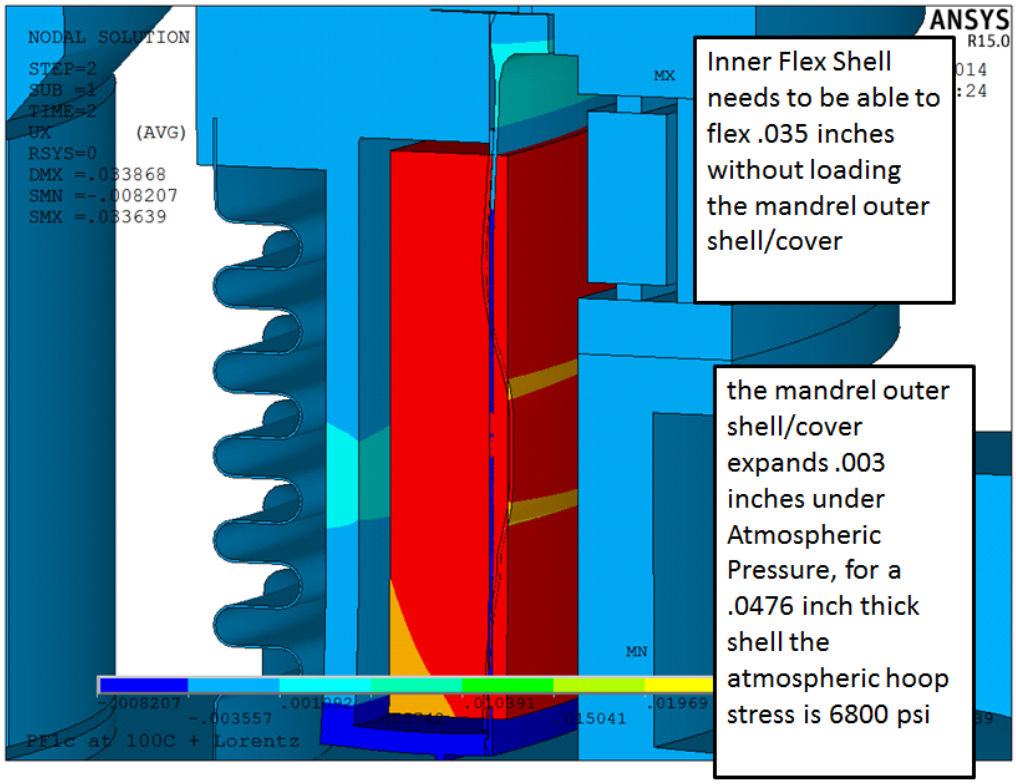


Figure 8.2-2 Coil and Flex Shell Thermal (100C) Radial Motion

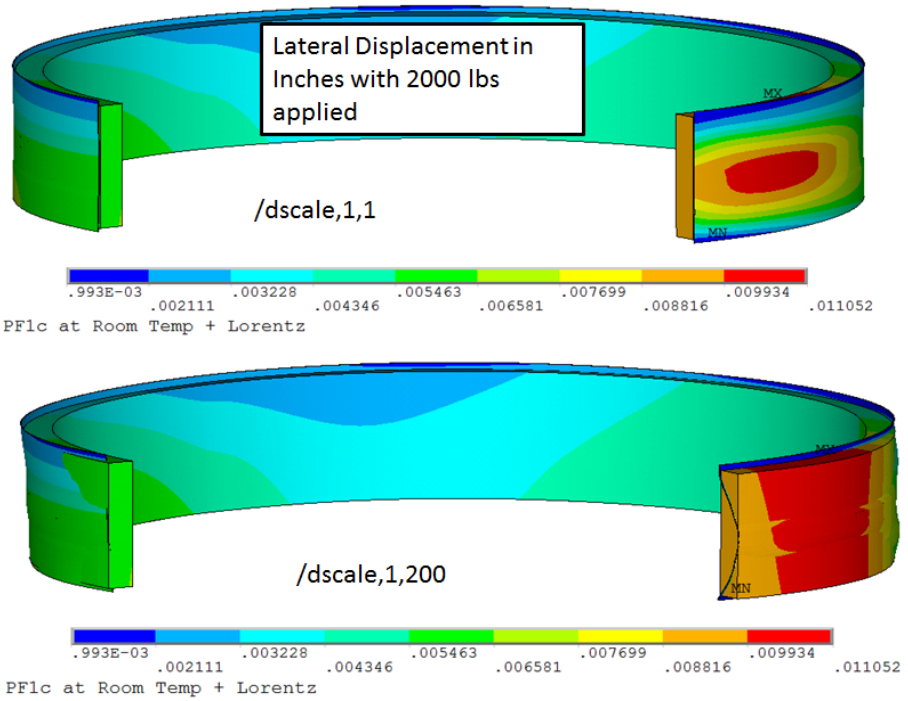


Figure 8.2-3 Lateral Displacements with 2000 Lbs Applied

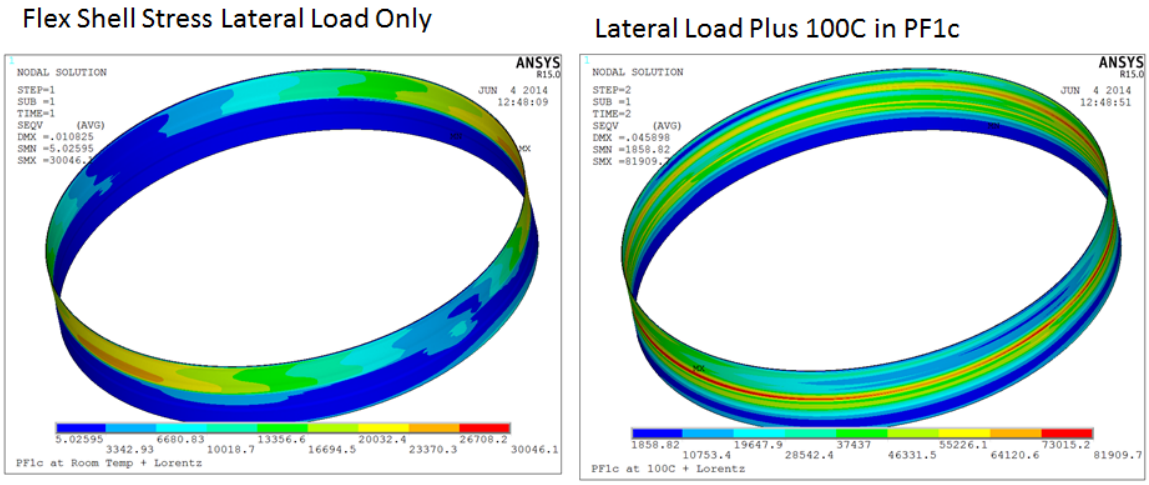


Figure 8.2-4 Stresses in Flex Shell with 2000 Lbs Lateral Load Applied

## 9.0 PF1c Mandrel/Case Outer Shell Closure Welds

The closure weld design developed from the O-ring seal detail needed for the VPI. Originally, one of the tiny lips that formed the O-ring slot, was to be welded to the 1/8 inch thick cover. This had been thinned from ¼ inch by Len Myatt [9]. The mandrel outer shell served as a centering device for the coils as they heat up and expand during the pulse. The proposed detail of 0.054 inch closure/seal weld was too small with respect to the shell thickness. All the bending stress from the shell flexure would concentrate in this weld. This was true of all inner PF mandrel shells, but was of special concern for the PF1c outer mandrel shell as this is a vacuum boundary for the machine. Shells in PF1a, and b were segmented and were welded with the small detail. This was partly intended to accommodate the closure weld, which started to

burn the insulation. For PF1a and b, the inner “nib” was being used to make the weld and this was too close to the winding pack.

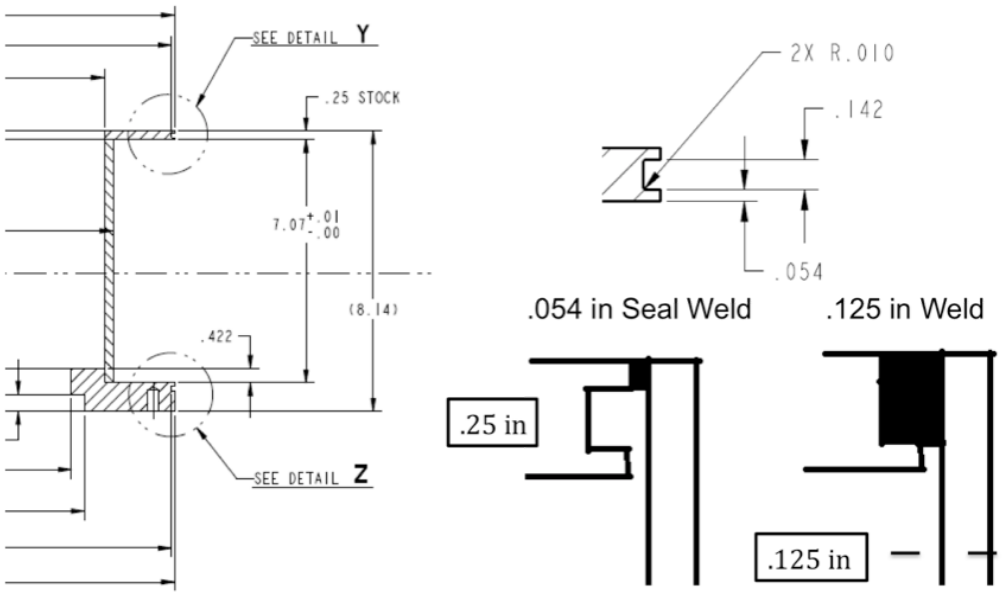


Figure 9.0-1

The shells were re-made to fit the outer nib and have been welded successfully. These welds may experience fatigue damage, but they will provide a centering force even with fatigue damage. PF1c was judged to require much more careful treatment to meet an adequate fatigue life.

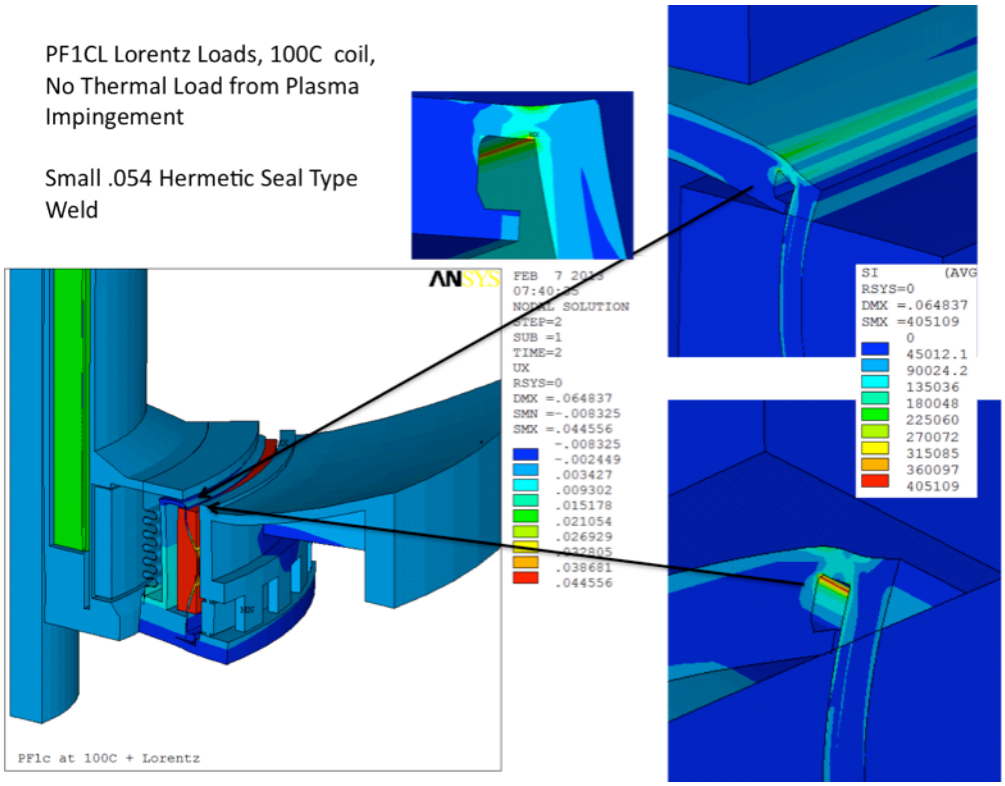


Figure 9.0-2 Stresses in the O-ring seal lips, if they are used to make the Closure Weld.

The stress in the .054-inch thick lip is 400 ksi; well above the fatigue limit.

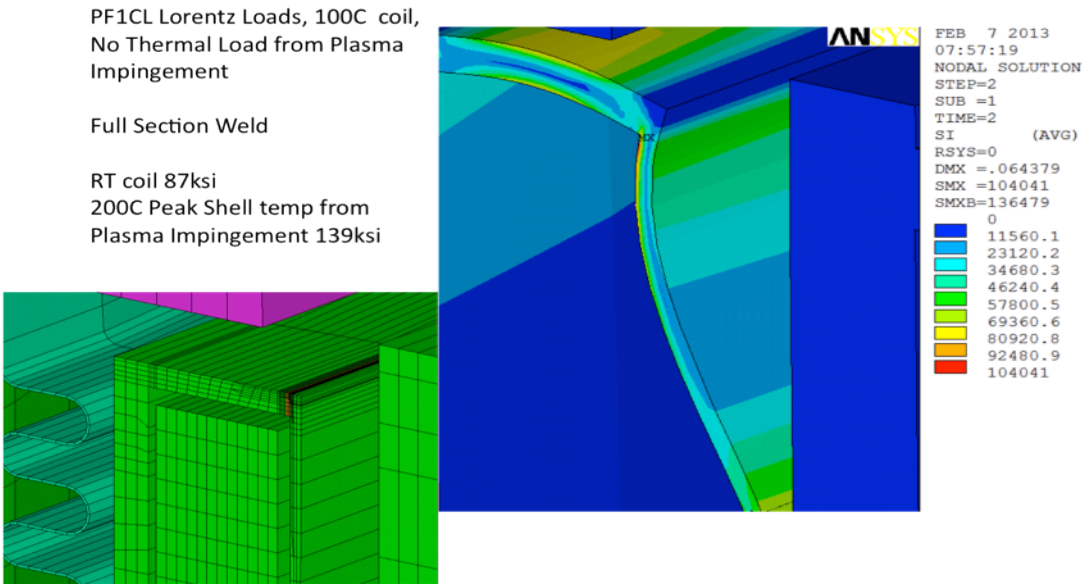


Figure 9.0-3

Figure 9.0-3 shows a full penetration weld in the ¼ inch mandrel to 1/8-inch shell weld. The full penetration weld is not feasible because of local heating of the insulation. It also has a relatively high stress at the corner, which would also be the root of the weld.

**From Len Myatt's Calculation of Record NSTXU-CALC-133-01-01**

The limiting stresses in the PF1c outer band shown in Fig. 4.3.11-9 are addressed here. High stresses at the top and bottom of the outer case wall develop because of the coil's thermal expansion. This problem is solved in the PF1a and PF1b coils by using a relatively thin outer band and limiting coil/band contact to a small region around its mid-height. Fig. 4.3.12.2-1 shows how the stress can be reduced to an acceptable level (as defined in Table 4.3.12-1) by employing a 1/8" thick outer band and limiting the extent over which the coil engages the band to <20 mm. This reduced peak stress is entered into the fatigue calculation spreadsheet and the revised CUF is 0.92 (<1.0⌉).
Fig.

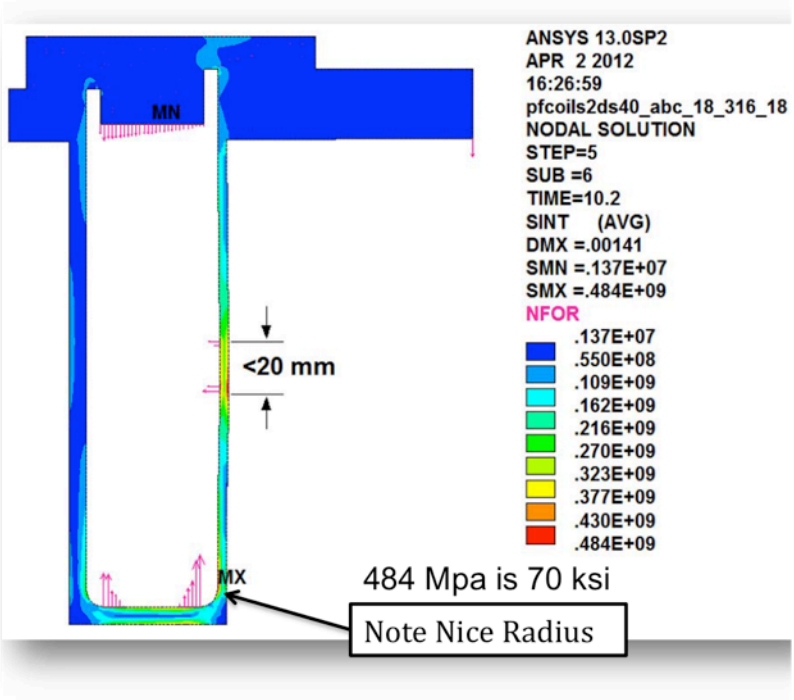


Figure 9.0-4

In Figure 9.0-4, the analysis in [9] shows a generous radius at the corner that ultimately would have to be the close-out weld. This provides an indication of what is needed to meet the fatigue criteria, but is very difficult to achieve given the manufacture and assembly sequence used.

## 9.1 Final Closure Weld Detail, July 2014, Silicon Band and Added Annular Plate

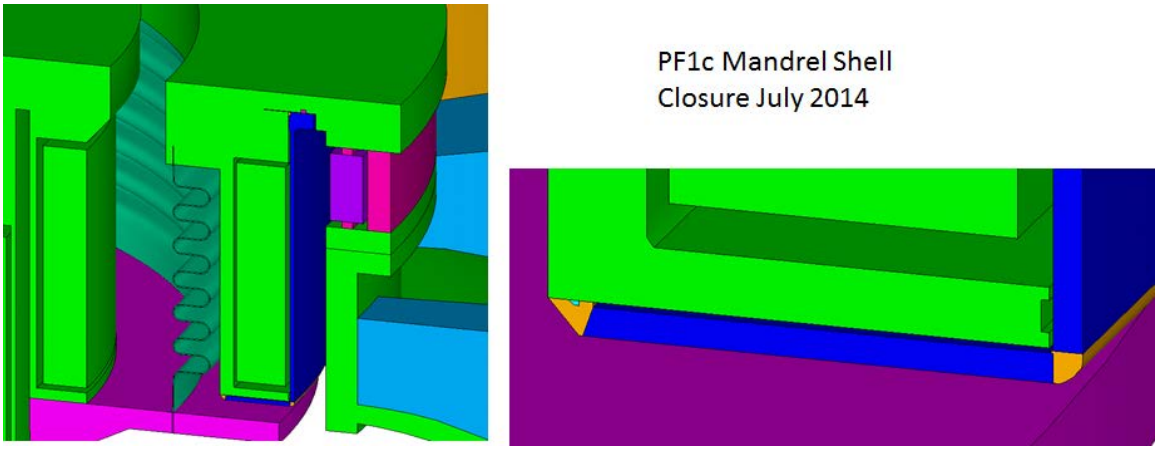


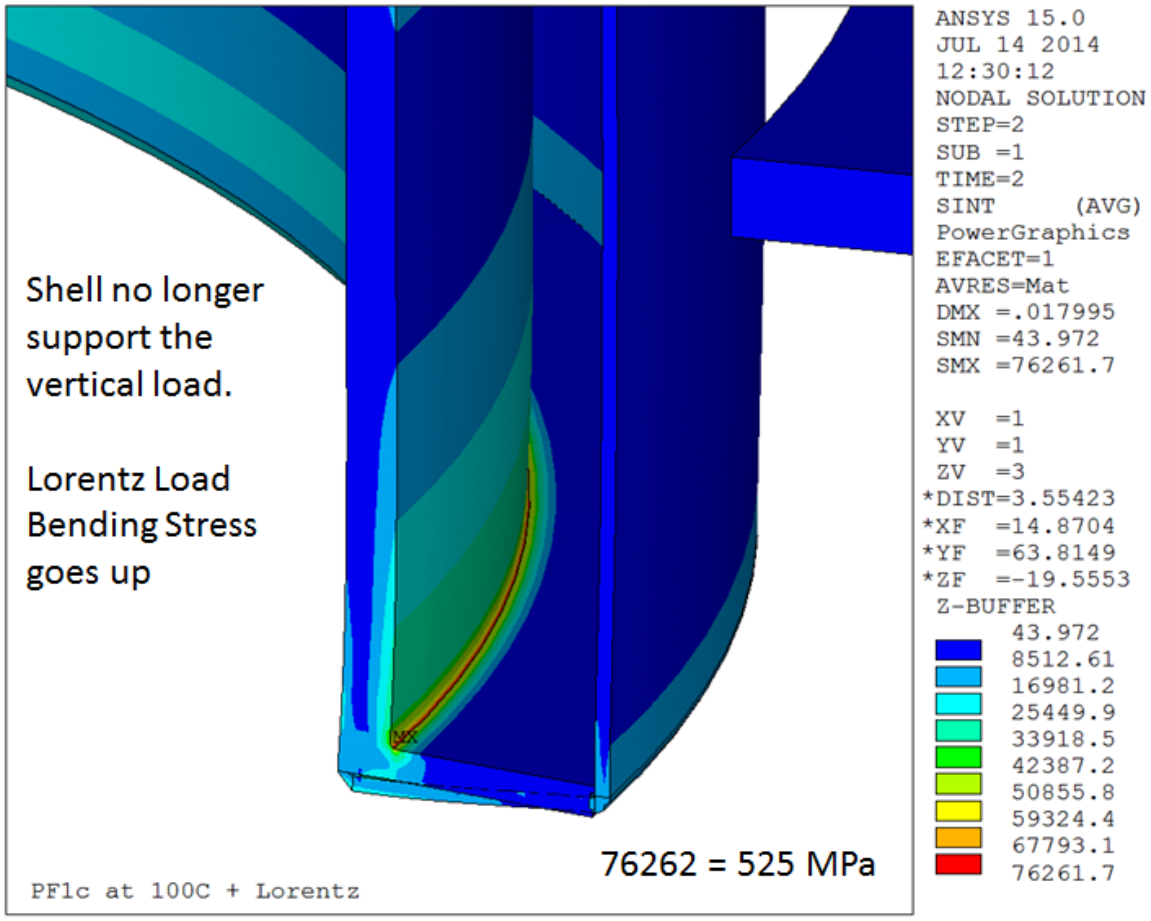

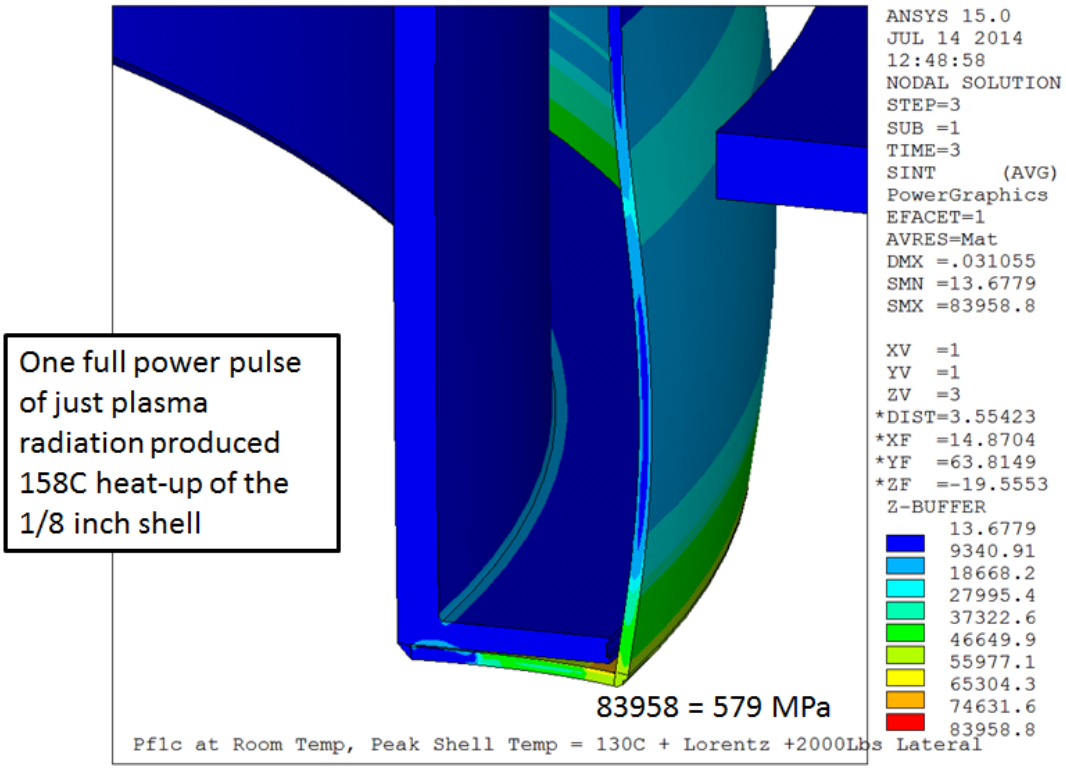
One full power pulse of just plasma radiation produced 158C heat-up of the 1/8 inch shell
ANSYS 15.0
JUL 14 2014
12:48:58
NODAL SOLUTION
STEP=3
SUB =1
TIME=3
SINT (AVG)
PowerGraphics
EFACET=1
AVRES=Mat
DMX =.031055
SMN =13.6779
SMX =83958.8
XV =1
YV =1
ZV =3
*DIST=3.55423
*XF =14.8704
*YF =63.8149
*ZF =-19.5553
Z-BUFFER
13.6779
9340.91
18668.2
27995.4
37322.6
46649.9
55977.1
65304.3
74631.6
83958.8
83958 = 579 MPa
Pf1c at Room Temp, Peak Shell Temp = 130C + Lorentz +2000Lbs Lateral

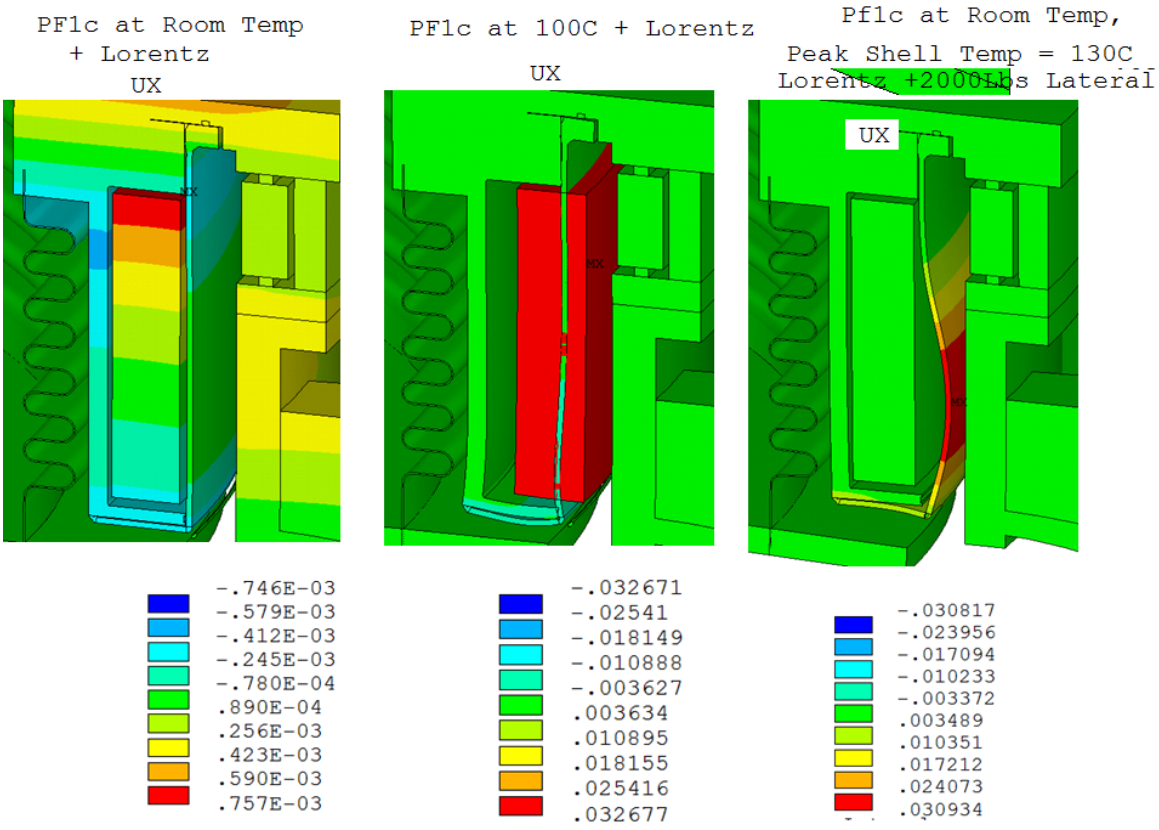
PF1c at Room Temp + Lorentz
UX
-.746E-03
-.579E-03
-.412E-03
-.245E-03
-.780E-04
.890E-04
.256E-03
.423E-03
.590E-03
.757E-03
PF1c at 100C + Lorentz
UX
-.032671
-.02541
-.018149
-.010888
-.003627
.003634
.010895
.018155
.025416
.032677
Pf1c at Room Temp,
Peak Shell Temp = 130C
Lorentz +2000Lbs Lateral
UX
-.030817
-.023956
-.017094
-.010233
-.003372
.003489
.010351
.017212
.024073
.030934

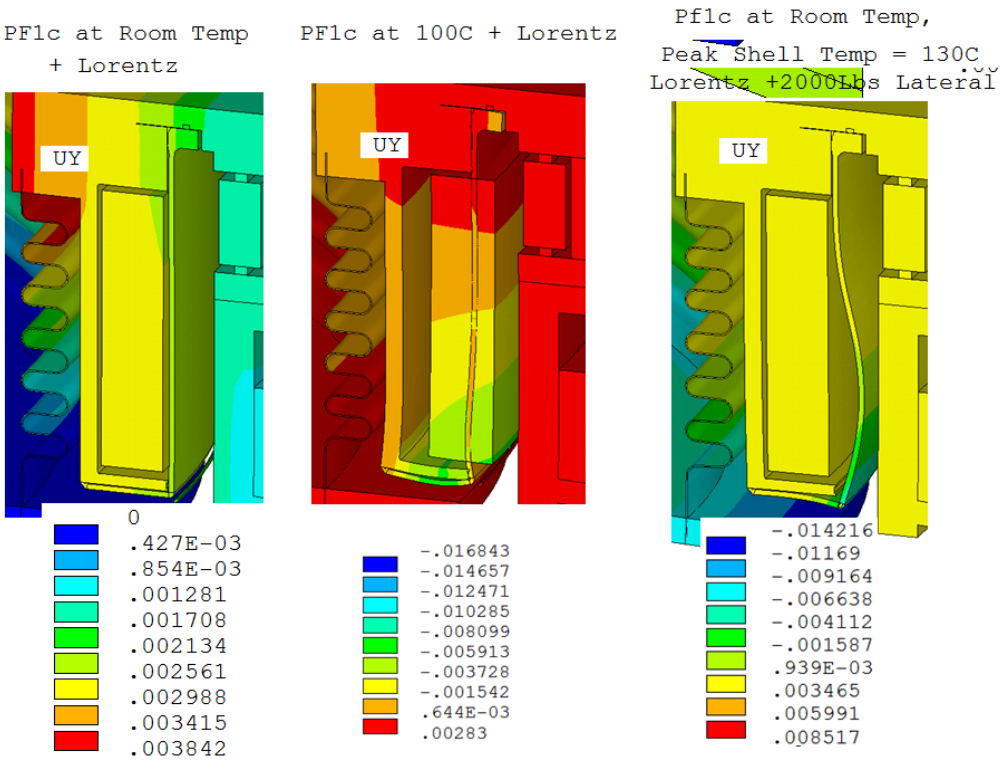
PF1c at Room Temp
+ Lorentz
UY
0
.427E-03
.854E-03
.001281
.001708
.002134
.002561
.002988
.003415
.003842
PF1c at 100C + Lorentz
UY
-.016843
-.014657
-.012471
-.010285
-.008099
-.005913
-.003728
-.001542
.644E-03
.00283
Pf1c at Room Temp,
Peak Shell Temp = 130C
Lorentz +2000Lbs Lateral
UY
-.014216
-.01169
-.009164
-.006638
-.004112
-.001587
.939E-03
.003465
.005991
.008517

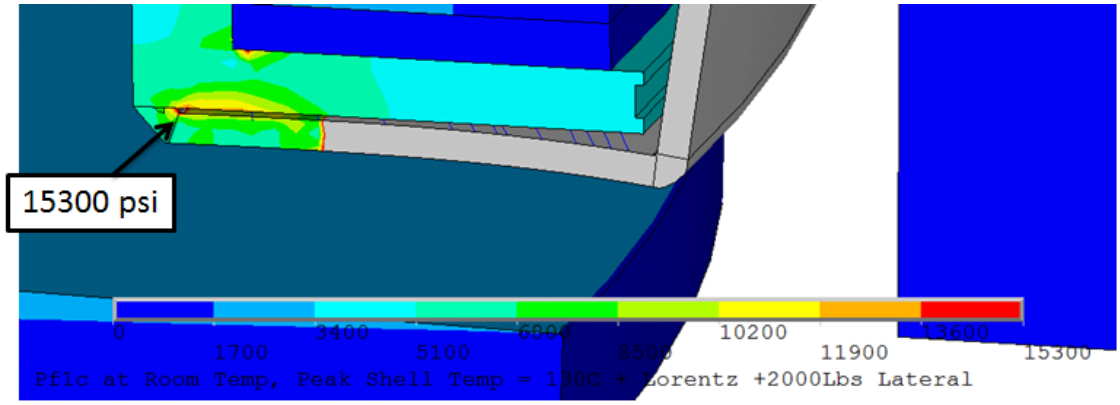
15300 psi
0
1700
3400
5100
6800
8500
10200
11900
13600
15300
Pf1c at Room Temp, Peak Shell Temp = 130C + Lorentz +2000Lbs Lateral

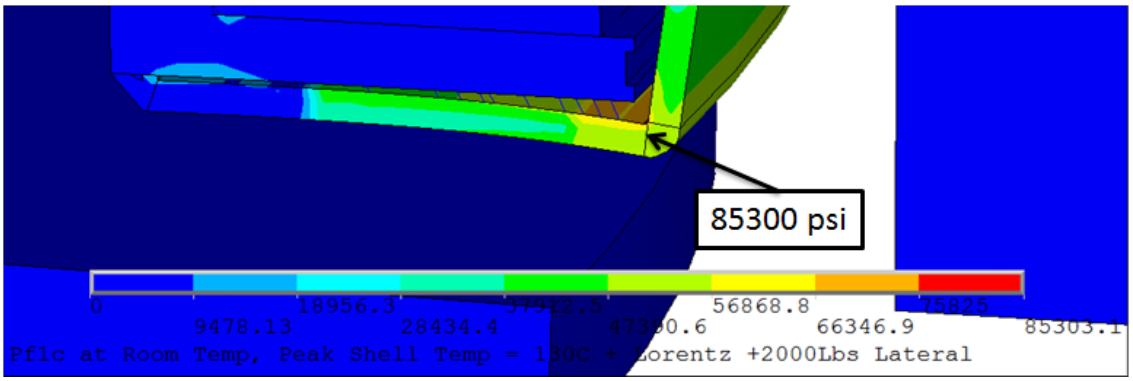
85300 psi
0
9478.13
18956.3
28434.4
37912.5
47390.6
56868.8
66346.9
75825
85303.1
Pf1c at Room Temp, Peak Shell Temp = 130C + Lorentz +2000Lbs Lateral

## 9.2 Final Closure Weld Fracture Mechanics Assessment

The PF1c closure weld is a 1/8 inch, one sided partial penetration weld with a 1/8 inch fillet. This butts against the PF1c mandrel and leaves the equivalent of a root crack. A fracture mechanics analysis of this weld was performed to provide an assessment of the potential for fast fracture of the weld and the weld's fatigue life.


Electromagnetic and Thermal Load Input

```
/title, Pf1c at Room Temp, Peak Shell
Temp = 130C + Lorentz +2000Lbs Lateral
esel,mat,17
nelem
t,all,20
f,all,fy,59782/(16*325)
f,all,fx,2000/(16*325)
esel,real,13
nelem
t,all,150
esel,real,12
nelem
t,all,200
eall
nall
solve
save
```

Figure 9.2-1 Electromagnetic and Thermal Load Input

For a one-sided partial penetration weld, the root of the weld forms an initial crack geometry that is not readily compared with handbook treatments of stress intensity factor (SIF). To calculate the SIF, the ANSYS crack tip element is used. Solid 90 elements with mid side nodes are used for the model. Wedge elements are arrayed around the crack tip. The midside nodes of the crack tip elements are positioned 1/4 of the length of the side. This causes a singularity that can be used by the KCALC ANSYS command to calculate the stress intensity factor (SIF), KI for a mode one crack, (and KII and KIII for the other modes) from a finite element model of a component including the crack tip. Higher order, 20 node elements must be used and the mid-side node of the elements at the crack tip must be positioned at one quarter the element edge length to force the appropriate discontinuity at the crack tip. Collapsed nodes must be at the crack tip. A routine in NTFTM2 takes an 8 node brick mesh and writes 20 node elements for input to ANSYS. Type 16 elements are written as crack tip elements with their collapsed nodes and ¼ point midside nodes positioned properly.

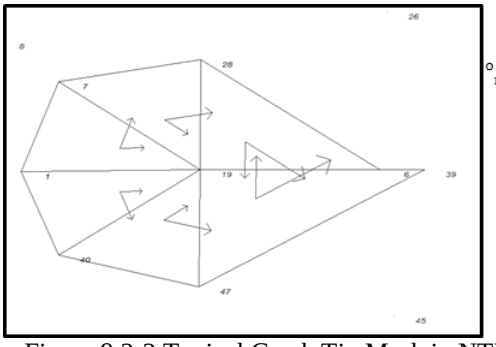

```
 El    typ mat rel     n1     n2     n3     n4     n5     n6     n7     n8
   13  16   7   0      1      7     19     19      0      0      0      0
 0.0000000E+00  0.000000000000000E+000
   14  16   7   0      7     28     19     19      0      0      0      0
 0.0000000E+00  0.000000000000000E+000
   15  16   7   0     28      6     19     19      0      0      0      0
 0.0000000E+00  0.000000000000000E+000
   34  16   7   0     47     39     19     19      0      0      0      0
 0.0000000E+00  0.000000000000000E+000
   35  16   7   0     40     47     19     19      0      0      0      0
 0.0000000E+00  0.000000000000000E+000
   36  16   7   0      1     40     19     19      0      0      0      0
 0.0000000E+00  0.000000000000000E+000
```

Figure 9.2-2 Typical Crack Tip Mesh in NTFTM2 Before Conversion to Solid 90 with Mid Side Nodes

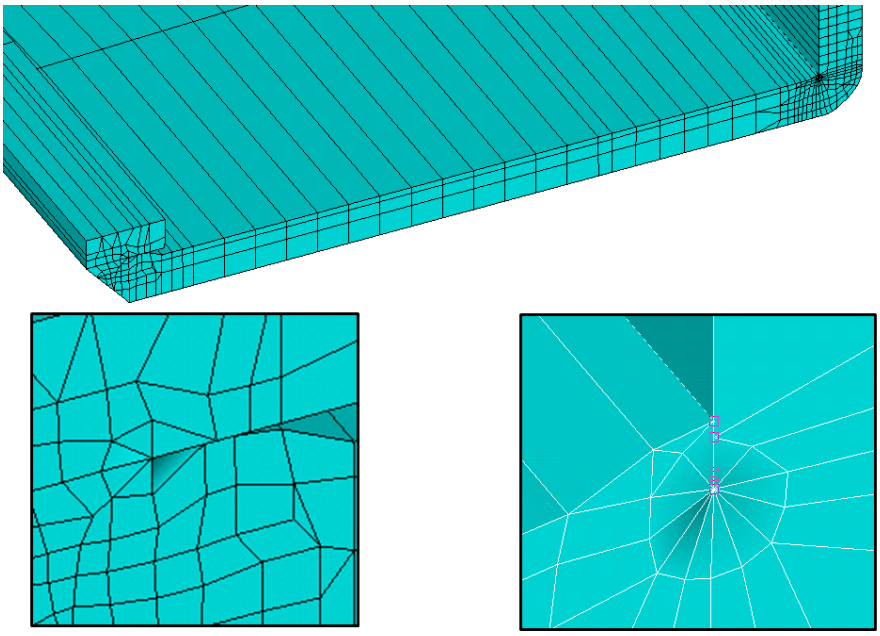

Figure 9.2-3 Typical Crack Tip at Closure Weld (Left) and Corner Weld (Right)

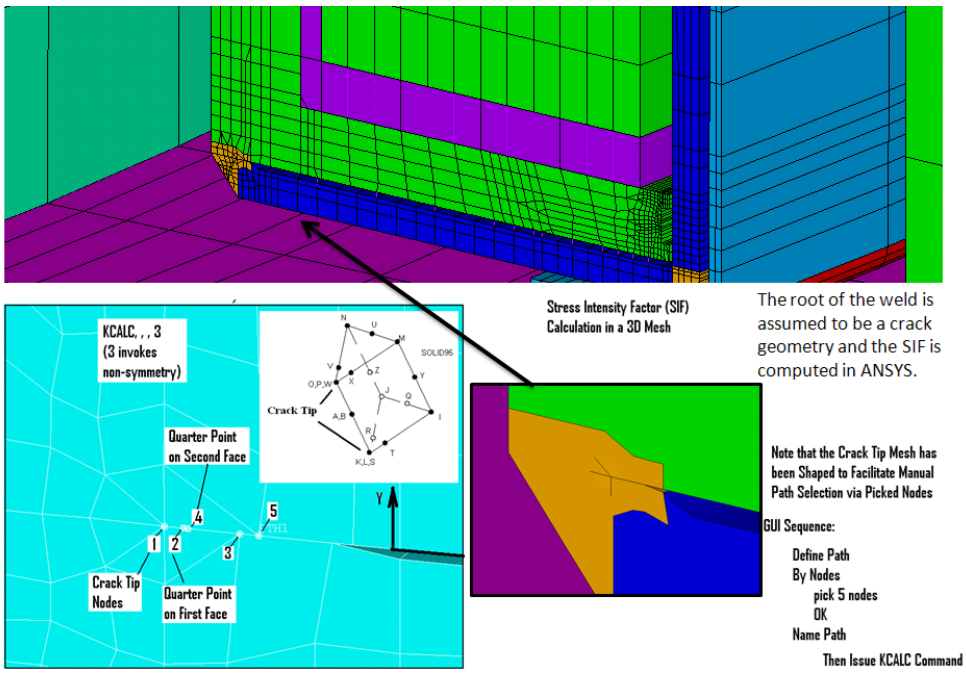


Figure 9.2-4 Fracture Mechanics Model of Closure Weld

A path is defined that describes the crack tip location. This is then used by ANSYS using the Kcalc macro – accessed from the nodal operations entry in the postprocessor GUI. This was done for a 3 dimensional model of the PF1c Case. The mesh must be re-generated for each crack depth to obtain the stress intensity factor a function of the crack depth.

The root of the weld is assumed to be a crack geometry and the SIF is computed in ANSYS. The PATH command is used to define a path with the crack face nodes (NODE1 at the crack tip, NODE2 and NODE3

on one face, NODE4 and NODE5 on the other (optional) face). A crack-tip coordinate system, having x parallel to the crack face (and perpendicular to the crack front) and y perpendicular to the crack face, must be the active RSYS and CSYS before KCALC is issued.

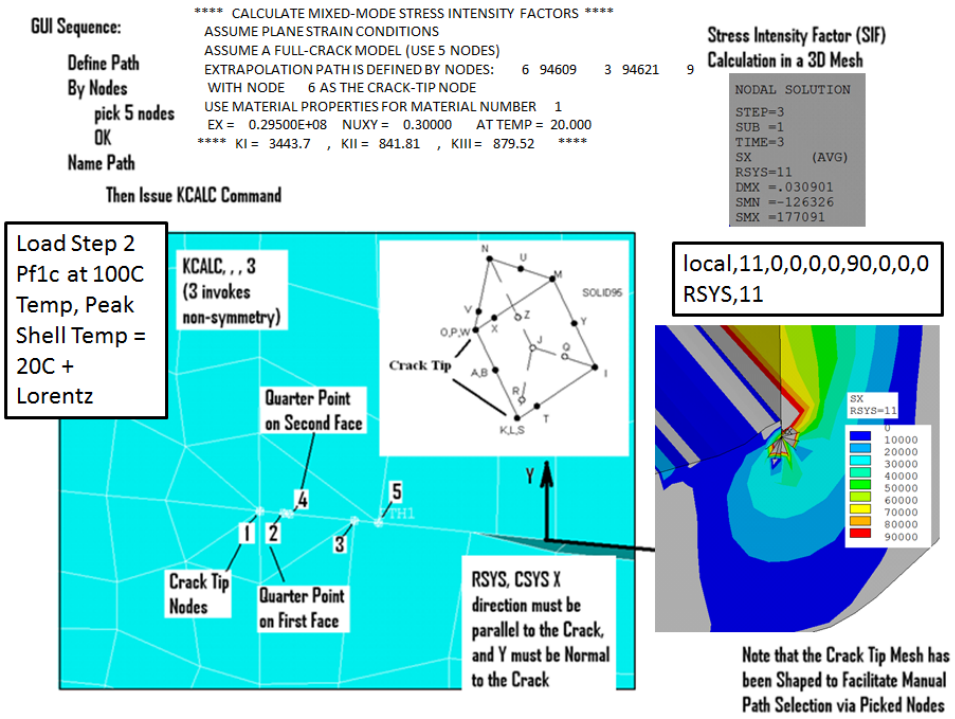


Figure 9.2-5 Fracture Mechanics ANSYS Model of Corner Weld – No CHI Heat

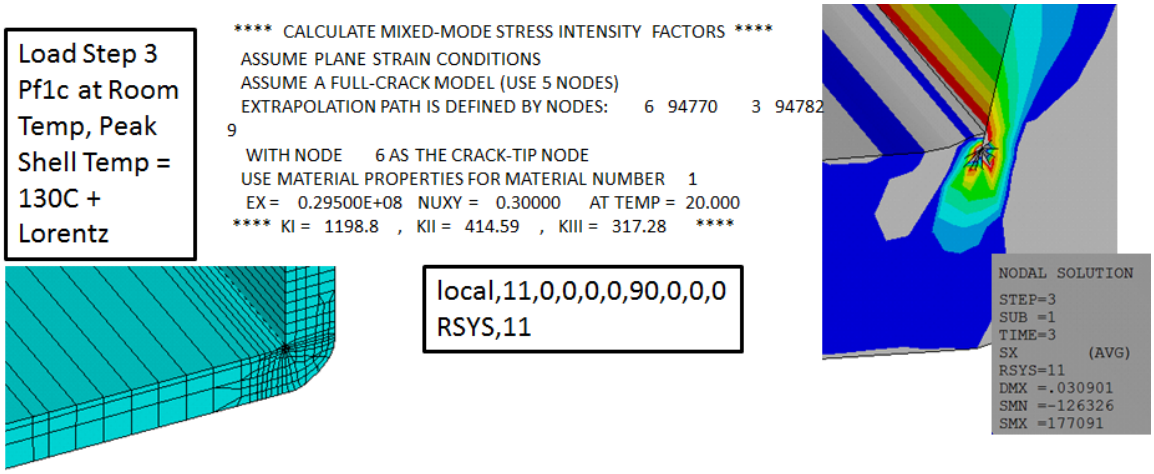


Figure 9.2-6 Fracture Mechanics ANSYS Model of Corner Weld – With CHI Heat, Peak Temp=130C

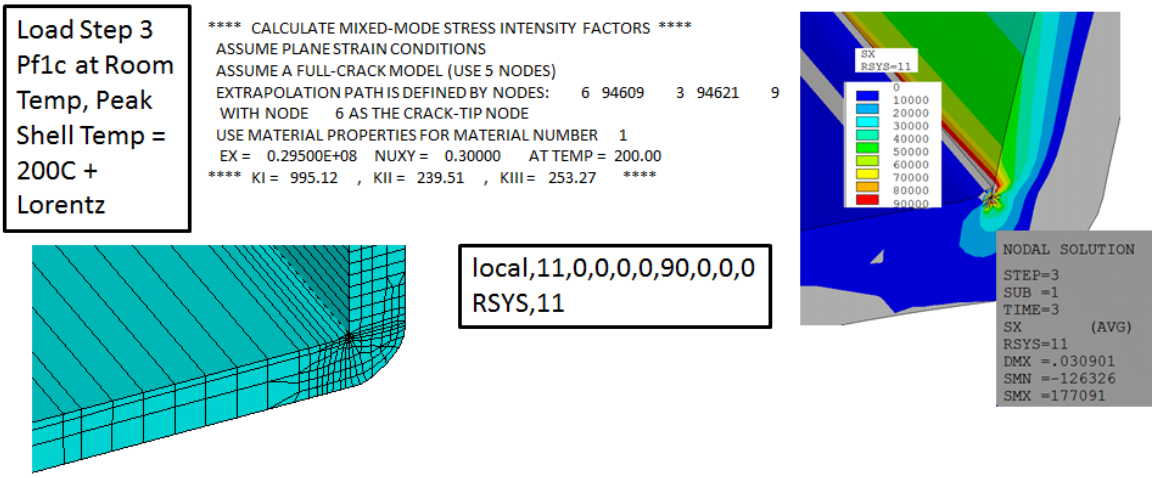


Figure 9.2-7 Fracture Mechanics ANSYS Model of Corner Weld – With CHI Heat, Peak Temp=200C

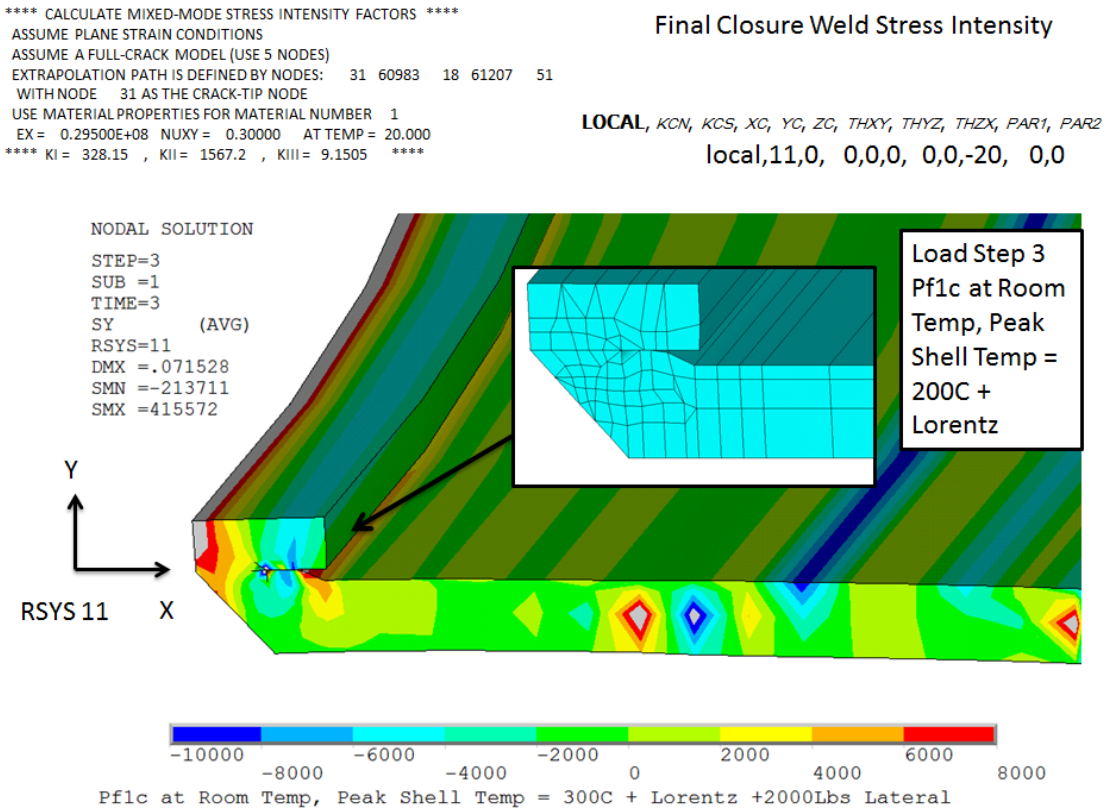


Figure 9.2-8 Fracture Mechanics ANSYS Model of Closure Weld – With CHI Heat, Peak Temp=200C

The model uses in-lb units so the 3135.9 stress intensity factor is in psi*root(in) to convert this to MPa root (m), the SIF is 3135.9*(1/39.37)^.5 *6895/1e6 = 3.44 MPa-root (m). This is quite low, but corresponds to a case peak temperature of 130C. The analysis was re-run with a peak temperature of 200C. The stress intensity went up slightly to 3125.6 psi-root(in).

The features in ANSYS that calculate stress intensity factors have been exercised. ANSYS can calculate the stress intensity value at the two postulated weld cracks.

$da/dN=C \times (\Delta K)^m$

Where, C and m are material (Paris) constants determined by testing

a is physical crack length
N is number of cycles
ΔK is stress intensity factor range
ΔK = YΔσ (π a)1/2
Δσ is the alternating component of the maximum principal tensile stress
Y is the stress concentration factor for a given crack geometry (based on an elastic calculation without plasticity corrections, see MC 2.6.3)

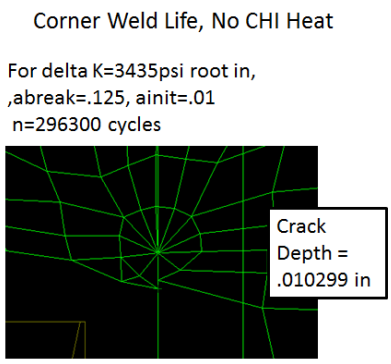


**Table 2. $\Delta K_{th}$ values and Paris equation parameters ($da/dN = C(\Delta K)^n$) at different temperatures for $R = 0.1$ (units are MPa√m and m/cycle)**

| Temperature (°C) | $\Delta K_{th}$ | $C$ | $n$ |
|---|---|---|---|
| 25 | 8.2 | $3.1\times10^{-13}$ | 3.3 |
| 475 | — | $6.8\times10^{-12}$ | 2.8 |
| 500 | 11.8 | $6.8\times10^{-12}$ | 2.4 |
| 600 | 6.5 | $5.5\times10^{-12}$ | 2.9 |
| 700 | 5.1 | $2.6\times10^{-11}$ | 2.6 |
| 800 | – | $2.4\times10^{-12}$ | 5.1 |

```
! Simple da/dn integral for 304 Stainless Steel
let t=.125/39.37
let ainit=.010299/39.37
let m=2.95
let c=5.43e-12
let fractTough=100
let deltak= 3443.7*6895/1e6/39.37^.5
let a=ainit
let abreak=t-ainit
Zoom
let counter = 0
!for i= 1 to 10000

do
!deltak is linear in crack length
let delk=deltak/ainit*a
!assume the delta k scales with the orig thick/remaining
thickness
let delk=delk*(t+ainit)/(t+ainit-a)
let i=i+1
let counter=counter+1
let dadn=c*delK^m
let a=a+dadn
if counter = 100 then
print i;",";delk;","; a
let counter = 0
end if
if a>abreak or delk>fractTough then exit do
!next i
loop
print "Cracked Through"
end
```

Figure 9.2-9 Life Prediction of Corner Weld .01 inch flaw – No CHI Heat

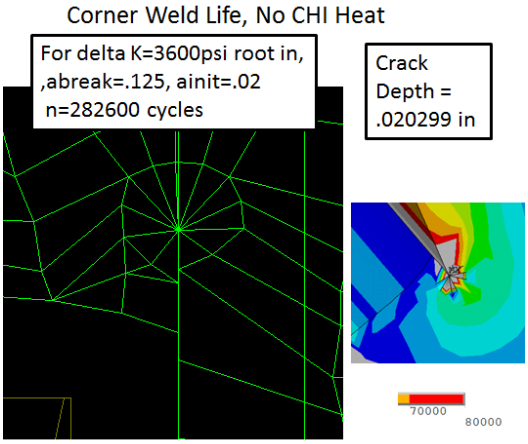


```
**** CALCULATE MIXED-MODE STRESS INTENSITY FACTORS ****
 ASSUME PLANE STRAIN CONDITIONS
 ASSUME A FULL-CRACK MODEL (USE 5 NODES)
 EXTRAPOLATION PATH IS DEFINED BY NODES:    6  94864    3  94876    9
  WITH NODE     6 AS THE CRACK-TIP NODE
 USE MATERIAL PROPERTIES FOR MATERIAL NUMBER   1
  EX =  0.29500E+08  NUXY =  0.30000    AT TEMP =  20.000
**** KI =  3600.1  ,  KII =  906.59  ,  KIII =  917.83   ****
```

```
! Simple da/dn integral for 304 Stainless Steel
let t=.125/39.37
let ainit=.020299/39.37
let m=2.95
let c=5.43e-12
let fractTough=100
let deltak= 3600.0*6895/1e6/39.37^.5
let a=ainit
let abreak=t-ainit
let counter = 0
!for i= 1 to 10000

do
!deltak is linear in crack length
let delk=deltak/ainit*a
!assume the delta k scales with the orig
thick/remaining thickness
let delk=delk*(t-ainit)/(t-ainit-a)
let i=i+1
let counter=counter+1
let dadn=c*delK^m
let a=a+dadn
if counter = 100 then
print i;",";delk;","; a
let counter = 0
end if
if a>abreak or delk>fractTough then exit do
!next i
loop
print "Cracked Through"
end
```

Figure 9.2-10 Life Prediction of Corner Weld .02 inch flaw – No CHI Heat

The worst of the weld stress intensities with a .02-inch initial flaw produces a life of 282,600 cycles.

## 9.3 Closure Weld Configuration Studies

These are concepts made from the O-ring seal geometry and ultimately not used. Either the stresses were too high or they were expected to overheat the coil insulation

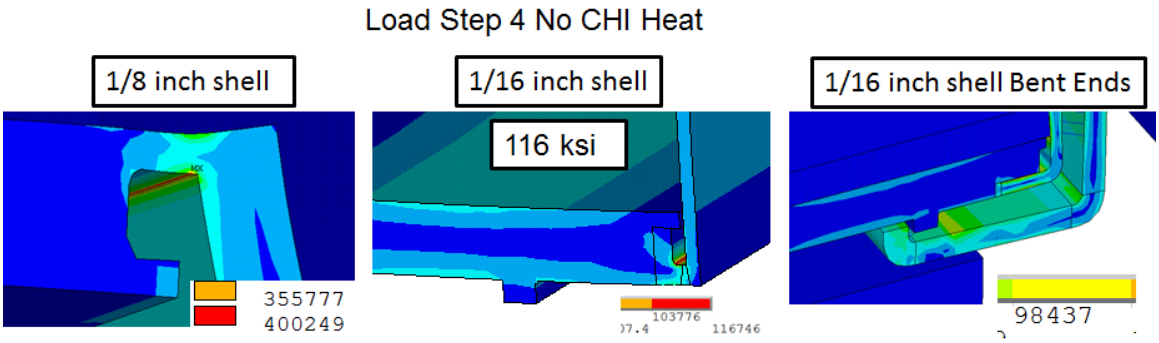


Figure 9.3-1 Early Closure Weld Concepts

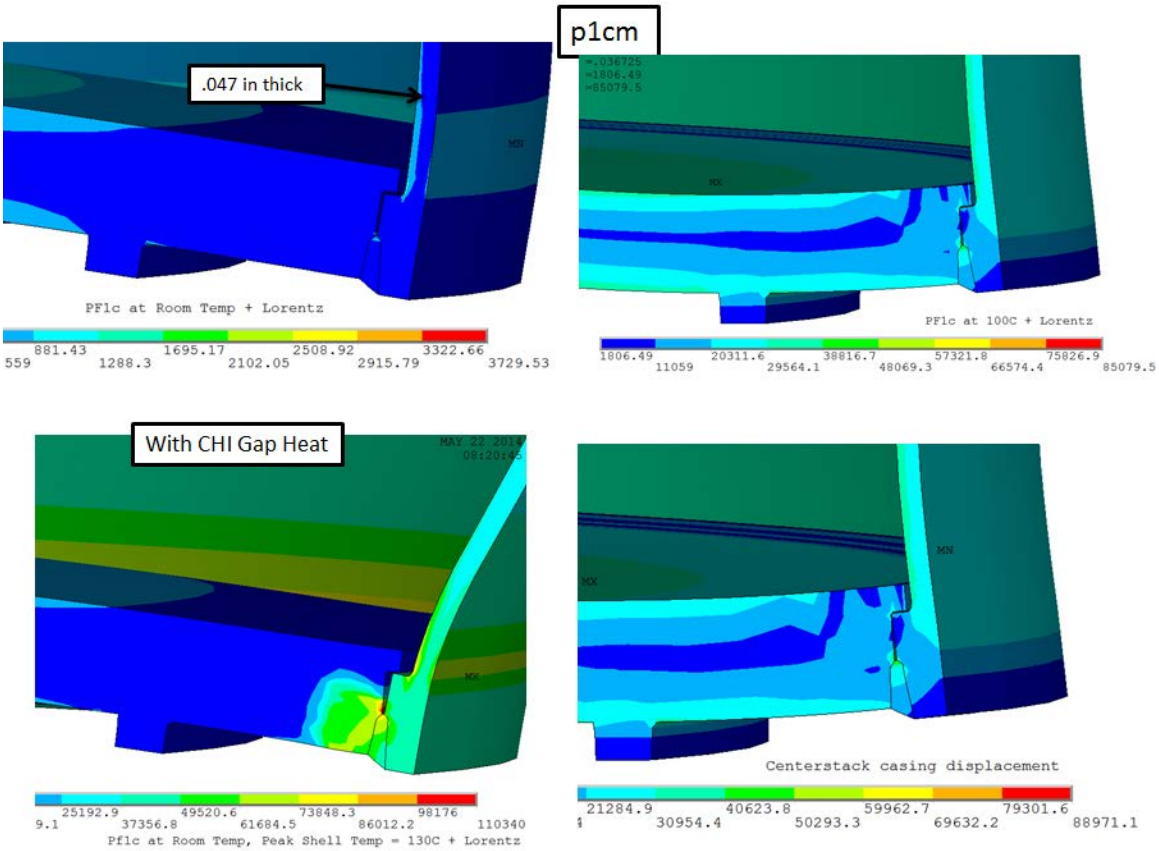


Figure 9.3-2 More Closure Weld Concepts

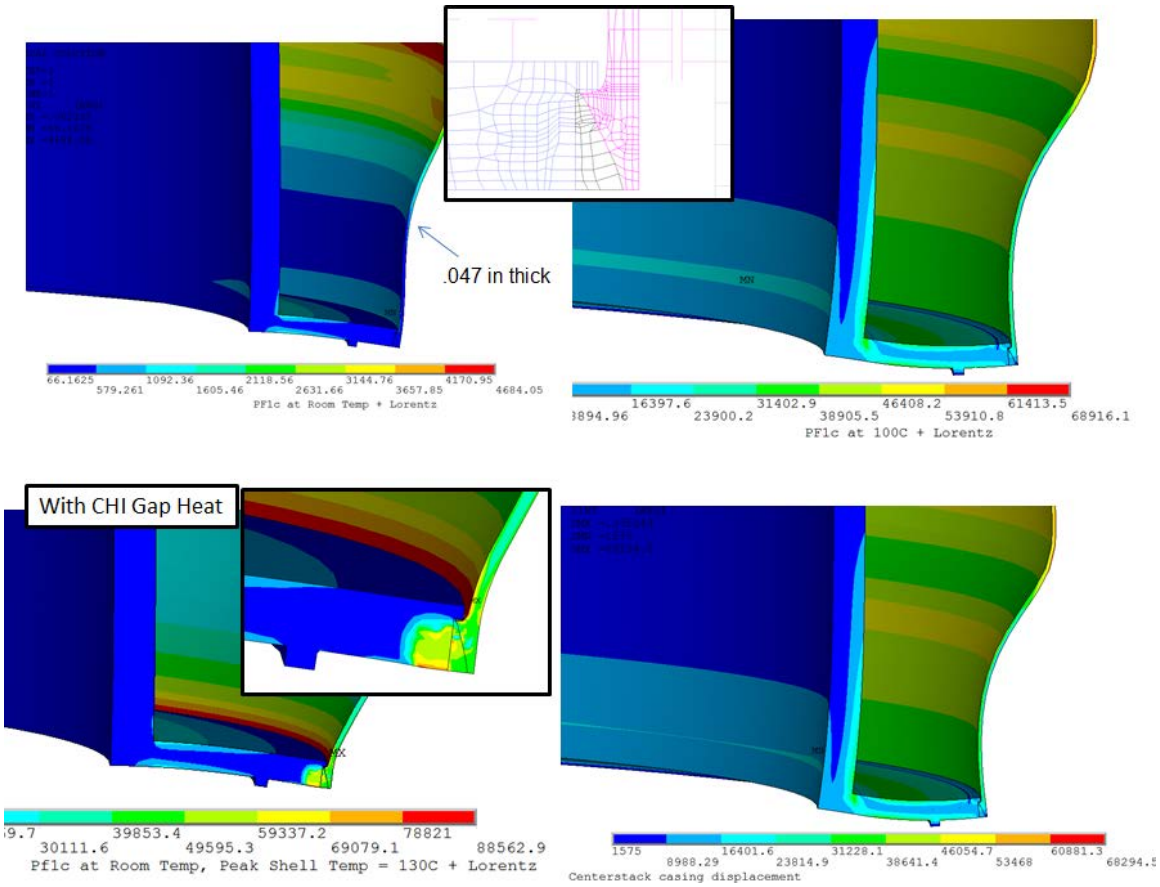


Figure 9.3-3 -Full Penetration Closure Weld

The weld detail shown in figure 9.3-3 was sure to burn the coils insulation.

## 10.0 PF1c Mandrel Shell and Heat Shield Thermal Transients

The thermal performance of the PF1c case and thermal shield is analyzed using a True Basic code that is included in Appendix E. Results of this program are tabulated below:

Table 10.0-1

| Shot Sequence | Pulse Time | Radiation Shield Thickness | Can Thickness | Figure | Shield Temp | Can Temp |
|---|---|---|---|---|---|---|
| 1 Full Power Rad Only | 5 | None | 1/8$^{th}$ in. | Figure 6.5.1-1 | NA | 430K 158C |
| 8 Full Power Rad Only | 5 | None | 1/8$^{th}$ in. | Figure 6.5.1-1 | NA | 248 C |
| 2 Full Power Shots | 1 sec | 1/16$^{th}$ inch | 1/8$^{th}$ in. | Figure 10.0-1 | 633K | 332K 60C |
| 2 Full Power Shots | 1sec | 1/8$^{th}$ inch shell | 1/8$^{th}$ in. | Figure 10.0-1 | 480K | 331K 60C |
| 2 Full Power Shots | 5 sec | Two .03” One .0625” | 1/8$^{th}$ in. | Figure 10.0-3 | 1873K | 379K 107C |
| 2 Full Power Shots | 5 sec | Two .03” One .125” | 1/8$^{th}$ in. | Figure 10.0-4 | 1178K | 352K, 80C |

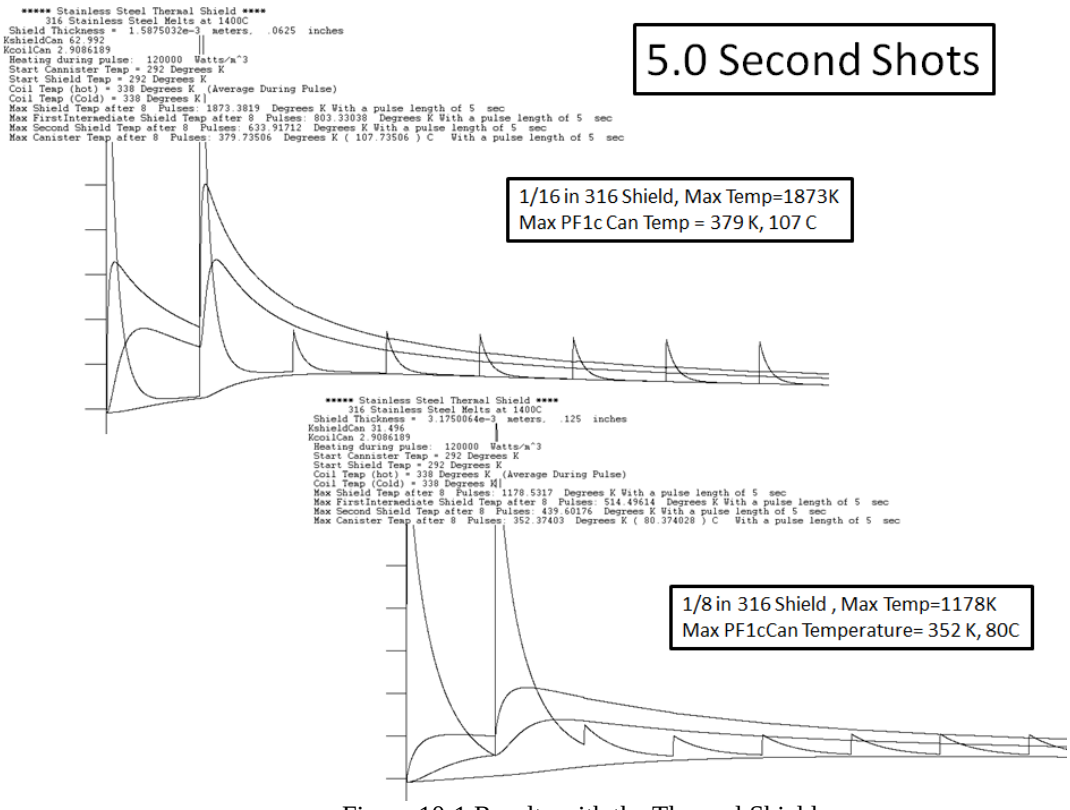


Figure 10-1 Results with the Thermal Shield

Appendix E is set up to produce the upper plot in figure 10.0-1.

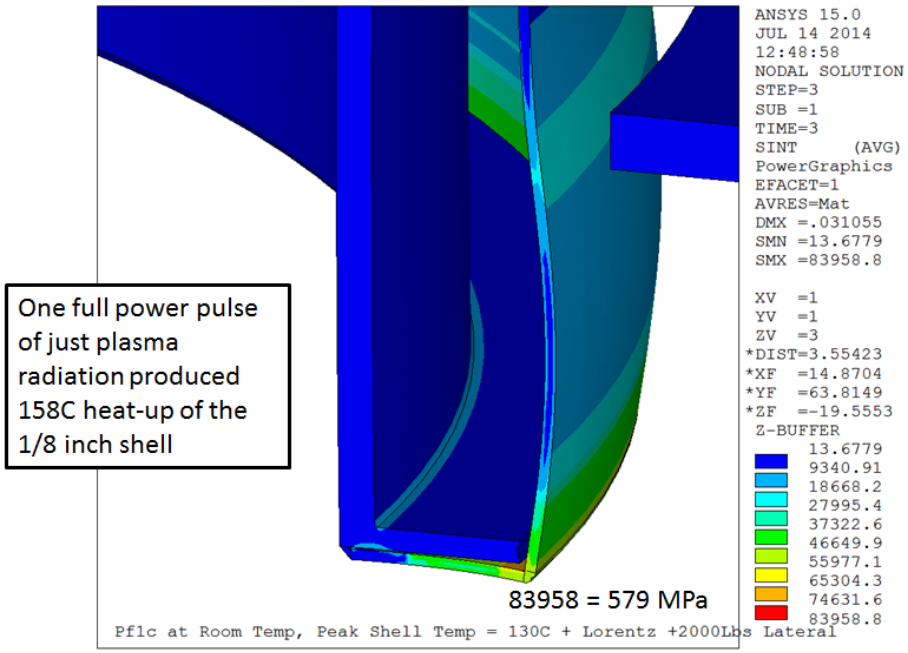


Figure 10-2

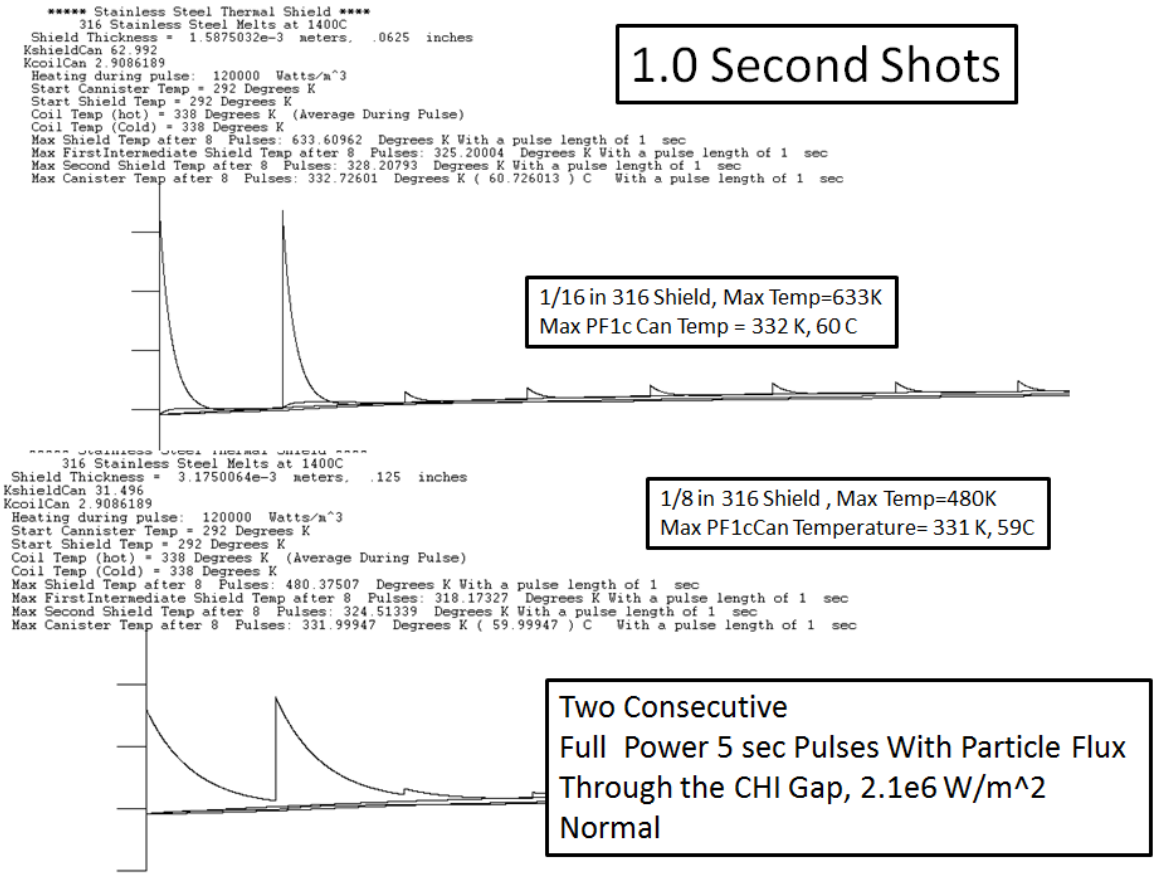


Figure 10-3

## 10.1 With Thermal Shield

Len Myatt recommended an 1/8 inch outer shell. This leaves the design with 1/8th of an inch for a thermal shield. The first option investigated was 1/16 inch of Molybdenum and a few layers of SST shim stock like was used on the C-Mod outer divertor. This is geometrically tight. The shield is also the electrode for the CHI so the shield design may be challenging. It is not needed early in the operation of the machine, but may be needed later.

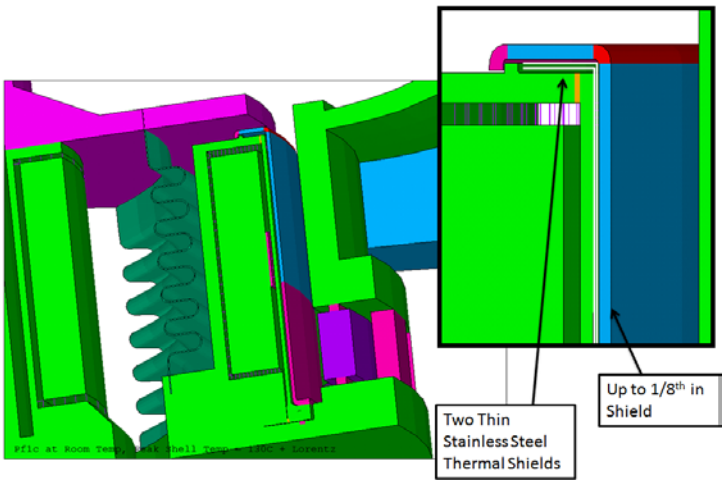


Figure 10.1-1 Thermal Shield Concept

### 10.1.1 Moly Shield

Again, no shield is being installed at initial start-up of the Upgrade. The following calculations are being included for future reference.

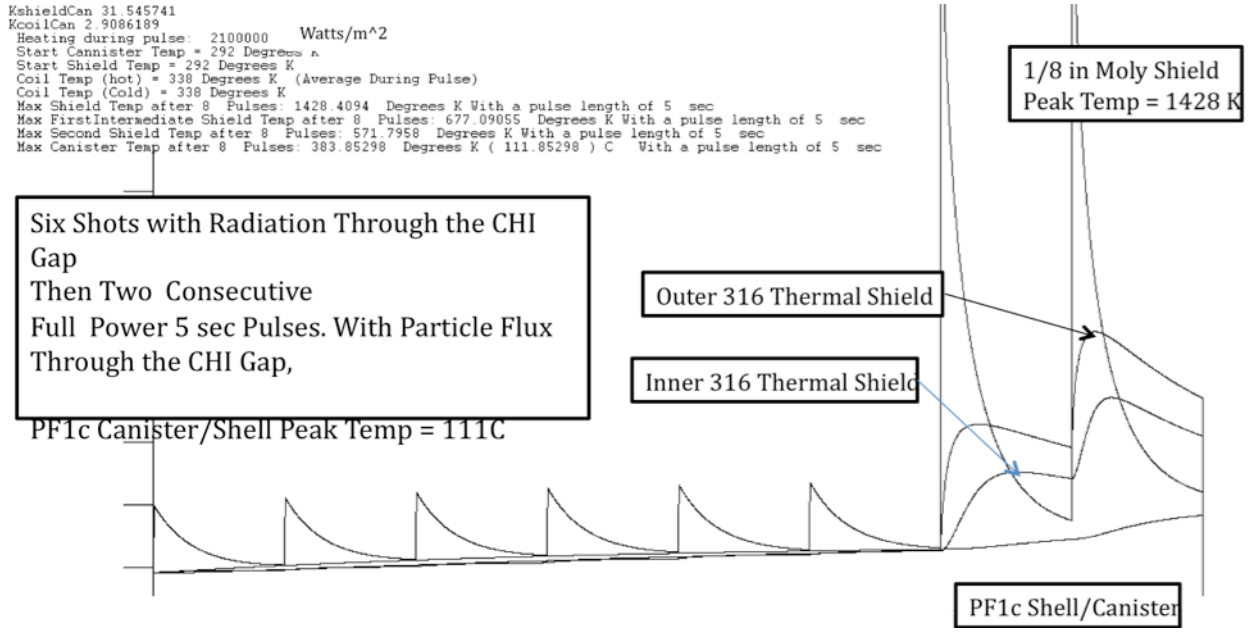


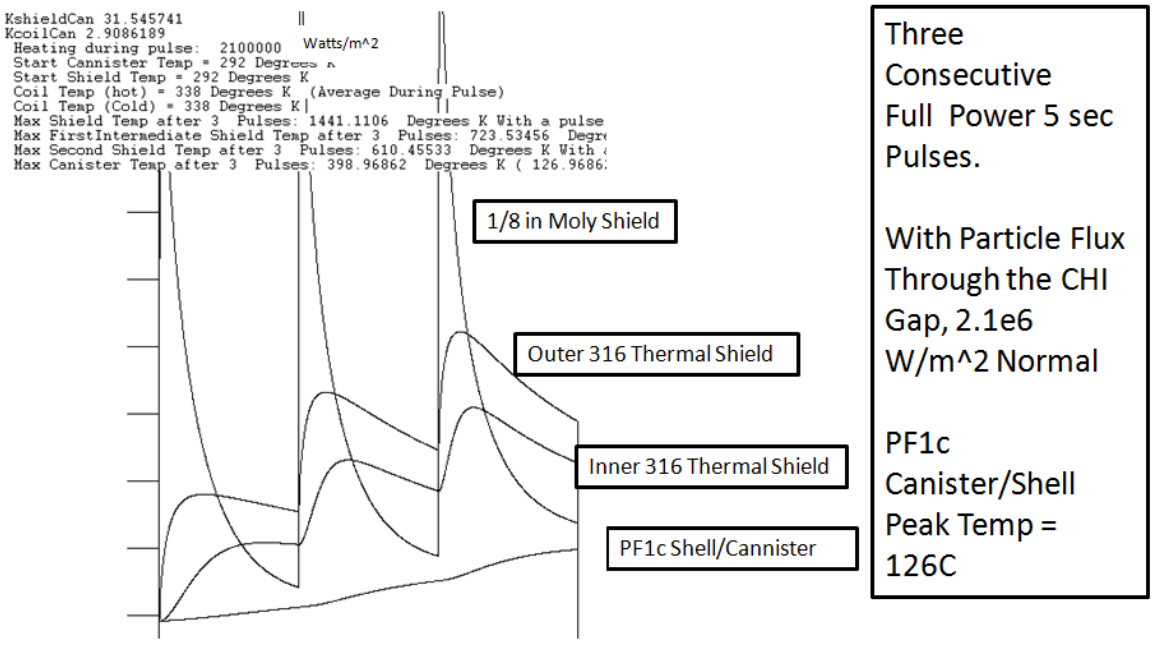

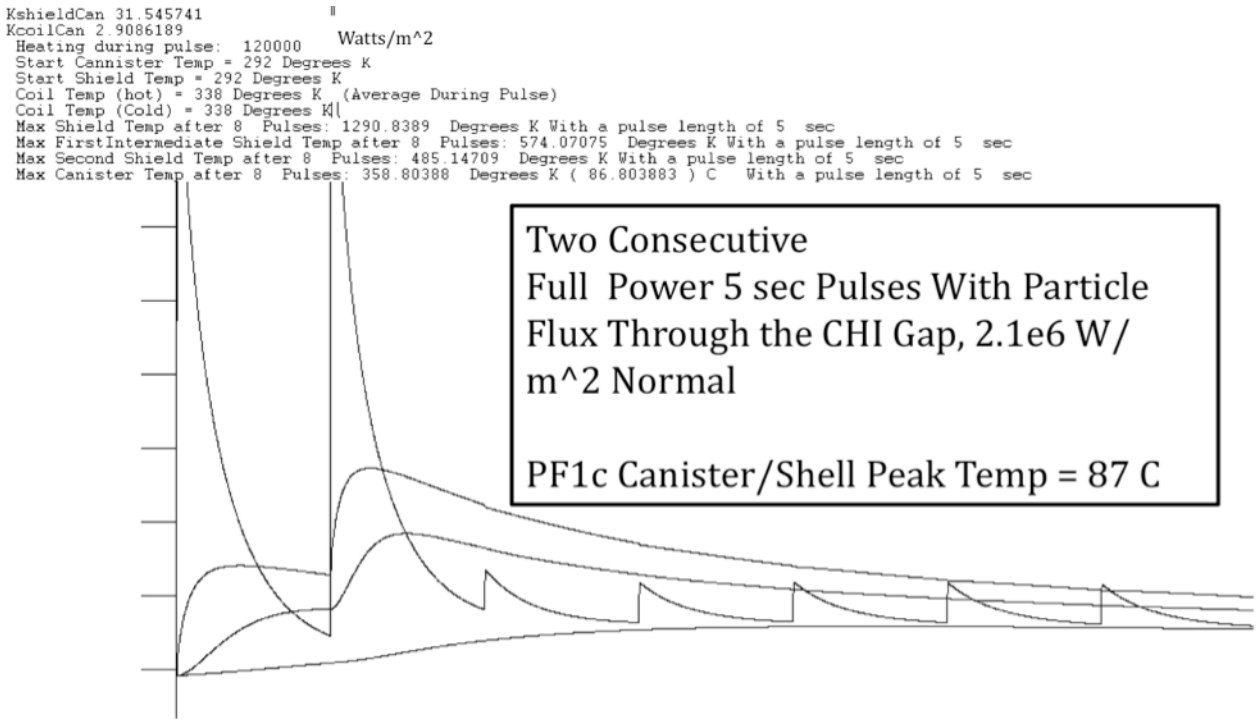


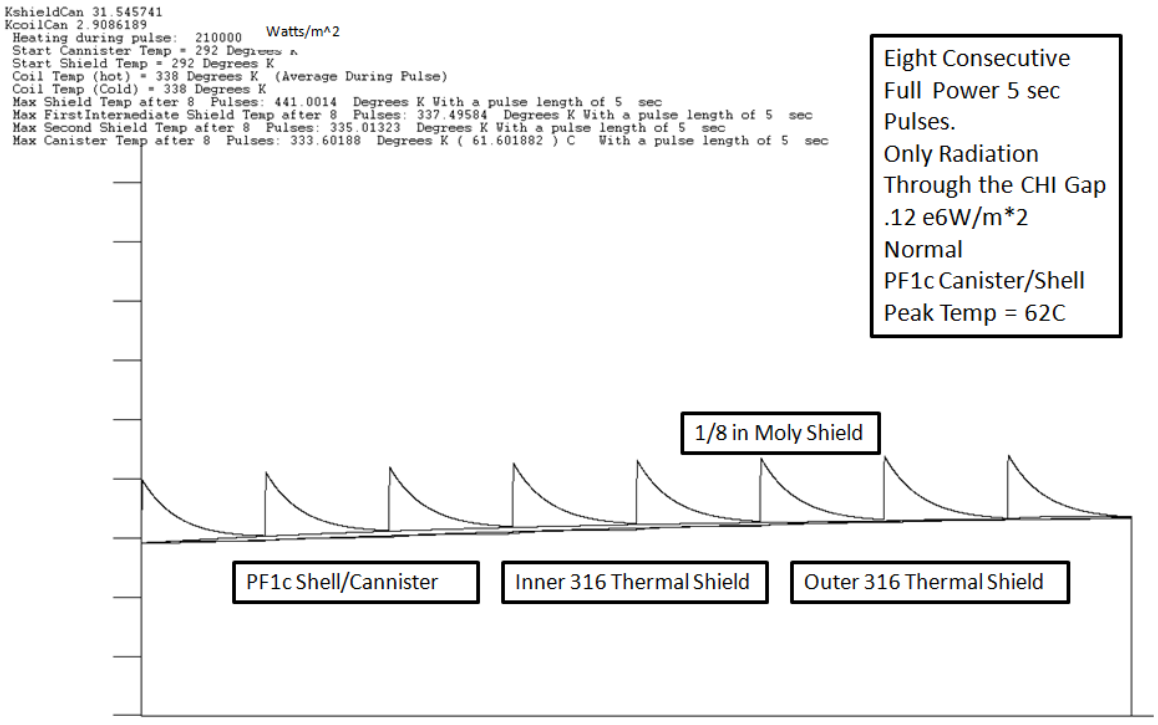


## 11.0 Transient Electromagnetic Disruption Results

Disruption loads on the PF1c case were calculated with an analysis and model developed for the passive plate simulation, [Ref 3-Appendix I]. Only the lower PF1c case was modeled (See section 7.0) A downward VDE was modeled, so the lower case needed to be detailed, but the results are representative for an upper PF1c and VDE.

The molybdenum thermal shield might have been interesting in terms of disruption response. The disruption model was re-run with only the stainless steel casing. The peak stress was about one MPa.

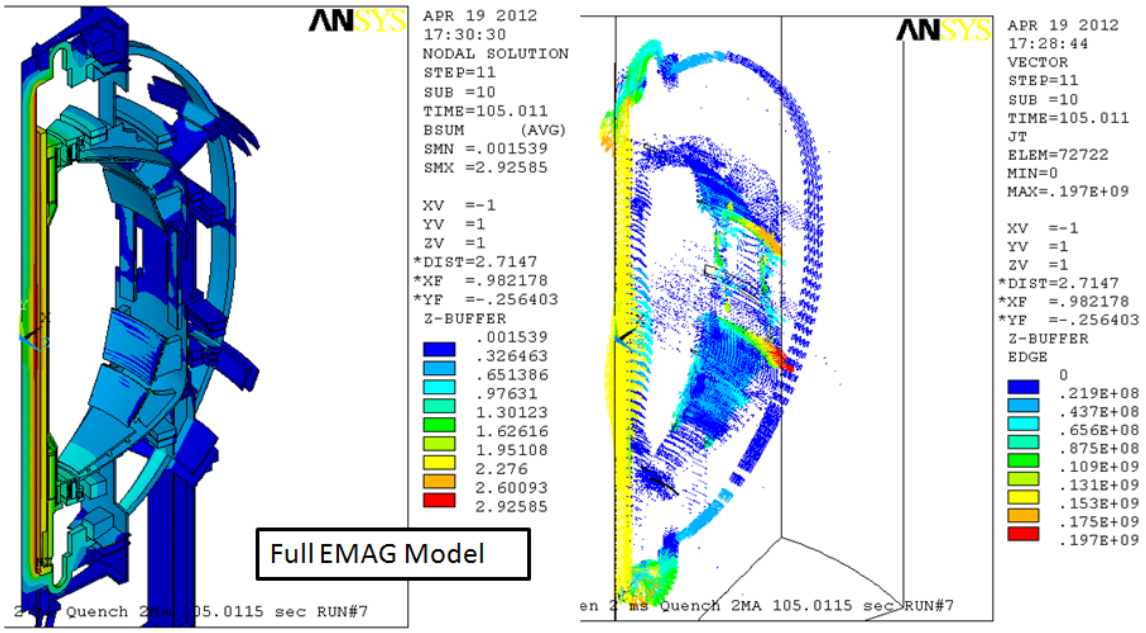


Figure 11.0-1 Electromagnetic Model

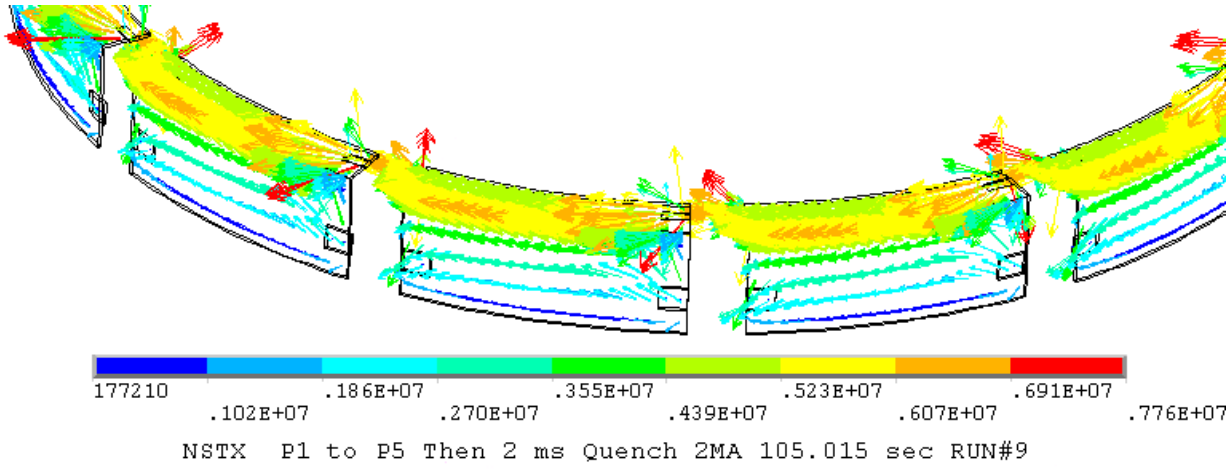


Figure 11.0-2 Results for Moly Thermal Shield - A shield was not included in the initial Upgrade equipment.

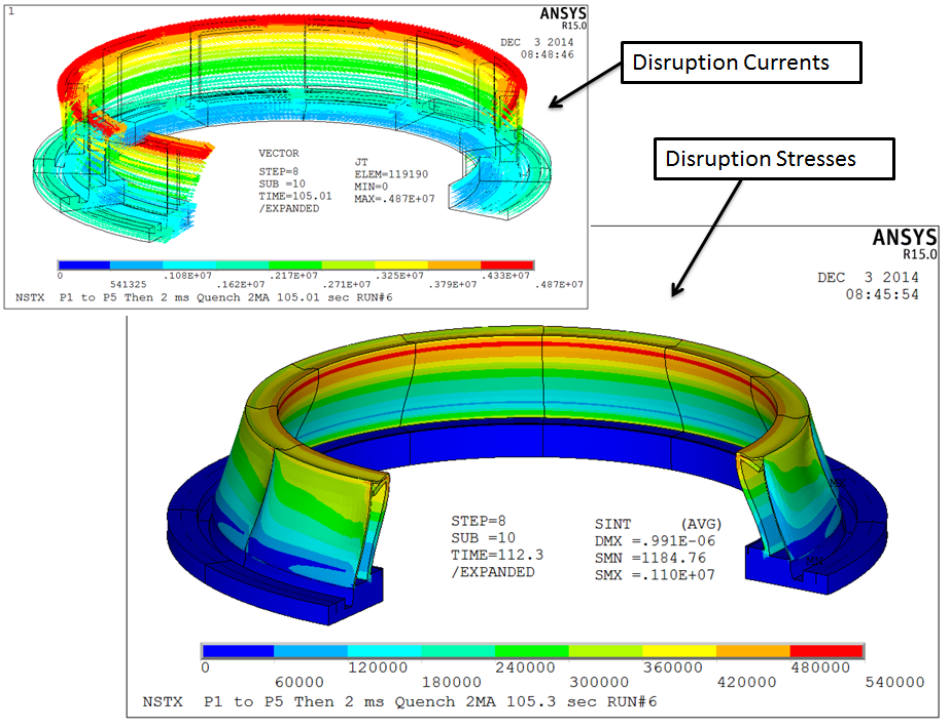


Figure 11.0-3 Results for a stainless steel PF1c Case

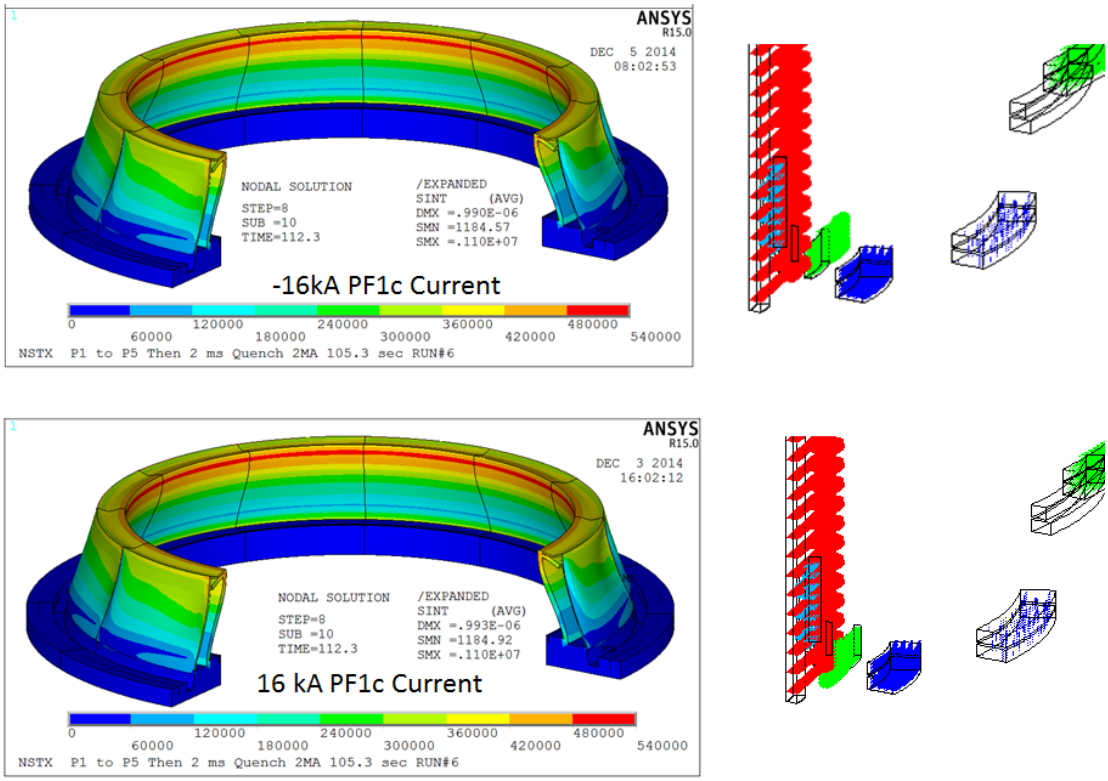


Figure 11.0-4 Results for a stainless steel PF1c Case

The very small difference in the stresses for +/- 16kA cases looks suspect, but the disruption stress in either case is small, only 1.1 MPa peak. So, disruption loads can be neglected.

Appendix A
email from Roger Ramen on PF1c Heat-Up During CHI Operations

**Temperature Rise of the PF1C casing during CHI operations**
**(R. Raman, 11-13-2012)**

Figure 1 shows the PF1C casing and two possible scenarios (A and B) for the current path along the surface of the PF1C casing. We will assume the worst-case scenario for this calculation. The present CHI capacitor bank has a capacitance of 50mF and a maximum charging voltage of 2kV. During 2016 it will be upgraded to a 3kV system at 50mF. The maximum bank energy would then be 225kJ. The frequency of the current waveform from the capacitor is about 100Hz, which means that the current will flow through the bulk of the material and not on a thin surface layer.

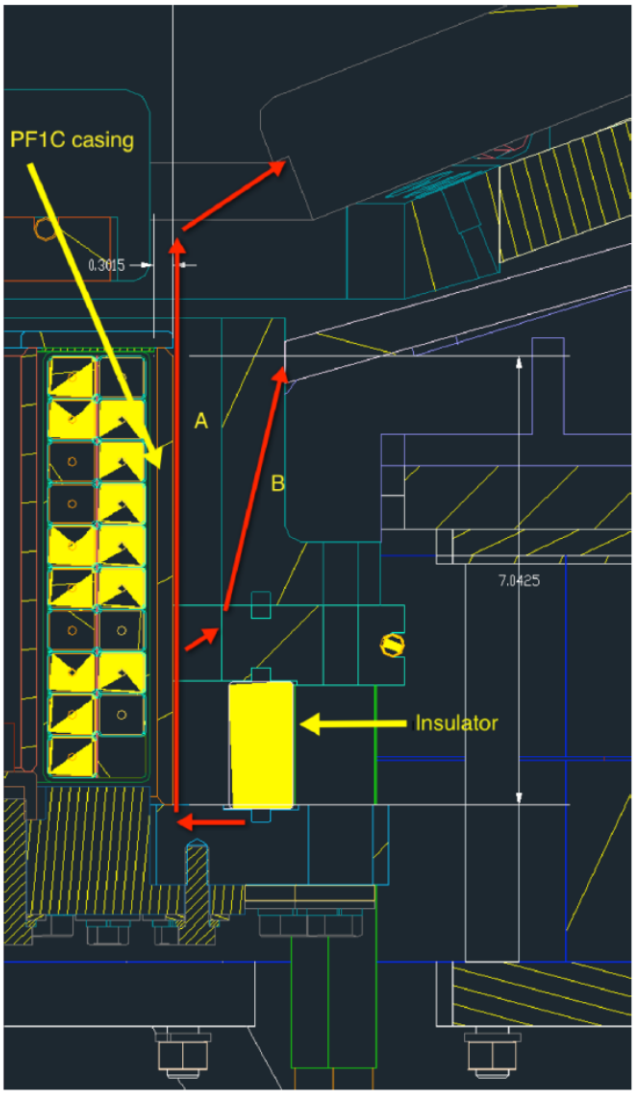

Figure shows two possible current paths along the PF1C casing. A similar current path can be assumed to exist along the PF1CU casing during an absorber arc.

The PF1C casing near the current path region has a radius of 58.06 cm, a thickness of 0.3177cm and a length of 17.78cm. It has a mass of 16.5kg and a specific heat of 500J/(kg.K). For stainless steel the corresponding resistance of this casing is 1.1E-5 Ohms. If all of this energy is somehow deposited in the casing (which is physically impossible), the casing temperature will increase by 28 degrees C. If the current flows along path B and energy is deposited in lower third of the casing length, the temperature will increase to about 80C.

Note that the capacitor bank represents an electrical power source. The energy from the capacitor bank must be transferred to the casing through the passage of electrical currents. The external circuit resistance is much

higher than the resistance of the casing so in case of a large current increase, most of the energy will be deposited in the external components and not in the casing.

The figures below are results from a more realistic calculation that considers the circuit parameters (Rext = 15mOhm, Lext= 100μH, Charging voltage of 3kV, C=50mF). This shows that the casing temperature will increase by less than 0.1C per pulse that are subjected to a very severe absorber arc. The normal peak currents anticipated during CHI discharges would be less than 20kA, which is much less than the 125kA current during a localized arcing, so that the heating during normal operation and during absorber arcs is insignificant.

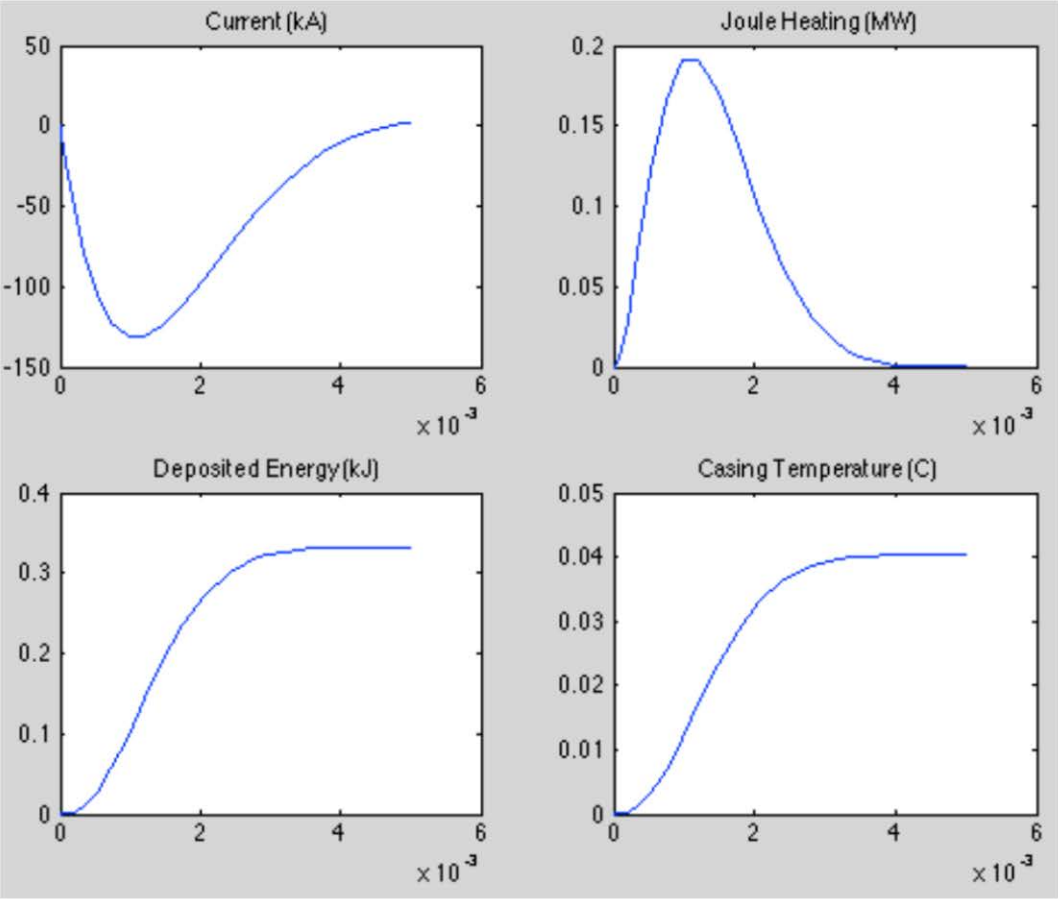

## Appendix B
## June 4 2014, Steel Flex Shell, and Proposed Weld Detail

Steve Raftopolis pointed out that a good vacuum design philosophy was to separate the functions of structural support and vacuum boundary. In this spirit, the centering spring was made up od an additional thin shell that was separate from the PF1c Outer can. It still had to bear on the top and bottom corners of the can but it would not flex the outer can shell as the coil thermally expanded and contracted. The closuire weld detail only had to take the stresses and deflections of the mandrel. These are significant though because of the large vertical Lorentz loads imposed on the coil.

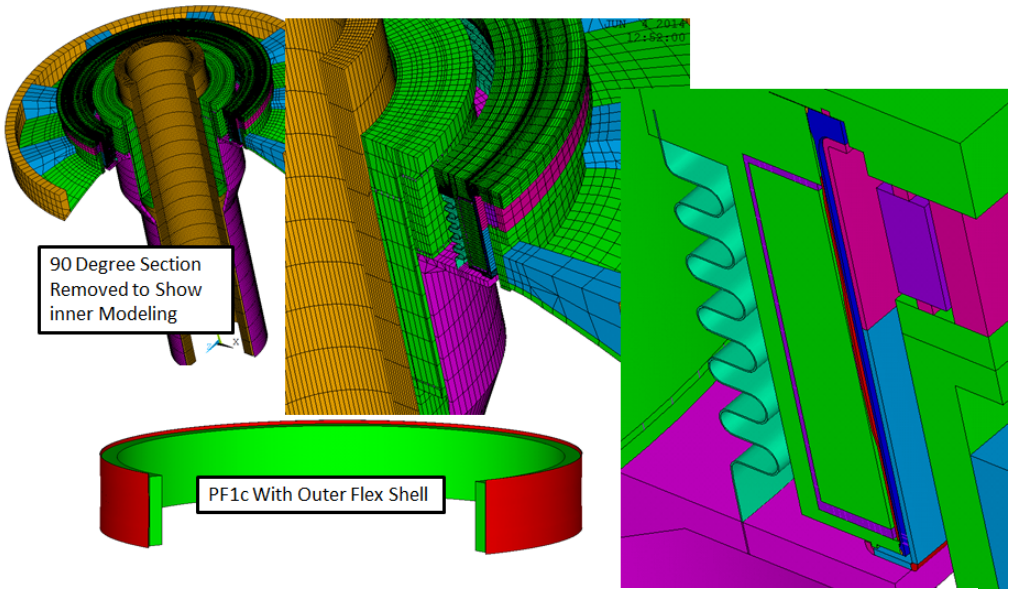


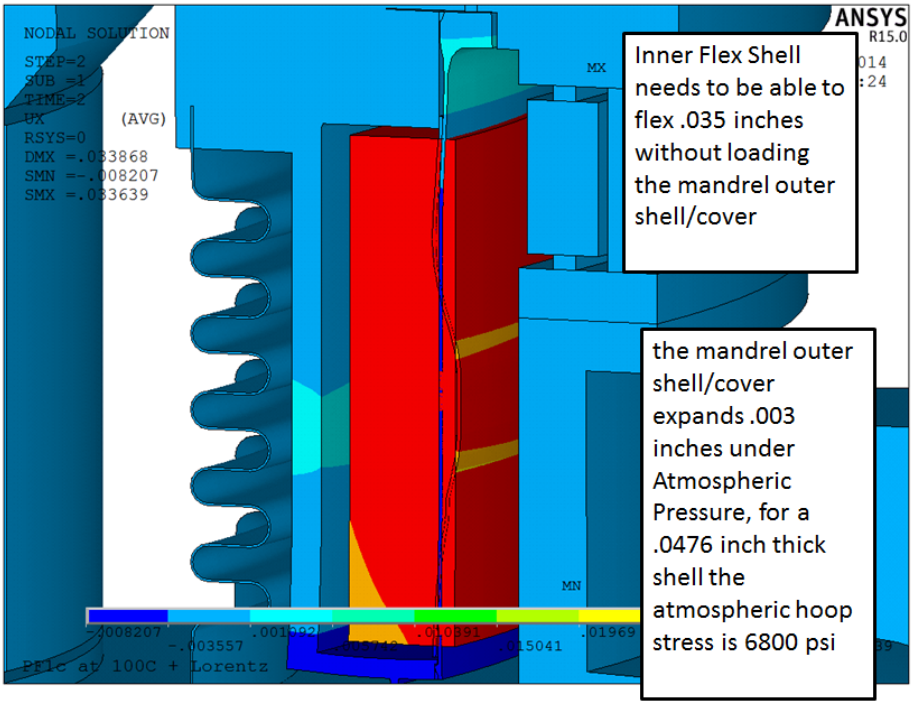

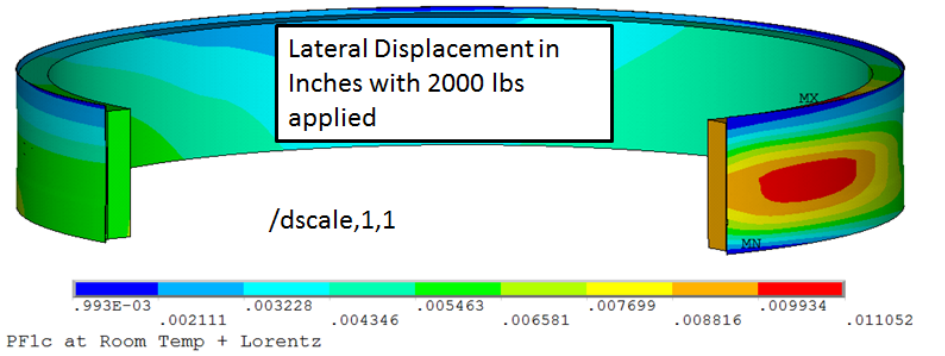


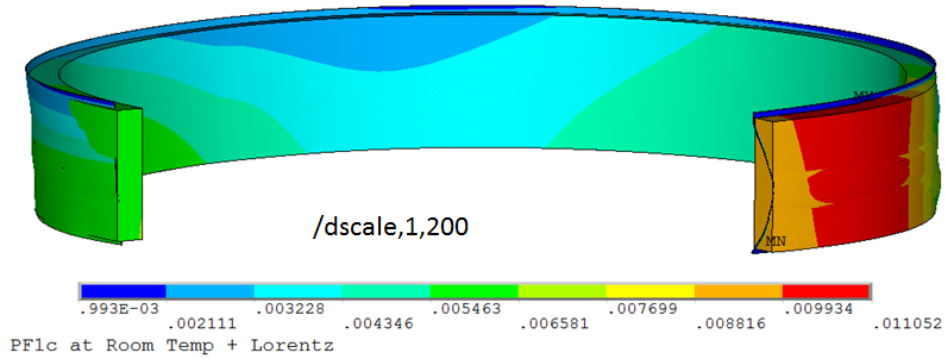


Flex Shell Stress Lateral Load Only

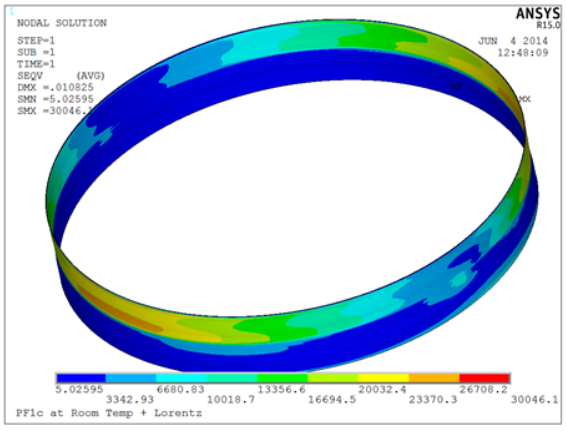


Lateral Load Plus 100C in PF1c

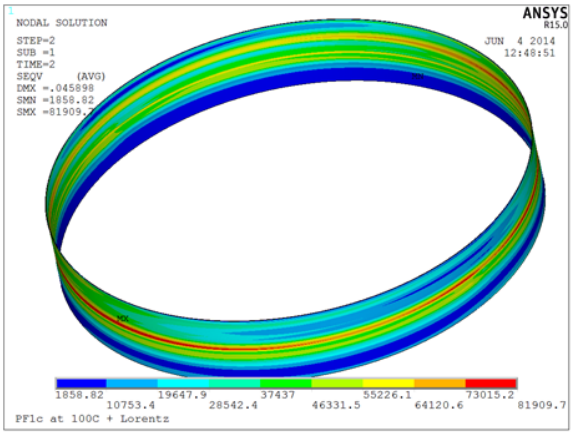

PF1c U Outer Shell and Weld Stress
(Does not include Hoop stress due to atmospheric pressure

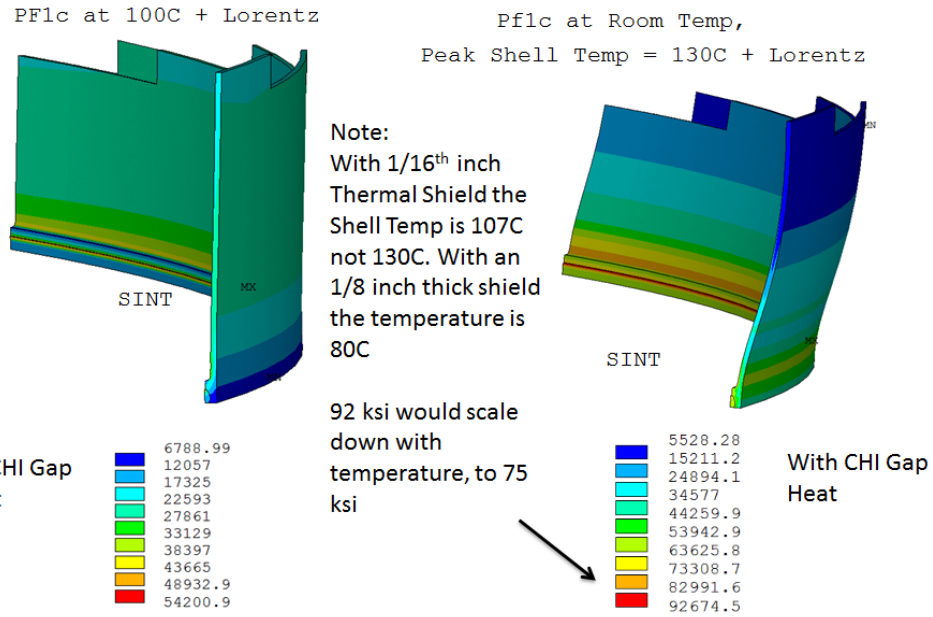


PF1c U Flex Panel Stress

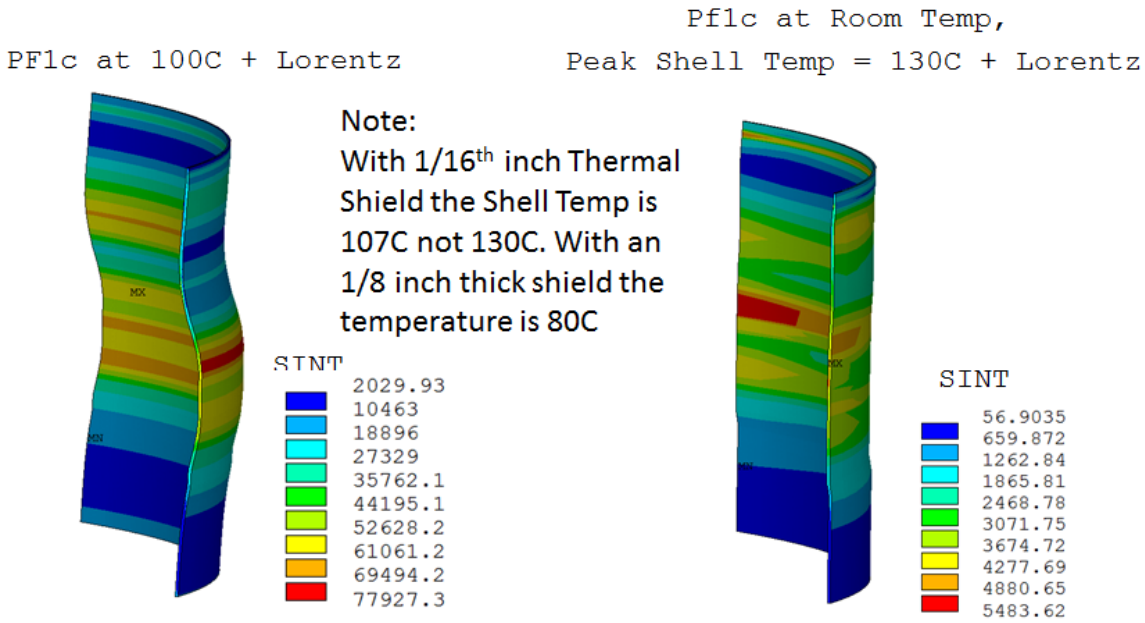


A feasibility issue with the internal flex shell is whether it can take the lateral loads that would result from a decentered coil. This is discussed in section 8.0 and also is an issue with any of the centering concepts.

## Appendix C

### "Rubber Bumpers"

PF1c Outer Shell and Centering System Studies
P Titus June 27 2014

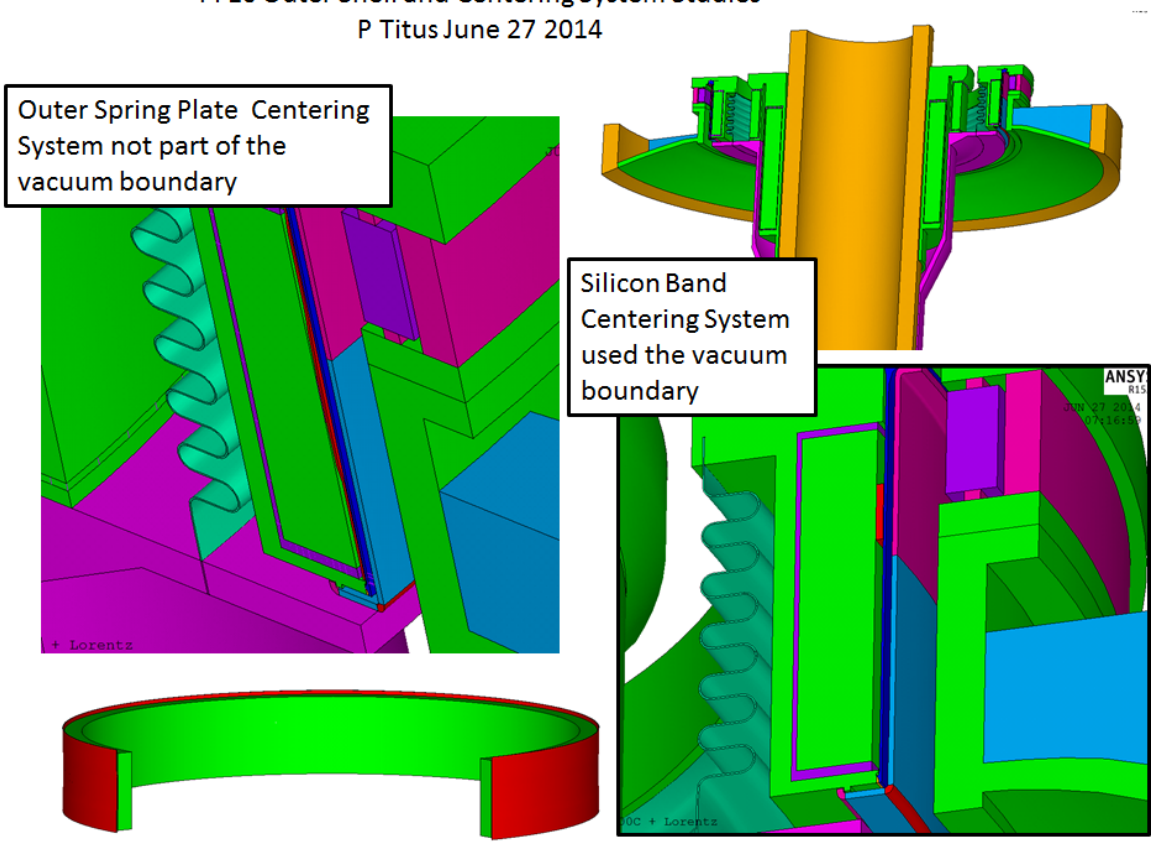


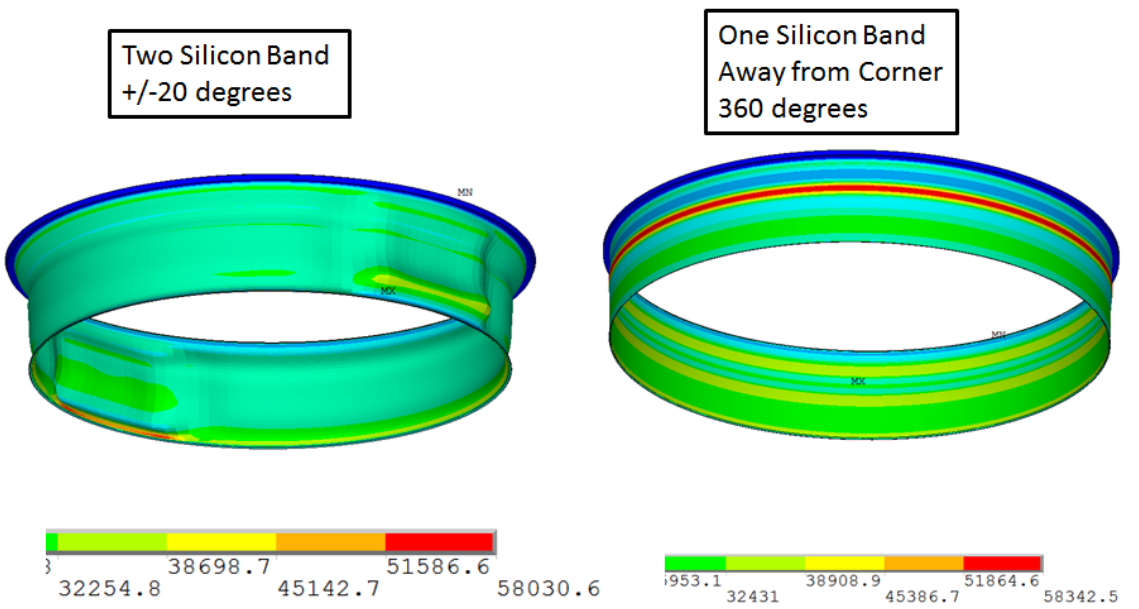

# Appendix D

## More on the Unused Moly Thermal Shield

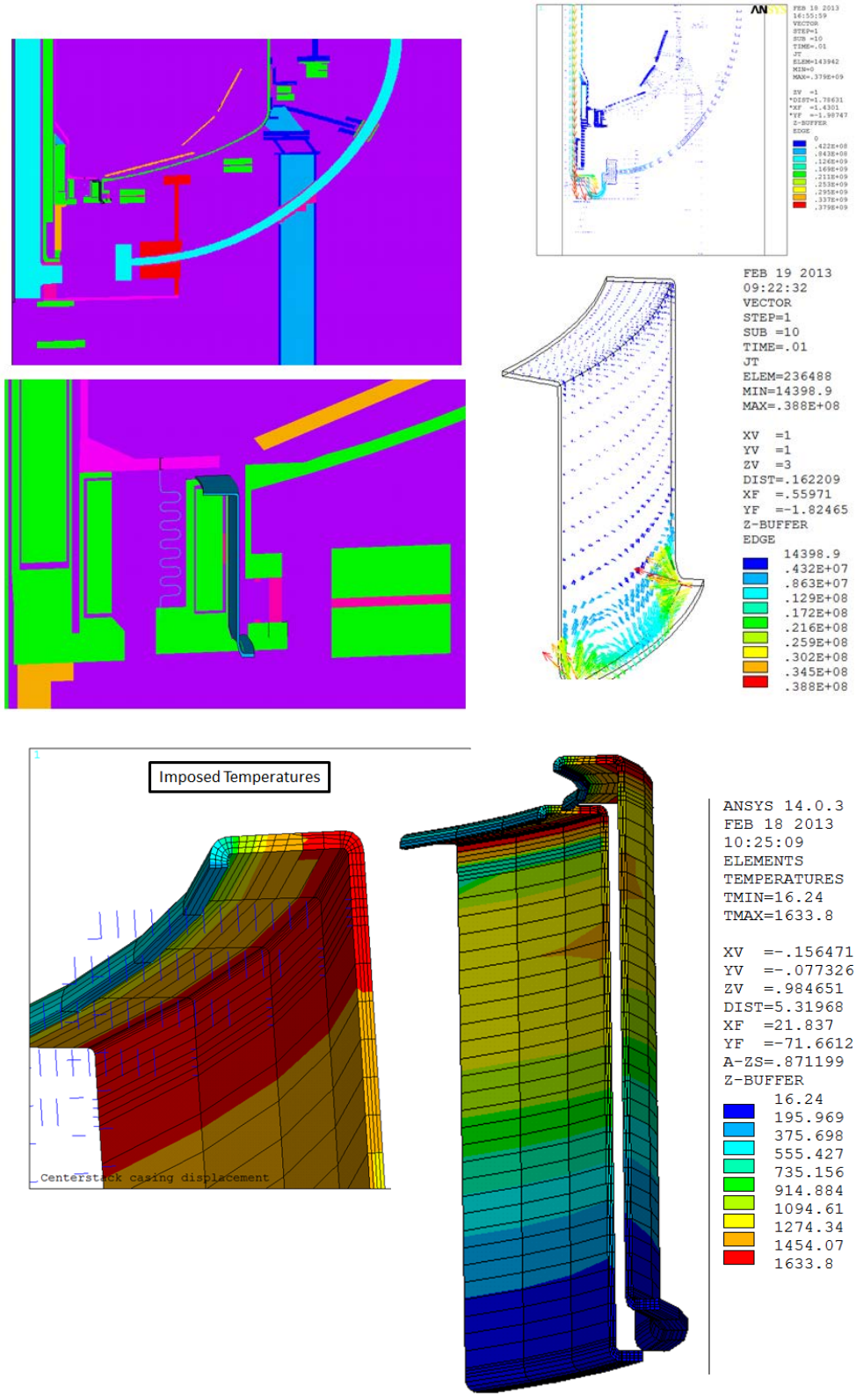

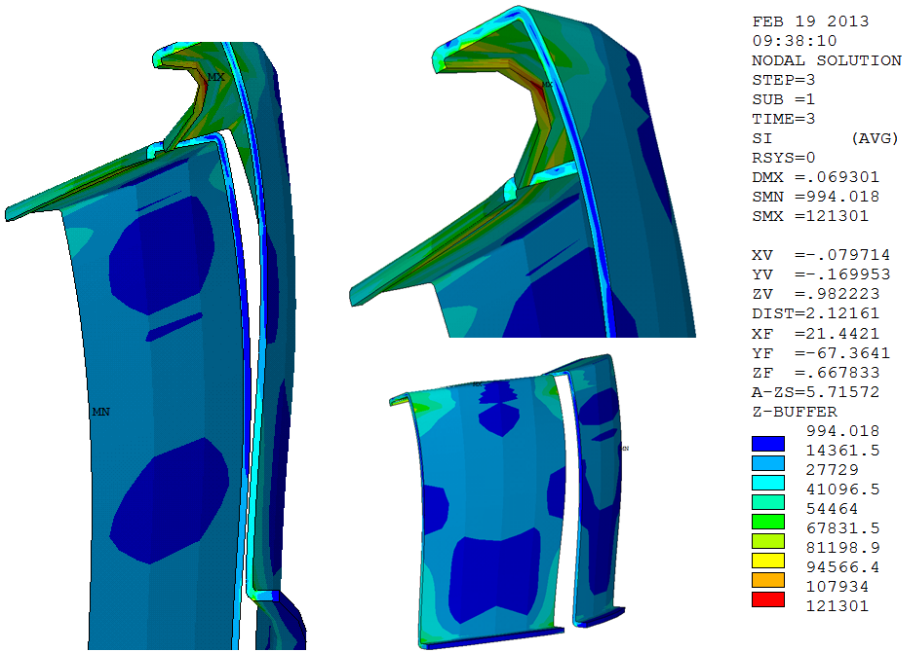


Pf1c at Room Temp, Peak Shell Temp = 130C + Lorentz

## Appendix E

## Thermal Shield Analysis Program

```
dim tempMoly(20000),tempcan(20000), tempcoil(20000),tempishld(20000),tempi2shld(20000)
let ian=100
let ibn=20
!print "Enter Thickness,Pulse Length in Sec.,Pulseheat"
!print "Material option, 1 for 718, 2 for Molybdenum:"
!input matopt
let matopt=2
let shieldthick=.00317/2   ! for 1/16 inch
let ishieldthick=.0003
let canthick=.00317
!     pulseheat=.455e6   ! watts/m^2   C-Mod
!           pulseheat=.116e6   ! watts/m^2   NSTX
let pulselength=5
let pulseheat=.12e6
let pulseheat=2.1e6
let pulseheat=2.1e6
let emisSO=.3             !emissivity of Shield Outer
let emisSI=.3            !Unoxidized moly emissivity of Shield Inner
let emisV=.3              !vessel emissivity
let emiscan=.3            !cannister emissivity
let emiscoil=.3
let tves=292             !Averge Vessel Surface temp
let numpulses=8
let cdtime=15.0
let cdtime=15
```

```
!if matopt= 1 then
   !718
let canspeheat=435
let candensity=8190.0

    !316
let canspeheat=500
let candensity=7900
let canTcon = 16.2  !Watts/m/degK
!end if

!if matopt=2 then    !Molybdenum
let shieldspeheat=280    !at 600C
let shieldspeheat=300    ! at 1000 C (reference Plansee Website)
let shielddensity=10220.0
let shieldTcon = 100
!end if

    !316

let shieldspeheat=280    !at 600C
let shieldspeheat=500    ! at 1000 C (reference Plansee Website)
let shielddensity=7900.0
let shieldTcon = 16.2


let epoxyTcon=0.6
let heliumTcon=.15
let airTcon=.01
let halfheightCan=.1
let EpoxyThick=.006
let Epoxywidth=.02
let Kcoilcan=(Halfheightcan/(canthick*canTcon) +epoxythick/(epoxywidth*epoxyTcon))^(-1)
let kcoilcan=kcoilcan+ heliumTcon/.06
let KShieldCan=ShieldTcon*(halfheightcan/(shieldthick*shieldTcon))
let shieldtempmax=0
let cantempmax=0

!     T1=(heatup+292)
let T1shield=tves
let t1ishield=tves
let t1i2shield=tves
let t1can=tves
let t1ves=tves
let t1coilhot=(392+284)/2    ! Average during pulse
let t1coilcold=(392+284)/2   ! Average during cooldown
!let t1coilcold=284   ! For Long Cooldowns the Coils will be cold for most of the cooling period

let k=0
let timestep=1
let numiter = pulselength/timestep

for np=1 to numpulses
if np>2 then let pulseheat=.12e6
                !During Pulse
```

```
let t1coil=t1coilhot
for j=1 to numiter
let k=k+1

let qshldtop=1*emisSO*emisv*5.67e-8*(t1shield^4-tves^4)/(emisSO+emisv-emisSO*emisv)
let qshldbot=1*emisSO*emisv*5.67e-8*(t1shield^4-t1ishield^4)/(emisSO+emisSO-emisSO*emisSO)

let qishldtop=qshldbot
let qishldbot=1*emisSO*emisv*5.67e-8*(t1ishield^4-t1i2shield^4)/(emisSO+emiscan-emisSO*emiscan)

let qi2shldtop=qishldbot
let qi2shldbot=1*emisSO*emisv*5.67e-8*(t1i2shield^4-t1can^4)/(emisSO+emiscan-emisSO*emiscan)

let qcantop=qi2shldbot
let qcanbot=1*emisSO*emisv*5.67e-8*(t1can^4-t1coil^4)/(emiscan+emiscoil-emiscan*emiscoil)

let qshield=pulseheat-qshldtop-qshldbot-kshieldcan*(t1shield-t1can)
let qishield=qishldtop-qishldbot
let qi2shield=qi2shldtop-qi2shldbot
let qcan=qcantop-qcanbot-KcoilCan*(t1can-t1coil)

let t1shield=t1shield+qshield*timestep/(shieldspeheat*shieldthick*shielddensity)
let t1ishield=t1ishield+qishield*timestep/(shieldspeheat*ishieldthick*shielddensity)
let t1i2shield=t1i2shield+qi2shield*timestep/(shieldspeheat*ishieldthick*shielddensity)
let t1can=t1can+qcan*timestep/(canspeheat*canthick*candensity)

let tempmoly(k)=t1shield
let tempishld(k)=t1ishield
let tempi2shld(k)=t1i2shield
let tempcan(k)=t1can
next j

let numCD=CDTime*60.0/timestep
!    do 40 j=1,numCD,1

                ! During Cooldown
let t1coil=t1coilcold
for j = 1 to numcd
let k=k+1
let qshldtop=1*emisSO*emisv*5.67e-8*(t1shield^4-tves^4)/(emisSO+emisv-emisSO*emisv)
let qshldbot=1*emisSO*emisv*5.67e-8*(t1shield^4-t1ishield^4)/(emisSO+emisSO-emisSO*emisSO)

let qishldtop=qshldbot
let qishldbot=1*emisSO*emisv*5.67e-8*(t1ishield^4-t1i2shield^4)/(emisSO+emiscan-emisSO*emiscan)

let qi2shldtop=qishldbot
let qi2shldbot=1*emisSO*emisv*5.67e-8*(t1i2shield^4-t1can^4)/(emisSO+emiscan-emisSO*emiscan)

let qcantop=qi2shldbot
let qcanbot=1*emisSO*emisv*5.67e-8*(t1can^4-t1coil^4)/(emiscan+emiscoil-emiscan*emiscoil)

let qshield=-qshldtop-qshldbot-kshieldcan*(t1shield-t1can)
let qishield=qishldtop-qishldbot
let qi2shield=qi2shldtop-qi2shldbot
let qcan=qcantop-qcanbot-KcoilCan*(t1can-t1coil)
```

```
let   t1shield=t1shield+qshield*timestep/(shieldspeheat*shieldthick*shielddensity)
let   t1ishield=t1ishield+qishield*timestep/(shieldspeheat*shieldthick*shielddensity)
let   t1i2shield=t1i2shield+qi2shield*timestep/(shieldspeheat*ishieldthick*shielddensity)
let   t1can=t1can+qcan*timestep/(canspeheat*canthick*candensity)

let  tempmoly(k)=t1shield
let  tempcan(k)=t1can
let  tempishld(k)=t1ishield
let  tempi2shld(k)=t1i2shield
let  tempcoil(k)=t1coil
!print t1
if t1shield>shieldtempmax then let shieldtempmax=t1shield
if t1ishield>ishieldtempmax then let ishieldtempmax=t1ishield
if t1i2shield>i2shieldtempmax then let i2shieldtempmax=t1i2shield
if t1can>cantempmax then let cantempmax=t1can
next j
!   40  continue
next np
set window -1000,10000,-100,1200
plot 10000,0;0,0;0,1200
for i=1 to 1200 step 100
plot -200,i;0,i
next i

for i=1 to 10000
plot i,tempmoly(i);
next i
plot i,tempmoly(i-1)

for i=1 to 10000
plot i,tempishld(i);
next i
plot i,tempishld(i-1)

for i=1 to 10000
plot i,tempi2shld(i);
next i
plot i,tempi2shld(i-1)

for i=1 to 10000
plot i,tempcan(i);
next i

print "KshieldCan" ;kshieldcan
print "KcoilCan" ;kcoilcan
print " Heating during pulse: ";pulseheat; " Watts/m^3"
print " Start Cannister Temp =";tves ; "Degrees K"
print " Start Shield Temp =";tves ; "Degrees K"
print " Coil Temp (hot) =";t1coilhot ; "Degrees K  (Average During Pulse)"
print " Coil Temp (Cold) =";t1coilcold ; "Degrees K"
print " Max Shield Temp after";numpulses;" Pulses:"; shieldtempmax; " Degrees K"; " With a pulse length
of";pulselength;" sec"
print " Max FirstIntermediate Shield Temp after";numpulses;" Pulses:"; ishieldtempmax; " Degrees K"; " With a
pulse length of";pulselength;" sec"
print " Max Second Shield Temp after";numpulses;" Pulses:"; i2shieldtempmax; " Degrees K"; " With a pulse length
of";pulselength;" sec"
```

```
print " Max Canister Temp after";numpulses;" Pulses:"; cantempmax; " Degrees K ("; (cantempmax-272);") C
With a pulse length of";pulselength; " sec"
end
```